Synthesis and Supramolecular Assemblies of Substituted Cycloparaphenylenes

---

Inauguraldissertation zur Erlangung des Doktorgrades (Dr. rer. nat.) der Naturwissenschaftlichen Fachbereiche im Fachgebiet Chemie der Justus-Liebig-Universität Gießen

vorgelegt von

Daniel Kohrs

aus
Holzminden

Betreuer: Prof. Dr. Hermann A. Wegner

Gießen 2023

Versicherung nach §17 der Promotionsordnung

Ich erkläre: Ich habe die vorgelegte Dissertation selbstständig und ohne unerlaubte fremde Hilfe und nur mit den Hilfen angefertigt, die ich in der Dissertation angegeben habe. Alle Textstellen, die wörtlich oder sinngemäß aus veröffentlichten Schriften entnommen sind, und alle Angaben, die auf mündlichen Auskünften beruhen, sind als solche kenntlich gemacht. Ich stimme einer evtl. Überprüfung meiner Dissertation durch eine Antiplagiat-Software zu. Bei den von mir durchgeführten und in der Dissertation erwähnten Untersuchungen habe ich die Grundsätze guter wissenschaftlicher Praxis, wie sie in der „Satzung der Justus-Liebig- Universität Gießen zur Sicherung guter wissenschaftlicher Praxis“ niedergelegt sind, eingehalten.

_____ _____

Datum Unterschrift

Dekan: Prof. Dr. Thomas Wilke

Erstgutachter: Prof. Dr. Hermann A. Wegner

Zweitgutachter: Prof. Dr. Richard Göttlich

“The whole of science is nothing more than a refinement of everyday thinking.”

Albert Einstein

Table of Contents

Abstract

Cycloparaphenylenes (CPPs) represent the shortest cutout of armchair single-walled carbon nanotubes (SWCNTs). These three-dimensional structures solely built from sp^2-hybridized subunits contain a considerable amount of strain arising from this unusual arrangement. This needs to be built throughout the synthesis and requires a strategy, targeting on a strain-reduced macrocycle prior to the formation of the CPP. One of these strategies which relies on a modular macrocyclization through palladium catalyzed Suzuki cross-coupling was combined with a [2+2+2] cycloaddition (CA) strategy to introduce *tert*-butyl (*t*-Bu) esters to the central building block. Thus, one [8] and two [10]CPP analogues equipped with *t*-Bu esters could be synthesized. The derivatives of [10]CPP were of particular interest as [10]CPP is, reasoned by its size, well suited to build inclusion complexes with the fullerenes C_{60} and C_{70}. The influence of the substituents on the association behavior to these carbon allotropes was investigated and quantified by fluorescence-quenching experiments as well as computational chemistry to gain further insight into the experimental results.

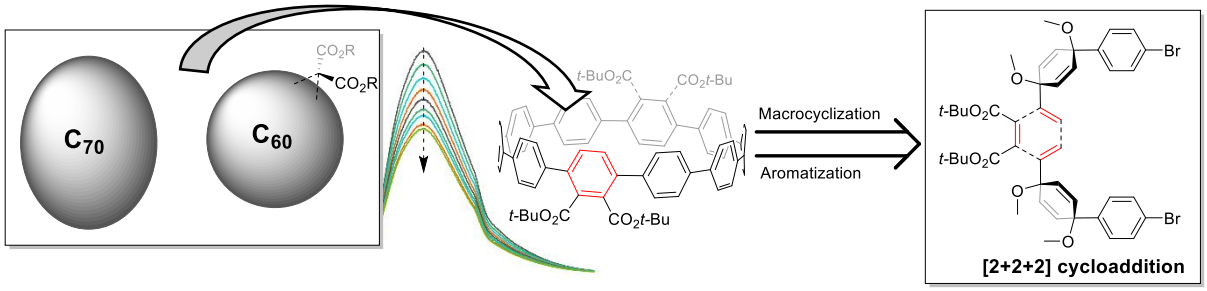

Supramolecular chemistry of substituted CPPs and their bottom-up synthesis centered around a [2+2+2] cycloaddition.

An interplay of multiple phenomena influenced the association, from which the increased dihedral angle, arising between the substituted and the neighboring phenyl rings, was attributed as the main contributor to decrease the association. Additional interactions emerging between the substituents and the fullerene were attenuating this effect and were differently strong for the two fullerenes. The achieved insights were compared to another functionalized [10]CPP analogue reported by the Wegner group. Further, malonyl ester derivatives of C_{60} with different alkyl chains were synthesized and used to investigate interactions occurring between the ester functionalities of the fullerene and *t*-Bu esters from one CPP derivative and were compared to results obtained for [10]CPP.

Zusammenfassung

Cycloparaphenylene (CPPs) stellen den kleinstmöglichen Ausschnitt von einwandigen *armchair* Kohlenstoffnanoröhren (SWCNTs) dar. Diese dreidimensionalen Strukturen, die ausschließlich aus sp^2-hybridisierten Untereinheiten bestehen, enthalten eine beträchtliche Spannung, die aus dieser ungewöhnlichen Anordnung resultiert. Diese muss während der Synthese aufgebaut werden, was durch einen vorherigen Aufbau eines spannnungsreduzierten Makrozyklus realisiert wird. Eine dieser Strategien, welche auf einer modularen Makrozyklisierung durch palladiumkatalysierte Suzuki Kreuzkupplung basiert wurde mit einer [2+2+2] Cycloadditionsstrategie kombiniert, um *tert*-Butyl (*t*-Bu) Ester in den zentralen Baustein einzuführen. Durch diese Verknüpfung konnten ein [8] und zwei [10]CPP-Analoga, ausgestattet mit *t*-Bu Estern, dargestellt werden. Die Derivate von [10]CPP waren von besonderem Interesse, da [10]CPP, aufgrund seiner Größe, gut geeignet ist, um Einschlusskomplexe mit den Fullerenen C_{60} und C_{70} einzugehen. Der Einfluss der Substituenten auf das Bindungsverhalten zu diesen Kohlenstoffallotropen wurde analysiert und anhand der Reduzierung der Fluoreszenz bei Zugabe quantifiziert. Um weitere Einblicke in die experimentellen Ergebnisse zu erhalten, wurden die Komplexe zusätzlich mittels Computerchemie untersucht.

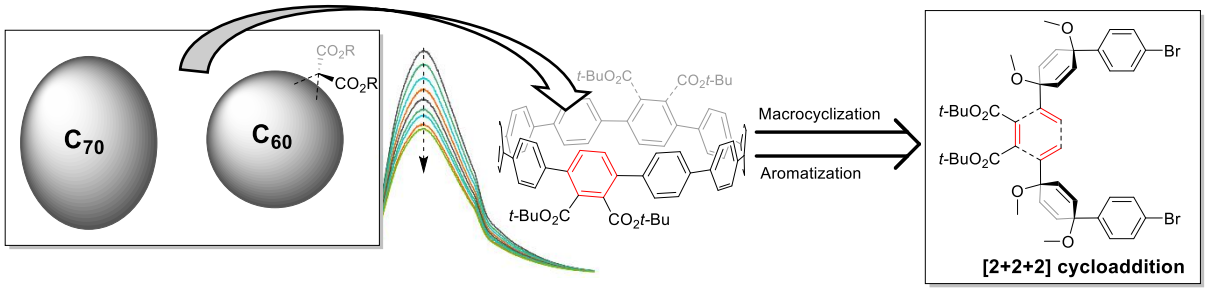

Supramolekulare Chemie substituierter CPPs und ihre Synthese mit einer im Mittelpunkt stehenden [2+2+2] Cycloaddition.

Es wurde herausgefunden, dass ein Zusammenspiel aus mehreren Phänomenen die Assoziation beeinflusste, von denen der vergrößerte Diederwinkel, der zwischen dem substituierten und benachbarten Phenylringen entsteht, den größten Einfluss auf die Assoziation ausübt. Zusätzliche Interaktionen, die zwischen den Substituenten und dem Fulleren auftauchen, haben diesen Effekt abgeschwächt und waren unterschiedlich stark für die beiden Fullerene. Die gewonnenen Einblicke wurden mit einem anderen funktionalisierten [10]CPP-Analogon der Wegner Gruppe verglichen. Zusätzlich wurden

Malonylesterderivate von C_{60} mit unterschiedlichen Alkylketten synthetisiert und Interaktionen zwischen den Estergruppen des Fullerens und *t*-Bu Estern eines CPP-Derivats untersucht und die erhaltenen Ergebnisse mit denen für [10]CPP verglichen.

1 Introduction

1.1 Weak Interactions in Chemistry

Supramolecular chemistry is a multidisciplinary subject at the borderline between physics, biology and chemistry.[1] It is present when two or more entities come in close proximity and interact via non-covalent interactions that keep molecules together without the need of any covalent bond. Even though *supramolecular chemistry* is defined as a research field based on interactions occurring intermolecularly,[2] e.g., in liquid crystals,[3] the underlying interactions also play an essential role in intramolecular systems like in the formation of secondary and tertiary structures of proteins.[4] Thus, an in-depth understanding of these *non-covalent interactions*, a term which describes the essence of these forces well, is crucial. Especially the research field of material science is a prime example in this regard. For instance, supramolecular chemistry and an exhaustive understanding of it was shown to be key for the improvement of different types of solar cells. Thus, the self-assembly of an electron acceptor was found to enhance the performance of an organic solar cell,[5] and an anion-π interaction in a perovskite solar cell equipped with a fullerene electron transport layer, promoted the charge-transport.[6]

Prominent representatives in the context of material science are single-walled carbon nanotubes (SWCNTs). These π-extended molecular architectures, experimentally discovered in the early 90s of the last century,[7] have a curved structure, solely consisting of sp^2-hybridized carbon atoms and can vary both in length and diameter.

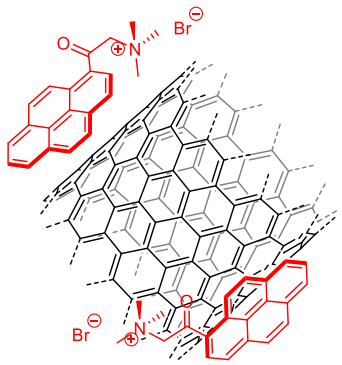

Figure 1: SWCNT functionalized through a supramolecular complexation with pyrenes.[8]

A supramolecular assembly of SWCNTs with functionalized pyrenes was found to facilitate solubility and even allows solubility in water, when ammonium ions were introduced to the

side chain (Figure 1).[8] The complex is mainly driven by π-π interactions occurring between the convex surface of the nanotubes and the two-dimensional pyrene. An in-depth analysis of this complex would be a challenging task because the one hand the exact structure of the nanotube is not well defined, as it consists of a mixture of different lengths and widths, and on the other hand the stoichiometry of pyrenes to the nanotube is unknown. Additionally, the side chains bear the possibility of additional interactions like CH-π interactions along with cation-π interactions, which make the analysis of these forces even more difficult.

One way of gaining insight into these interactions in general is the quantification within a suitable system. Molecular balances are a useful tool for this purpose and manifold systems were presented in the past decades.[9] Especially, when one force in the occurring interaction is dominant, an in-depth study is facilitated. One prominent example of such a system was reported by Wilcox and coworkers (Figure 2, left). The rotation around the C_{phenyl}-C_{phenyl} bond is at room temperature slow enough to observe different ^{1}H NMR signals for the intramolecularly interacting and the non-interacting state, which made the investigation of CH-π interactions by measurement of the ^{1}H NMR spectrum possible.[10]

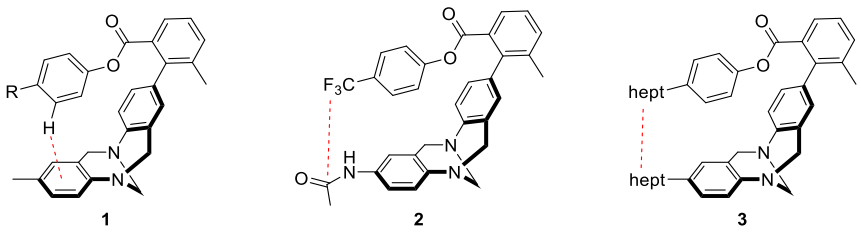

Figure 2: Example of a rotational balance system, the original Wilcox balance (left),[10] adapted version by Diederich (middle),[11] and adapted version by Cockroft (right).[12]

This rotational balance motif was also used by Diederich and coworkers (Figure 2, middle) in order to investigate fluorine-amide interactions,[11] as well as by Hunter and coworkers for the investigation of solvent effects, altering the electron densities of the interacting aromatic rings.[13] Further, Cockroft and coworkers equipped the interacting aromatics with long alkyl chains to exploit this system to investigate London dispersion.[12] These examples showcase the manifold applications of a system which is adapted to fit the needs. Additional systems were published relying on the rotational interconversion between two states – an interacting and a non-interacting one whose equilibrium was used to quantify the emerging interaction. Examples include systems based on thiobarbiturate,[14] thiourea,[15] or a bicyclic *N*-arylimide.[16] Similarly, the bond isomerism could be used in this regard.

Cyclooctatetraene, for instance, was applied in this manner, as the equilibrium between the two isomers **4** and **5** has been used for the investigation of London dispersion (Scheme 1, left).[17] Further, the azobenzene scaffold, which is, in contrast to most systems, not analyzed via its equilibrium but the kinetics of the back-isomerization from the less favored *cis* state **6-*cis*** into the favored *trans* state **6-*trans***, can be employed (Scheme 1, right).[18–22]

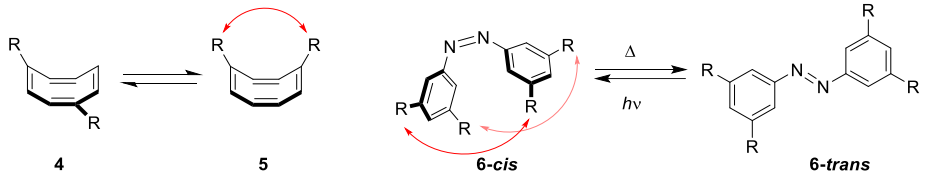

Scheme 1: Molecular systems build on the isomerization of cyclooctatetraene (left) and azobenzene (right).[17–22]

Besides these intramolecular systems for the quantification of weak interactions, there are examples of intermolecular systems which were used for this purpose as well. In one example, the group of Albrecht used ^{1}H NMR spectroscopy to investigate the dimerization equilibrium between titanium tris-catecholate **7** and its dimeric form **8** (Scheme 2).[23]

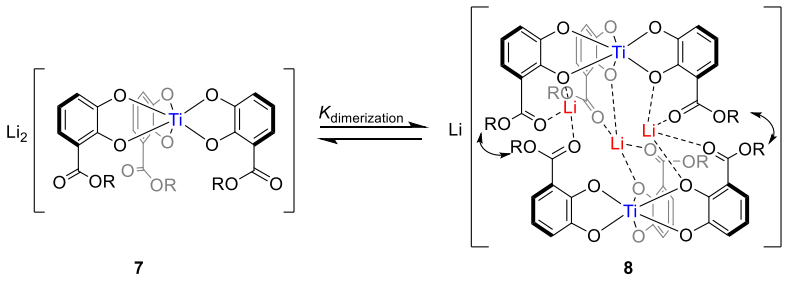

Scheme 2: Dimerization equilibrium of titanium tris-catecholate **7** influenced by London dispersion.[23]

Different alkyl groups as residues on the ester functionalities led to different dimerization constants with a maximum for *n*-heptyl. The non-covalent interactions, influencing the dimerization were dominated by London dispersion interactions and their enthalpy as well as entropy contributions could be quantified.[23] A second example of intermolecular balances for the evaluation of London dispersion interactions was published by the group of Chen who utilized proton-bound *N*-heterocyclic dimers in the gas phase as well as in solution.[24] Even though these systems give an accurate idea about interactions like London dispersion, CH-π, cation-π, or solvophobic effects, a more complex interplay of such interactions is hard to investigate with these balance systems. This becomes even clearer when considering extended structures like the beforehand presented SWCNTs. One way to circumvent this obstacle is to design suitable model systems to shine light onto these more

complex systems. In this manner, the molecular class of cycloparaphenylenes (CPPs) comes into play, which represents the shortest repeatable section of a SWCNT.

1.2 Cycloparaphenylenes

CPPs preserve the π-conjugated cyclic nature of SWCNTs, granting them a radially arranged molecular orbital with increased electron density in their cavity (Figure 3) making them host-candidates for supramolecular inclusion complexes.

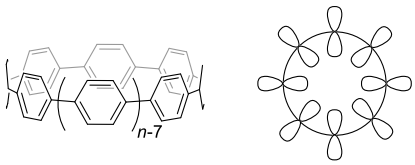

Figure 3: Representative sketch of [*n*]CPPs on the example of [8]CPP (left) and the schematic representation of π-orbitals from the aerial view.

Besides, this unusual arrangement of sp^2-hybridized subunits yields size-dependent properties, like strain energy,[25] as the curvature is distributed over a varying number of ring units, altering the geometric distortion from planarity. In contrast to this, CPPs show a size-independent UV-Vis absorption (Figure 4, left).

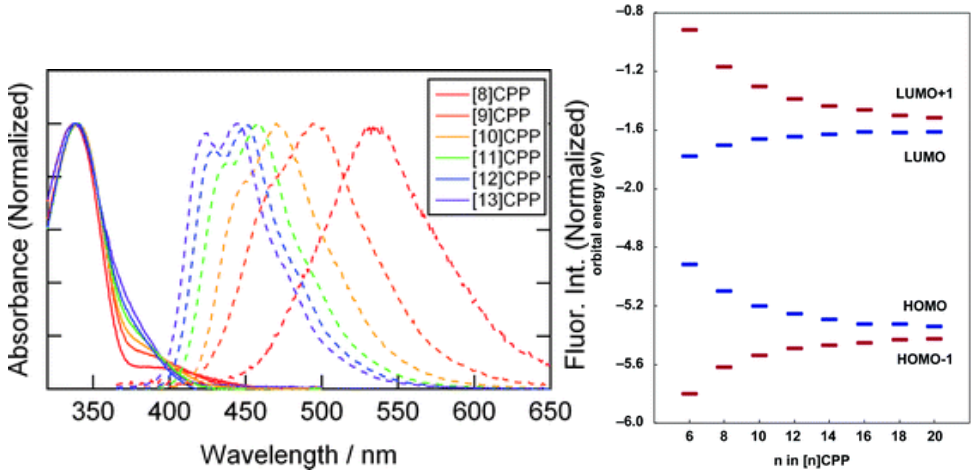

Figure 4: Absorbance (solid lines) and fluorescence (dashed lines, excited at 350 nm) of [8]-[13]CPP in THF (left),[26] reproduced from Ref. [26] with permission from the Royal Society of Chemistry; orbital energy diagram for different sized CPPs on the TD-DFT level of theory B3LYP/6-31G(d),[27] reproduced from Ref. [27] with permission from the Royal Society of Chemistry.

The responsible orbital-transition does not take place between the highest occupied molecular orbital (HOMO) and the lowest unoccupied molecular orbital (LUMO) as this is symmetry forbidden. This transition occurs as a longer wavelength side maximum due to dynamic conformational change.[27] The degenerate transitions HOMO-1 → LUMO as well as HOMO → LUMO+1 are the main contributor for the UV-Vis absorption and result in a

maximum absorbance at 340 nm. Additionally, CPPs show fluorescence upon excitation at this wavelength, which is contrary to their excitation size dependent making CPPs an interesting target for organic light-emitting diodes (Figure 4, left),[28] supported by the possibility to produce thin films.[29]

Further, CPPs bear a size-dependent strain (Figure 5, left),[25] which influences geometric parameters like the distortion of single rings from planarity as well as twisting of ring-planes to each other, altering the orbital energies.[27] Additionally, the deformations affect the aromaticity. This fact can be rationalized by nucleus independent chemical shifts (NICS), which have smaller values for more aromatic compounds. The numbers reveal a drastic decrease of aromaticity for CPPs with less than eight ring units (Figure 5, right).[30] The large strain in these cyclic molecules is one parameter which has to be built throughout the synthesis and is one reason which hampered earlier success in their bottom-up synthesis.

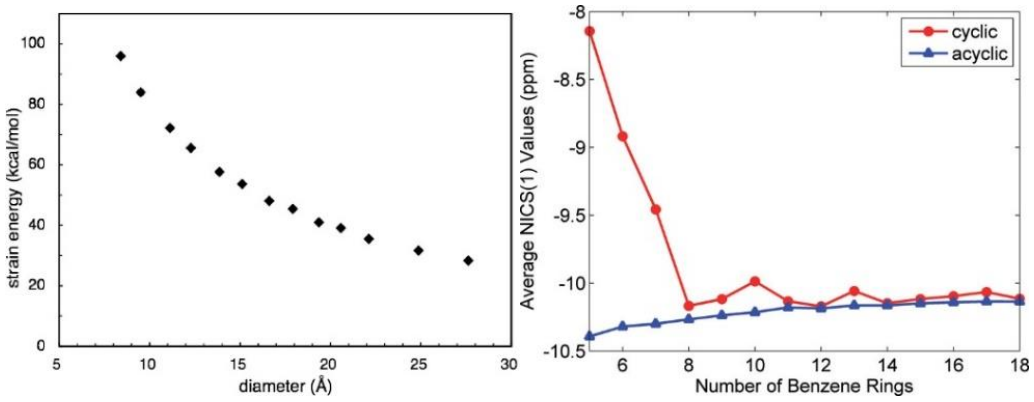

Figure 5: Size-dependent strain energies of [*n*]CPPs (left),[25] adapted with permission from Ref. [25]. Copyright 2010 American Chemical Society; NICS (1) values as probe for aromaticity of different sized CPPs in comparison to their open-chain analogues (right),[30] reproduced with permission from Ref. [30]. Copyright 2010 American Chemical Society

1.2.1 Synthetic Approaches

The first successful synthetic approach, giving access to CPPs was reported in 2008 by Jasti and Bertozzi.[31] Key in their strategy was the synthesis of strain-reduced macrocycles by incorporating cyclohexadiene moieties as sources of curvature prior to the formation of the target compounds (Scheme 3). The bottom-up synthesis starts from the readily available small molecules *p*-diiodobenzene (**9**) and *p*-benzoquinone (**10**), which already carry every carbon and hydrogen atom of the target compounds. Lithiation of *p*-diiodobenzene (**9**) with *n*-butyllithium (*n*-BuLi) in tetrahydrofuran (THF) gave a nucleophilic aromatic moiety from which two equivalents were added in a *syn*-selective fashion to *p*-benzoquinone (**10**).

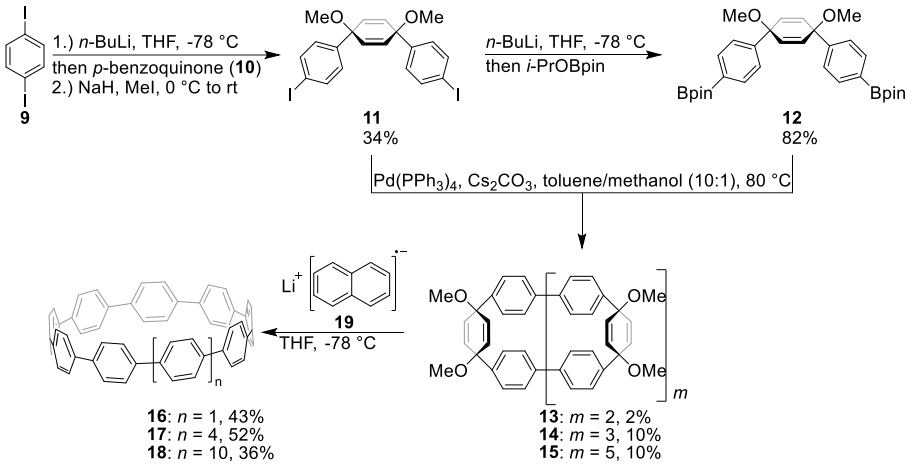

Scheme 3: Synthetic strategy towards CPPs by Bertozzi and Jasti centered around a random-cross-coupling.[31]

After etherification with methyliodide (MeI) bent diiodide building block **11** was obtained. The sterically less favored *syn* addition can be explained by electrostatic repulsion occurring between the in situ generated alkoxide and the nucleophile. This addition was reported with a diastereoselectivity of 80% for a similar case.[32] For the formation of the pre-bent macrocycles **13**-**15** the Suzuki coupling was chosen. Thus, one portion of diiodide building block **11** was converted into its size-corresponding boronic ester **12** and coupled with building block **11**. This synthesis was not size-selective and furnished macrocycles with nine, twelve and eighteen ring units. The final treatment with lithium naphthalenide (**19**) as a strong single-electron reductant yielded a mixture of [9], [12] and [18]CPP. Despite the breakthrough in the research field of synthetic carbon allotropes, this approach has a lack of size-selectivity at this point. Further development especially focusing on this obstacle followed within the next years. Utilizing central key building blocks for different sized CPPs allows a high flexibility through a modular combination (Scheme 4). In this manner, key synthons **12**, **23** and **24** delivered [7]-[12]CPP through a sequence of two consecutive Suzuki cross-couplings followed by reductive aromatization.[32,33]

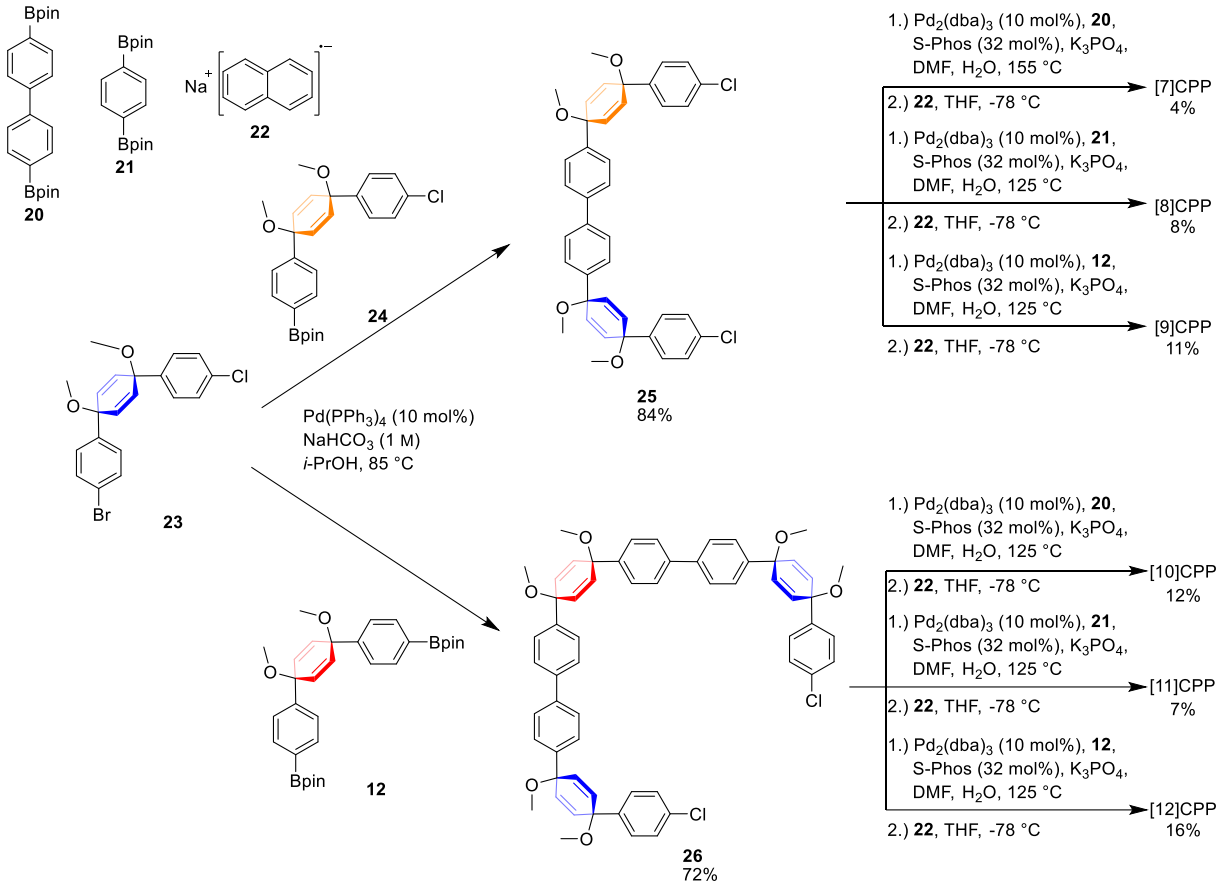

Scheme 4: Modular syntheses to [7]-[12]CPP relying on three central building blocks.[32,33]

The three essential building blocks employed for this synthesis were the Bpin/Bpin synthon **12** already reported in the first approach by Bertozzi and Jasti,[31] as well as mixed halogen derivative **23** and mixed Bpin/chloride derivative **24**. To access the latter ones, phenol **27** was, after conversion to its trimethylsilyl (TMS) ether, oxidized using the iodine (III) species phenyliodine(III) diacetate (PIDA) to achieve hydroxy ketone **28** (Scheme 5).

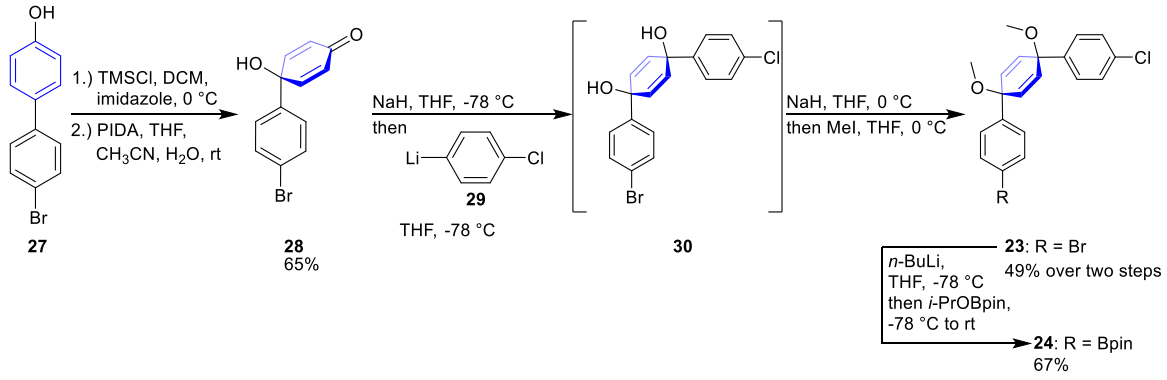

Scheme 5: Synthesis of key synthons **23** and **24**.[32]

To this electrophile was added 4-lithium-chlorobenzene (**29**) in a *syn*-selective fashion. The resulting diol **30** was deprotonated without any purification and converted to the Br/Cl building block **23**. After selective lithiation and reaction with *i*-PrOBpin the Cl/Bpin building

block **24** was obtained. Another strategy employing cyclohexadiene moieties utilized building block **37** which contains five ring units (Scheme 6) as the central compound to access [8] and [10]CPP on a gram scale (Scheme 7).[34] The build-up of the key compound is similarly approached as in the other modular synthesis. Angled ketone **28** is targeted from phenol **27** through silylation followed by oxidation with PIDA. To this ketone *t*-Bu dimethylsilyl (TBDMS) protected phenol **31** which was prepared beforehand from phenol **27** through silylation reaction was added after lithiation. The resulting four-membered synthon **33** could be deprotected using tetra-*n*-butylammonium fluoride (TBAF) as fluorine source to furnish phenol **34** which could again be oxidized using PIDA to obtain an angled unit in building block **35** with more curvature.

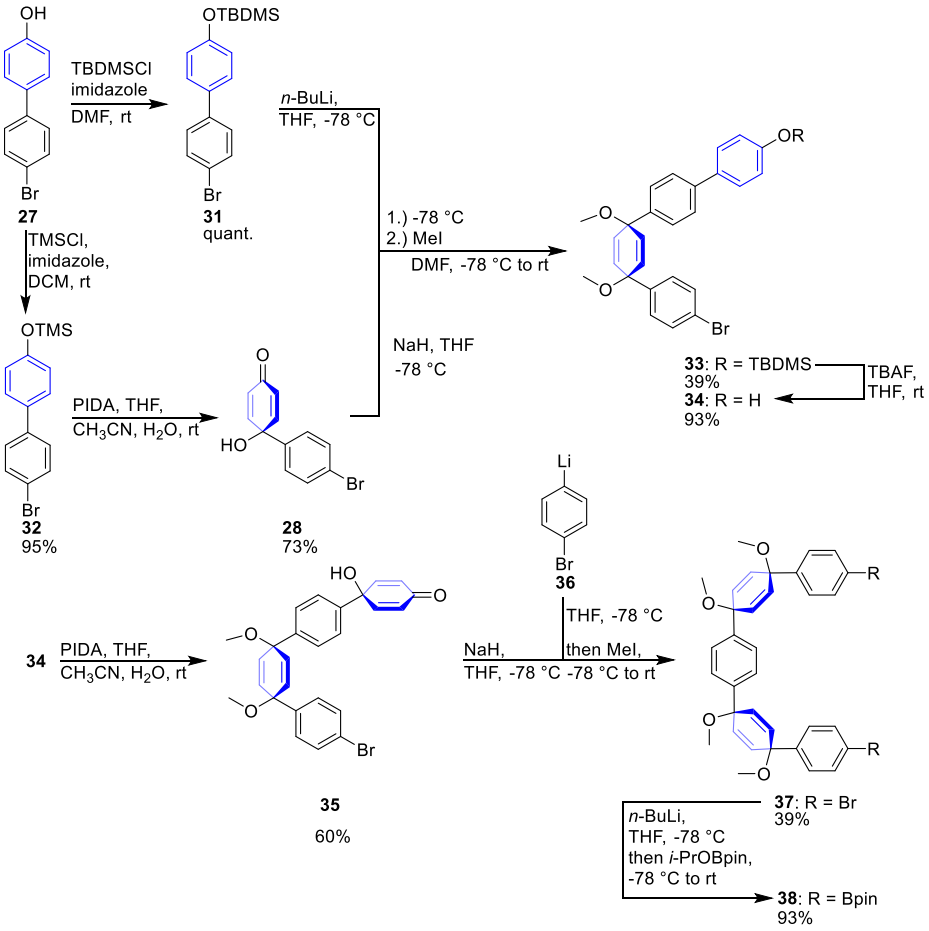

Scheme 6: Synthesis of key synthons **37** and **38** for the gram scale synthesis of [8] and [10]CPP.[34]

To obtain five-membered building block **37**, ketone **35** was subjected to a sequence of deprotonation with NaH, addition of lithium-bromobenzene (**36**) and quenching with MeI and *N*,*N*-dimethylformamide (DMF) to form the methoxy ethers in the final step. Lithium-halogen exchange using *n*-BuLi followed by addition of *i*-PrOBpin gave its size corresponding

boronic ester **38**. Thus, two five-membered building blocks with orthogonal reactivity for a Suzuki cross-coupling were obtained and were used to synthesize ten-membered macrocycle **39** using palladium(II) acetate [$Pd(OAc)_2$] as catalyst (Scheme 7). Exposing five-membered building block **37** to the same conditions, but with three-membered building block **12** from the original procedure by Bertozzi and Jasti[31] as cross-coupling partner, gave eight-membered macrocycle **41**. The final treatment with sodium naphthalenide (**22**) yielded [8]CPP from **41** and [10]CPP from **39**, each on a gram scale. The availability of bulk material is an important benefit of this strategy.

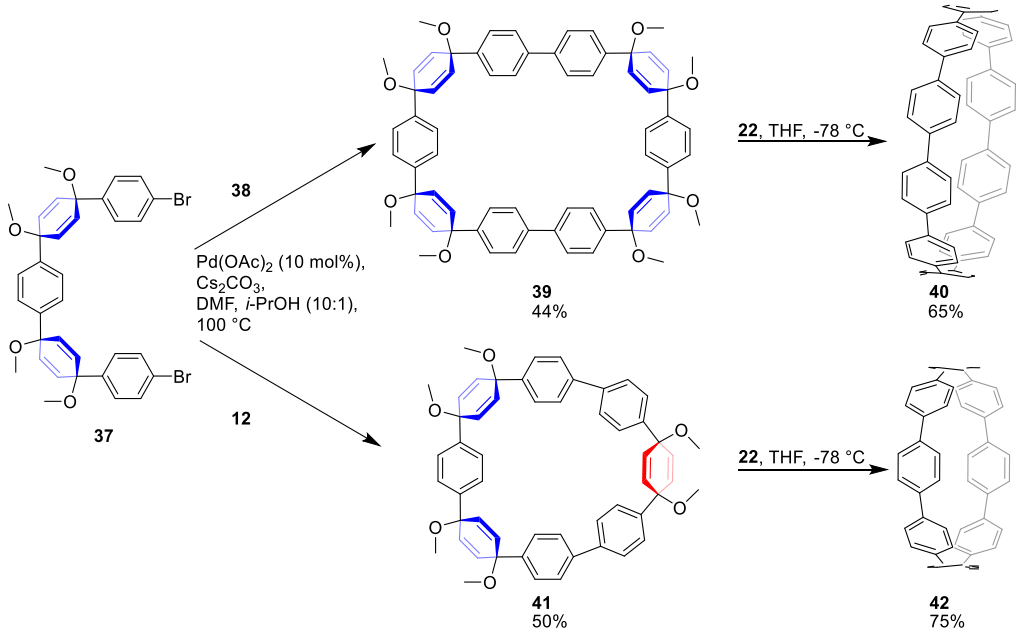

Scheme 7: Cross-coupling / reductive aromatization sequence for [8] and [10]CPP on a gram-scale.[34]

A similar cross-coupling / aromatization sequence was applied to obtain [6]CPP from five-membered dibromide **37** and 1,4-Bpin substituted phenyl **21** as one-membered building block.[35] Additionally, [5]CPP was synthesized from five-membered boronic ester **38** through oxidative coupling followed by a two-step aromatization procedure.[36]

Shortly after the first successful synthesis of a CPP was published by Bertozzi and Jasti, a second strategy was presented by the group of Itami. As in the earlier approach, three-membered building blocks played a crucial role in the strategy. Furthermore, a cross-coupling between a bis-iodide as well as a bis-boronic ester were central in the ring-formation, with the main difference of cyclohexane moieties instead of cyclohexadiene moieties as angled phenyl surrogates (Scheme 8),[37] following the general idea of approaches by Vögtle and coworkers even though they were not able to achieve the final

CPP.[38] Further size selectivity was achieved through a step-wise cross-coupling approach. These key intermediates were synthetically accessed from 1,4-diiodobenzene (**9**), which was, after lithiation, added to cyclohexane-1,4-dione (**43**) to obtain curved diiodide **44**. One fraction was converted to its corresponding methoxymethyl (MOM)-ether **45**; the other was converted to its size corresponding boronic ester **46** by applying a Miyaura borylation. Two equivalents of diiodide **44** were connected to one equivalent of boronic ester **46** forming the enlarged diiodide **47**, which was subjected to a ring-closing cross-coupling with another equivalent of boronic ester **46**.

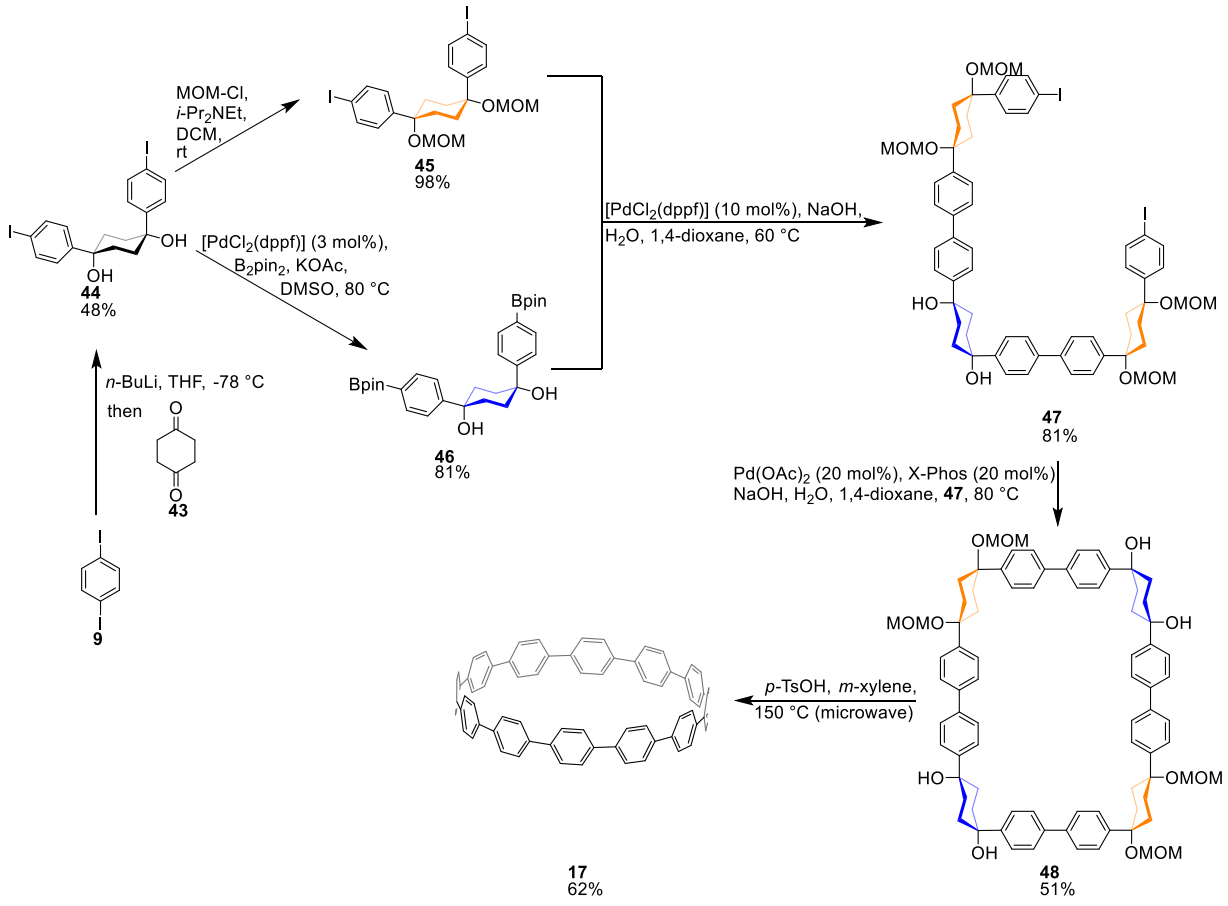

Scheme 8: Size selective synthesis of [12]CPP by Itami and coworkers.

Through the sequence of two consecutive cross-coupling reactions a twelve-membered ring could be selectively achieved which is the important benefit of this approach. With the cyclohexane moieties as sources of curvature, oxidation is necessary to furnish the CPP. This conversion is accomplished by treatment of **48** with *p*-toluenesulfonic acid (*p*-TsOH) as strong acid at 150 °C together with microwave irradiation. Similar to the cyclohexadiene approach, a modular strategy based on building blocks with three ring units was

developed,[39] and additionally concise syntheses giving faster access of CPPs by substitution of the cross coupling step through the nickel mediated Yamamoto-coupling.[40,41]

The third strategy towards CPPs, which is presented by Yamago and coworkers, is with regard to the number of steps, even more efficient and is the only approach which does not rely on phenyl surrogates as sources of curvature.[42] Here, a tetranuclear platinum complex is formed instead from bis-tin biphenyl **49** in a size-selective fashion followed by a change of the ligand on the metal from 1,5-cyclooctadiene (cod) to 1,1'-bis(diphenylphosphino)ferrocene (dppf). The final oxidative C-C coupling furnishing [8]CPP (Scheme 9) follows a strategy originally used by Bäuerle and coworkers towards thiophene macrocycles utilizing Pt-macrocycles as well as the extrusion by an external oxidant in the final step.[43] Advancement of this strategy include the formation of tetranuclear Pt-complexes through nickel mediated homo-coupling.[44] Additionally cyclohexadienes as phenyl surrogates were combined with Pt-macrocycles,[45] and the metal was changed to gold which gives triangular instead of square-shaped macrocycles and further extends the sizes of CPPs accessible with this strategy.[46]

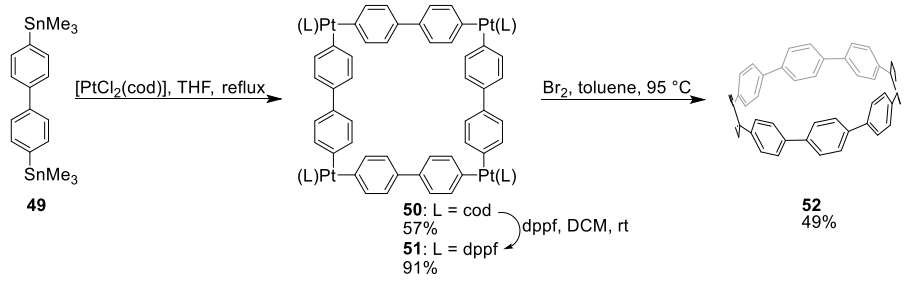

Scheme 9: Synthesis of [8]CPP using a tetranuclear platinum complex.[42]

With these three strategies, which are all centered around the formation of a strain-relieved macrocyclic precursors, CPPs with different ring sizes are accessible in modular, as well as concise strategies. Besides the size, substitution is another parameter to alter the properties of a CPP.

1.3 Substituted Cycloparaphenylenes

One possibility to synthesize substituted CPPs, probably the most intuitive one, is to use the CPP itself as starting material to introduce substituents via post-functionalization. It was demonstrated, that for [8]CPP and smaller derivatives, strain induced addition of bromine followed by treatment with a superbase gives brominated CPPs.[47] A second example of this

strategy allows the use of larger CPPs. This strategy is centered around η^6-complexes consisting of a CPP and a chromium atom.[48] This metal complex unveiled an increased acidity of the complexed phenyl ring (Scheme 10). Thus, this ring could efficiently be deprotonated by using *n*-BuLi as strong base. Afterwards, an electrophile (TMSCl, $ClCO_2Me$ or MeOBpin) was added to introduce the substituent, followed by quenching with water and exposure to air and ambient light which led to decomplexation.

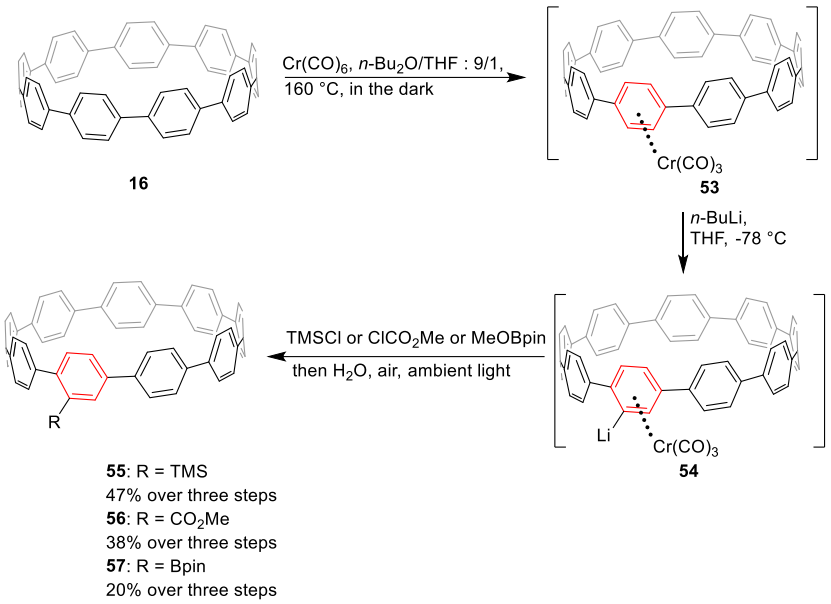

Scheme 10: Post-functionalization relying on increased acidity by metal complexation.[48]

These strategies can build on well-established syntheses as they start with the readily synthesized CPP. Additionally, pre-functionalized building blocks can be used throughout the bottom-up synthesis of the nanoring. Especially for π-extended analogues this approach was widely used,[49,50] and even yielded a polymeric structure of CPP subunits connected through biphenylenes, giving a tubular extension towards a nanotube-structure.[50] The same strategy of using substituted building blocks was also applied to furnish fluorinated CPPs in order to achieve nanotube-like solid-state structures,[51] or altered electronic properties compared to their unsubstituted analogue.[52] Also, a brominated building block was used as key compound for the design of CPP dimers with a phenyl group as a bridge.[53]

Between these two extrema, namely introducing the substituents after the CPP synthesis and carrying the substituents throughout the whole synthesis, lies the strategy of introducing substituents within the synthesis. In the year 2014, two different approaches were reported, which opened the research field of substituted CPPs. One strategy relied on a

combination of a literature known Wittig reaction, with Lewis-acid catalyzed Diels-Alder reaction for the formation of a pre-bent building block which is converted to the macrocyclic precursor by Yamamoto coupling (Scheme 11).[54] The following oxidative treatment delivered the substituted nanohoop. This strategy could, after slight modification, deliver nanohoops containing methyl esters and *N*-phenylphthalimido groups,[55] as well as naphthyl units.[56]

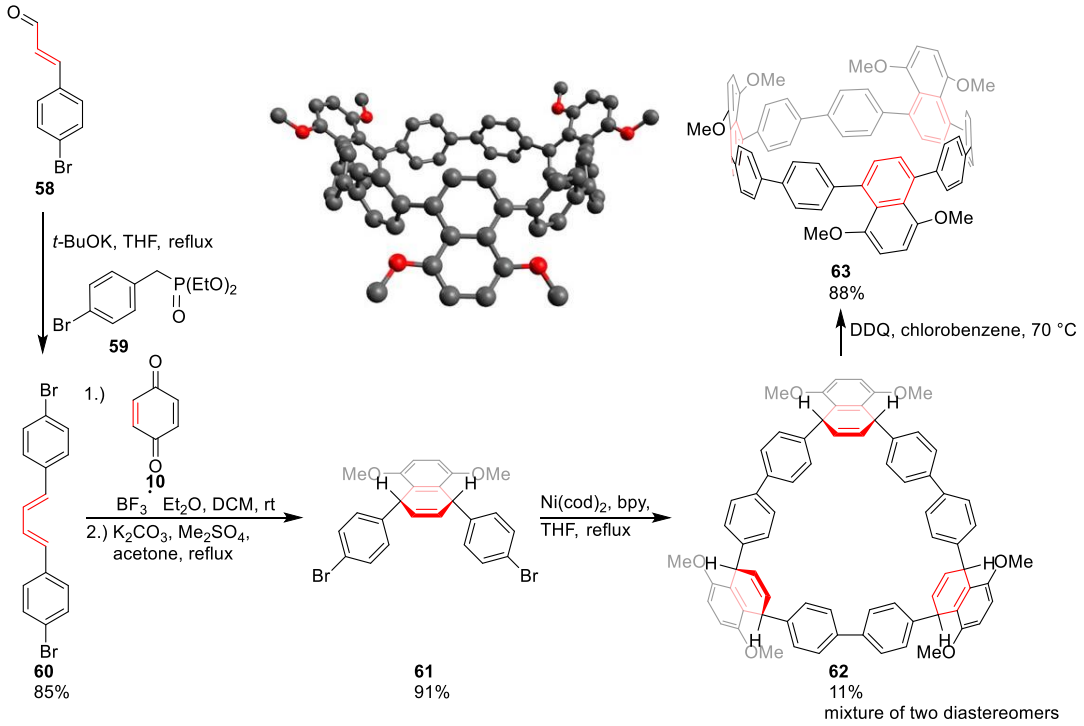

Scheme 11: Synthetic approach towards substituted CPPs by Wang and coworkers and solid-state structure of the target compound (top, center),[54] reprinted with permission from Ref. [54]. Copyright 2014 American Chemical Society

The fact, that substituents need to be introduced throughout the synthesis includes an additional challenge to the strategy but also opens the toolbox for a larger variety of synthetic techniques. One of these methods is the [2+2+2] cycloaddition (CA), in which three alkyne units are converted to one aromatic moiety. This was utilized in the second approach towards substituted CPPs from 2014, which was reported by the Wegner group.[57] This strategy focusses on the formation of alkyne-incorporated macrocycles, which are then exposed to different conditions for the key [2+2+2] CA delivering differently substituted [8]CPP analogues after oxidative aromatization. This strategy builds on the utilization of cyclohexane units as sources of curvature, commencing with diiodide **46**, a building block from the first synthesis of Itami,[37] using an optimized procedure, published one year later.[39] This building block was connected to the protected alkyne **69** via Sonogashira

coupling, furnishing alkyne **70** which undergoes a second Sonogashira coupling to build the size-defining macrocycle **71**. This macrocycle could then be used to introduce different substituents to the CPP precursor by Rh^{I} catalyzed [2+2+2] CA in yields between 46 and 68%. Oxidative treatment of this CPP precursor furnished four substituted CPPs with different substituents R^1 and R^2 (Scheme 12). Especially the fact, that R^2 is introduced rather late in the synthesis is a mayor benefit of this approach.

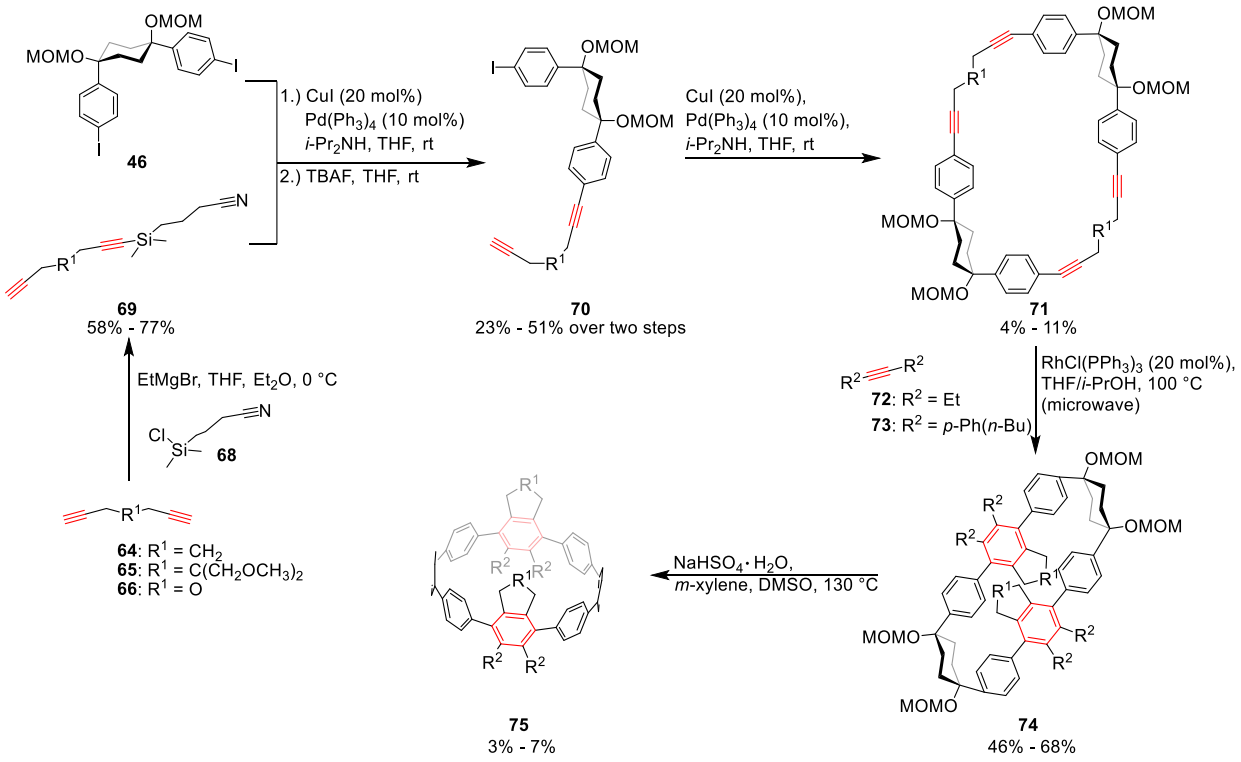

Scheme 12: Synthesis of substituted [8]CPPs by Wegner and coworkers.[57]

A later adapted approach towards substituted CPPs by Tanaka and coworkers employed a [2+2+2] CA not only to form the substituted rings, but also to form the macrocyclic precursor.[58] This strategy has the benefit of killing two birds with one stone, the challenging macrocyclization step in the synthesis as well as the crucial introduction of substituents into the molecular scaffold. The drawback on the other hand is a decreased flexibility when it comes to different sized CPPs. The synthesis utilized cyclohexadiene moieties as phenyl surrogate with sp^3-hybridized sources of curvature (Scheme 13). The starting building block for this was synthesized analogously to the first synthesis following the approach by Jasti and Bertozzi.[31] Also in this strategy, a [2+2+2] CA should introduce substituents to the CPP precursor. The necessary alkynes are, like in the approach by Wegner and coworkers, introduced by a Sonogashira-coupling. In this case, TMS-acetylene (**76**) is thus introduced

which gave, after deprotection, terminal alkyne **77** as central compound in this strategy. Contrary to the approach discussed before, the [2+2+2] CA has a second purpose, namely the efficient formation of a macrocycle. A threefold [2+2+2] CA constructed the twelve-membered macrocyclic CPP precursor **79**.

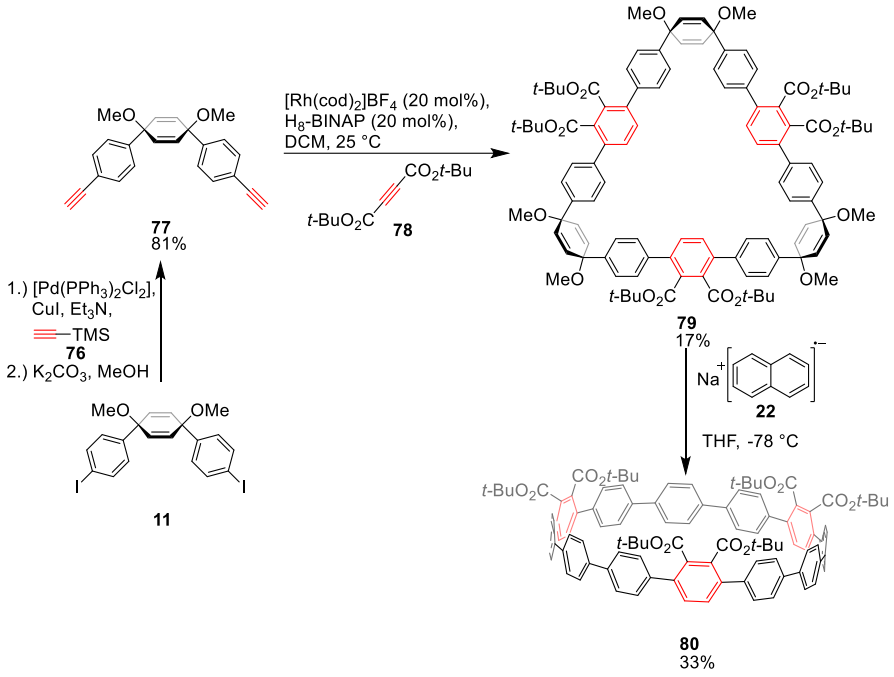

Scheme 13: Synthetic strategy towards *t*-Bu ester substituted [12]CPP by Tanaka and coworkers.[58]

Reductive aromatization gave [12]CPP analogue **80** decorated with six *t*-Bu esters as substituents (Scheme 13). Modification of this method enabled the opportunity to further increase the degree of substitution in the case of an [8]CPP derivative via step-wise cross-alkyne cyclotrimerization,[59] or to expand the boundaries towards smaller substituted CPPs in the case of a [6]CPP derivative (Scheme 14).[60] For this purpose, the general motif of the original procedure was applied with the difference of a protection group on one alkyne unit. Thus, a selective cross-cyclotrimerization of one alkyne is possible (Scheme 14, red marked alkyne).

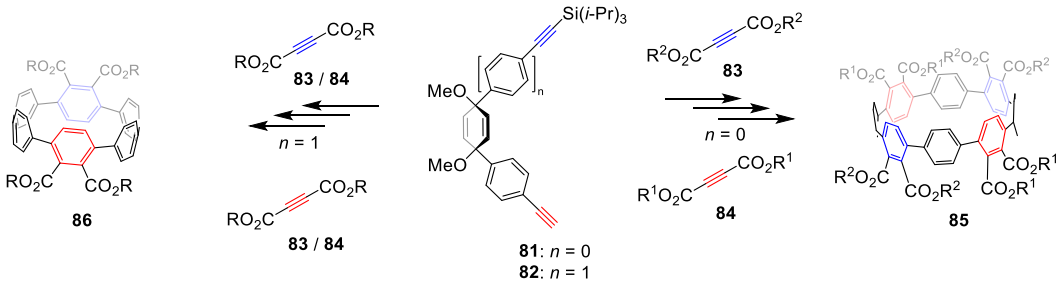

Scheme 14: Additional ring sizes and substitution pattern accessible via Tanaka's route.[59,60]

Deprotection followed by a second cross-cyclotrimerization (Scheme 14, blue marked alkyne) gave then the macrocycles. Further, alternating donor-acceptor nanohoops were built with this method by incorporating Wang's strategy of substituted CPPs into the [2+2+2] CA approach.[61] The *t*-Bu ester substituted CPP analogues revealed strongly altered solid-state structures compared to their unsubstituted parent molecules.[58–61] The observed tubular arrangements were attributed to additional non-covalent interactions compared to their unsubstituted analogues.

1.4 Supramolecular Chemistry of Cycloparaphenylenes

On the very basis of supramolecular chemistry, the interaction between two or more molecules is described, which is also at play in the self-assembly in single crystals. The synthesis of CPPs was long-awaited as they represent promising candidates as model substrates, and growth seeds for SWCNTs.[62] However, their crystal structure does not show the expected SWCNT-like tubular arrangement, but with the exception of [6]CPP,[35] rather a herringbone pattern, as exemplarily shown by the first crystal structure obtained for a CPP (Figure 6).[40] The cavity of CPPs can be used to bind solvents or small aromatic molecules.[63] This ability was exploited in a study in which pyridinium ions are brought into the cavity of the CPP, whose host ability was compared with an electron-enriched derivative.[64]

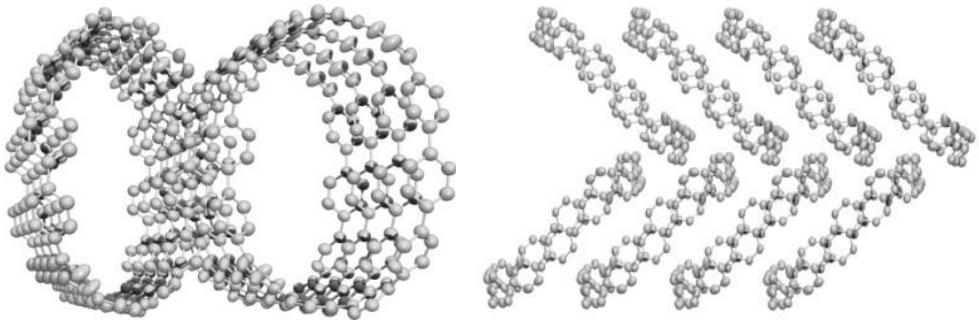

Figure 6: First report for a single-crystal structure of [12]CPP, aerial view (left) and side-view (right); solvent molecules and protons omitted for clarity,[40] reproduced with permission form Ref. [40]. Copyright 2011 John Wiley and Sons

These arrangements could be altered to the desired tubular one by structural modification of the nanoring. Thus, partly fluorinated CPPs can be used to obtain the desired tubular structures which were self-assembled to maximize C-H-F interactions.[51] Furthermore, the introduction of London dispersion donors into the structure by utilizing *t*-Bu esters had a similar effect but with different ring-to-ring distances.[58–61] Besides these solid-state

structures, also other ring-to-ring interactions were obtained. Bringing different sized CPPs with the correct size-difference together made the formation of Russian-doll type structures possible representing the shortest cutout of multiwalled nanotubes (Figure 7, left).[65] Furthermore, catenanes based on CPPs were found,[66] and also systematically synthesized using a template approach (Figure 7, right).[67]

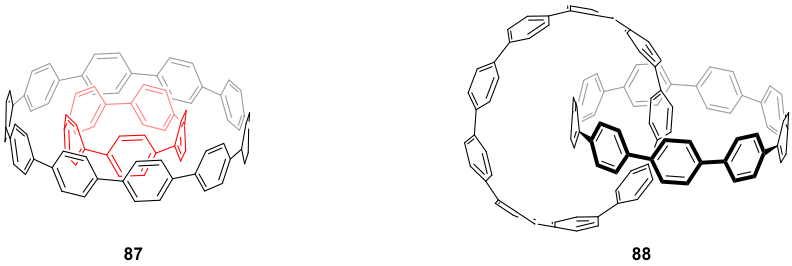

87 88

Figure 7: Supramolecular assemblies built solely from CPPs: CPP in CPP complex (left) and catenane (right).[65,67]

The radially distributed π-orbitals in CPPs grants them an electron enriched cavity, which has the ability to host fullerenes as guest molecules, which are strong electron-acceptors. The supramolecular chemistry between fullerenes and CPPs was initiated by the early study of Yamago and coworkers in which the size-selective complexation of [10]CPP by buckminsterfullerene (C_{60}) was investigated.[68] This assembly formed the foundation for future research on this molecular motif, which resembles a short segment of SWCNT-fullerene peapod structures (Figure 8).[69]

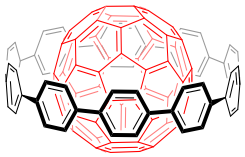

89

Figure 8: Supramolecular complex consisting of [10]CPP and C_{60} fullerene.[34,68]

This complex exhibits strong association, which is rationalized by its good fit in size. The different magnetic environment led to a shift in the ^{1}H NMR spectrum, which was the qualitative proof of a size selectivity as in an NMR sample of a mixture of different sized CPPs only the one of [10]CPP showed a shift upon addition of solid excess C_{60}. The extraordinary intense fluorescence of CPPs, more precisely the quenching of it was used in order to quantify the association,[68] as ^{1}H NMR is only a good quantitative tool for association constants smaller than ~10^5 M^{-1} (Figure 9).[70] The fact, that the fluorescence is, in a certain range, linearly dependent on the concentration was exploited. With a strong association of (2.79 +/-0.03) · 10^6 M^{-1}, the complex is stabilized by about 38 kJ/mol. This can be attributed

to the size and shape of the two molecular entities which is supported by DFT calculations on a M062X/6-31G(d) level, even though this method seemed to be inappropriate for the quantification of the binding energy.[68] This particular good fit is a result of the structural motif it resembles. The CPP⊂C_{60} scaffold mimics a peapod version of two graphene layers interacting with each other. With diameters of 0.70 nm for C_{60},[71] and ~1.39 nm for [10]CPP,[72] the inter-layer distance in this curved π-complex matches the distance of 340 pm known for graphene layers in graphite.[71]

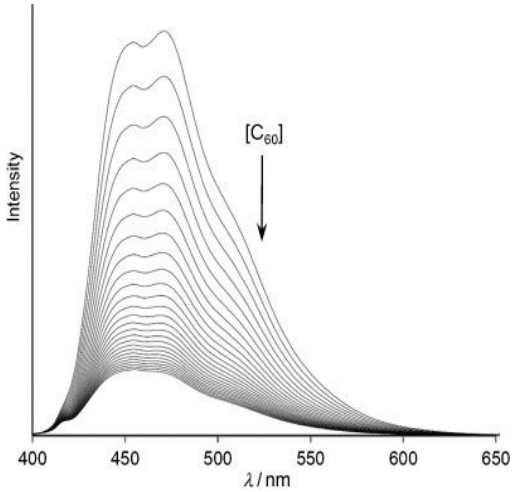

Figure 9: Fluorescence quenching of [10]CPP by the addition of C_{60},[68] reproduced with permission from Ref. [69]. Copyright 2011 John Wiley and Sons

This structural motif paved the way for further CPP-fullerene based supramolecular assemblies. One of these includes the next-larger fullerene derivative C_{70}. The ellipsoidal structure of this carbon allotrope makes the binding situation more complex. The geometry of C_{70} reveals two diameters. The larger one is suitable for [11]CPP while the shorter one fits into [10]CPP. These two different binding states were verified by ^{1}H NMR in which [10]CPP showed a downfield shift, while [11]CPP showed an upfield shift.[73] This goes hand in hand with different local aromaticities on the fullerene surface located at the six- and five-membered rings. These differences were investigated by nucleus independent chemical shift (NICS) analysis and induce different magnetic fields leading to an influence on the ^{1}H NMR spectrum.[74] In the same study, the influence of substitution on the fullerene was tested. Van't Hoff analysis of the complexation in 1,2-dichlorobenzene revealed that the binding to [10]CPP is only slightly exotherm, while the one to [11]CPP is in fact endotherm. Both complexes were strongly entropy driven for which the desolvation of the solvent from the fullerene and CPP was the driving force for the complexation event. To further verify the "standing" orientation of C_{70} in [11]CPP and the "lying" one in [10]CPP, C_{70} was

functionalized with a diethylmalonyl-group. Thus, the "standing" orientation in [11]CPP was sterically not possible and let to a reduction of the association, while the "lying" orientation in [10]CPP didn't incorporate the pole position anyways and the association was the same as with unsubstituted C_{70} which further supports the findings (Figure 10).

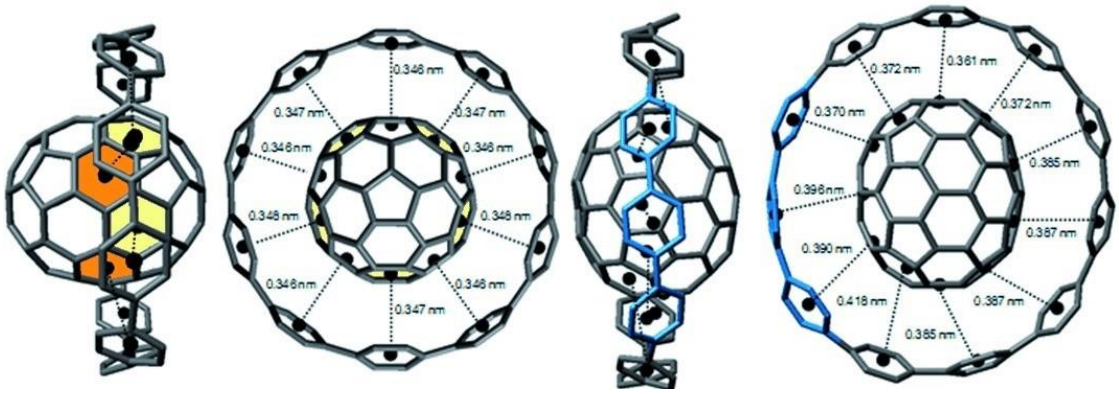

Figure 10: Side- and aerial view on computed structures for the supramolecular complexes of C_{70} with [10]CPP in the "lying" orientation (left) and in [11]CPP in the "standing" orientation (right) achieved on the M062X/6-31* level of theory,[73] reproduced with permission from Ref. [74]. Copyright 2013 John Wiley and Sons

Single crystal analysis of the substituted derivative of C_{70} with [10]CPP and the unsubstituted with [11]CPP further supported their findings. Additionally, the supramolecular activity of C_{70} was investigated with a large π-extended derivative of [12]CPP.[75] With its hexa-peri-hexabenzocoronene-units it forms a larger cutout of an armchair SWCNT. It was thus used as a model substrate to gain insight into the supramolecular chemistry of SWCNTs for which CPPs can be regarded as model substrates. The π-π interactions between CPPs and fullerenes were also exploited in order to improve the efficiency of a fullerene-based organic solar cell system.[76] On top, one special class of fullerenes, namely metallofullerenes were exploited in this regard. Thus, a supramolecular charge-transfer complexes consisting of $Li^+@C_{60}$ and [10]CPP,[77] and other sized CPPs,[78] as well as a complex possessing partial charge-transfer was found in $La@C_{82}$ and [11]CPP.[79] Furthermore, this binding motif could also be utilized in order to purify metallofullerenes as exemplarily shown on the example of $Gd@C_{82}$, which is extracted by the addition of [11]CPP from a raw soot, without the necessity of chromatography.[80] This is a prime example in which the fundamental understanding of interactions, as well as shape- and size complementarity were key for the implementation of fundamental knowledge in an application. Besides the structural modulation of the fullerene by size and encapsulated metal atoms, also dumbbell shaped fullerenes as well as heteroatom-substituted fullerenes were investigated for their

supramolecular properties. The Wegner group, together with the research groups of Ewels and Tagmatarchis investigated the association behavior of the dumbbell shaped bis(azafullerene) dimer **90** with [10]CPP (Figure 11).[81] Structurally, each buckyball represents an *N*-doped C_{60}, which are connected via one carbon atom next to the nitrogen. As this fullerene derivative possesses two binding sites, it fulfills the fundamental requirement to complex two nanohoop-shaped molecules, in this case [10]CPP. The main finding was an influence of the first complex on the association of the second.

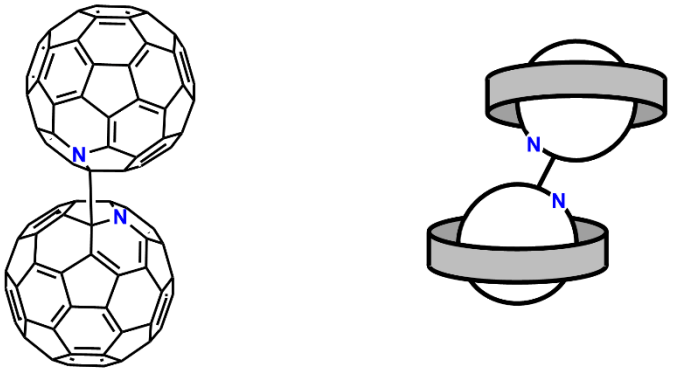

90 **91**

Figure 11: Left: molecular structure of bisazafullerene dumbbell; right: schematic representation of the supramolecular complexation of bisazafullerene dumbbell with [10]CPP.[81]

The first association event promoted the second one driven by a maximization of π-π, CH-π and London dispersion interactions. This 2:1 complex could be utilized to generate C_{59}N-radicals which are stabilized within the [10]CPP in solution,[82] as well as in the solid state.[83] Similarly C_{120}, a dimerization product of C_{60} in which the buckyballs are connected via a four-membered ring,[84] as well as sugar-bridged fullerene dumbbells were investigated in regard to their binding behavior to [10]CPP.[85] The excitation of a porphyrin unit, covalently connected to [10]CPP, led to a charge transfer to different fullerenes which were bound in the cavity of the CPP.[84] For the charge separated states lifetimes of up to 0.5 µs were found and showcase the potential of supramolecular complexes of CPPs for organic electronics. Furthermore, the binding motif between CPP and fullerene led to the formation of a [2]rotaxane while using one fullerene as a binding site and two others as stopper-units.[86] In this structure, the central fullerene moiety which binds the CPP needs to be connected on two sides to a linker unit. The connection was made through cyclopropanation on the fullerene by malonyl esters, which was developed by Bingel and coworkers in the 90s (Scheme 15).[87] Mechanistically, a stepwise cyclopropanation occurs in a regioselective

fashion on one of the [6,6] bonds which fuse two six membered rings and have a higher double bond character compared to the [5,6] bonds.

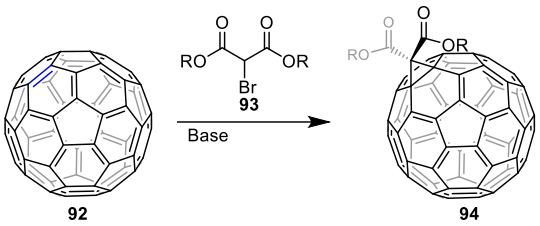

Scheme 15: Representation of the cyclopropanation of C_{60} under Bingel conditions.[87]

Later, Hirsch and coworkers shed light on the distribution of diastereomers achieved after a second cyclopropanation reaction (Figure 12, left).[88] Experimentally, seven different diastereomers were observed. The von Delius group used the complexation with [10]CPP in order to block reaction sites in the fullerene which led to a more selective double addition to the fullerene core supplying a reduced number of three diastereomers (Figure 12, middle).[86]

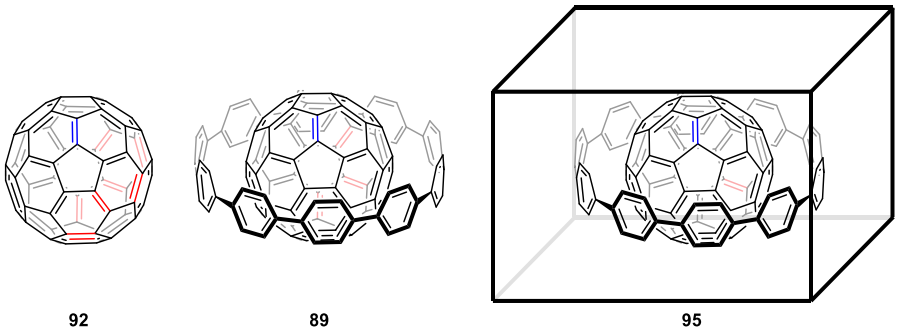

Figure 12: Reactive [6,6] double bonds in C_{60} (red marked) leading to different diastereomers after a first addition on the blue marked double bond (left for C_{60}, middle for $C_{60} \subset$ [10]CPP and right for $C_{60} \subset$ [10]CPP in a schematic represented supramolecular box).[86,88,89]

An even higher selectivity of a single diastereomer is achieved by a collaborative work with the group of Ribas in which the inclusion complex of C_{60} and [10]CPP is placed in a *supramolecular box* consisting of a porphyrin-Zn^{II}-containing, Pd^{II}-based tetragonal nanocapsule, which further blocks binding sites and provides a yield of 90%.[89]

In conclusion, great effort was spent on the design and exploitation of supramolecular assemblies centered around fullerenes and CPPs with a special focus on gaining fundamental understanding. In contrast to this, studies investigating interactions occurring between substituents on the fullerene and on the CPP form an open question. A new synthetic

strategy towards substituted CPPs and the implementation of the analogues in supramolecular studies were focus of this thesis to tackle this obstacle.

2 References

[1] J. M. Lehn, *Science* **1993**, *260*, 1762–1763.

[2] V. I. Minkin, *Pure Appl. Chem.* **1999**, *71*, 1919–1981.

[3] H. K. Bisoyi, Q. Li, *Chem. Rev.* **2022**, *122*, 4887–4926.

[4] S. Deechongkit, H. Nguyen, E. T. Powers, P. E. Dawson, M. Gruebele, J. W. Kelly, *Nature* **2004**, *430*, 101.

[5] Y. Liu, C. Zhang, D. Hao, Z. Zhang, L. Wu, M. Li, S. Feng, X. Xu, F. Liu, X. Chen, Z. Bo, *Chem. Mater.* **2018**, *30*, 4307–4312.

[6] X. Sun, L. Y. Ji, W. W. Chen, X. Guo, H. H. Wang, M. Lei, Q. Wang, Y. F. Li, *J. Mater. Chem. A* **2017**, *5*, 20720–20728.

[7] a) S. Iijima, T. Ichihashi, *Nature* **1993**, *363*, 603–605; b) D. S. Bethune, C. H. Klang, M. S. de Vries, G. Goman, R. Savoy, J. Vazquez, R. Beyers, *Nature* **1993**, *636*, 605–607.

[8] N. Nakashima, Y. Tomonari, H. Murakami, *Chem. Lett.* **2002**, *31*, 638–639.

[9] a) M. A. Strauss, H. A. Wegner, *Eur. J. Org. Chem.* **2019**, *2019*, 295–302; b) F. Biedermann, H.-J. Schneider, *Chem. Rev.* **2016**, *116*, 5216–5300; c) I. K. Mati, S. L. Cockroft, *Chem. Soc. Rev.* **2010**, *39*, 4195–4205.

[10] S. Paliwal, S. Geib, C. S. Wilcox, *J. Am. Chem. Soc.* **1994**, *116*, 4497–4498.

[11] F. Hof, D. M. Scofield, W. B. Schweizer, F. Diederich, *Angew. Chem. Int. Ed.* **2004**, *43*, 5056–5059.

[12] L. Yang, C. Adam, G. S. Nichol, S. L. Cockroft, *Nat. Chem.* **2013**, *5*, 1006.

[13] S. L. Cockroft, C. A. Hunter, *Chem. Commun.* **2006**, 3806–3808.

[14] U. Berg, I. Pettersson, *J. Org. Chem.* **1987**, *52*, 5177–5184.

[15] L. Rummel, M. H. J. Domanski, H. Hausmann, J. Becker, P. R. Schreiner, *Angew. Chem. Int. Ed.* **2022**, *61*, e202204393.

[16] a) J. Hwang, B. E. Dial, P. Li, M. E. Kozik, M. D. Smith, K. D. Shimizu, *Chem. Sci.* **2015**, *6*, 4358–4364; b) J. Hwang, P. Li, M. D. Smith, K. D. Shimizu, *Angew. Chem. Int. Ed.* **2016**, *55*, 8086–8089.

[17] M. H. Lyttle, A. Streitwieser Jr., R. Q. Kluttz, *J. Am. Chem. Soc.* **1981**, *103*, 3232–3233.

[18] C. Di Berardino, M. A. Strauss, D. Schatz, H. A. Wegner, *Chem. Eur. J.* **2022**, *28*, e202104284.

[19]L. Schweighauser, M. A. Strauss, S. Bellotto, H. A. Wegner, *Angew. Chem. Int. Ed.* **2015**, *54*, 13436–13439.

[20]M. A. Strauss, H. A. Wegner, *Angew. Chem. Int. Ed.* **2019**, *58*, 18552–18556.

[21]M. A. Strauss, H. A. Wegner, *ChemPhotoChem* **2019**, *3*, 392–395.

[22]M. A. Strauss, H. A. Wegner, *Angew. Chem. Int. Ed.* **2021**, *60*, 779–786.

[23]D. van Craen, W. H. Rath, M. Huth, L. Kemp, C. Räuber, J. M. Wollschläger, C. A. Schalley, A. Valkonen, K. Rissanen, M. Albrecht, *J. Am. Chem. Soc.* **2017**, *139*, 16959–16966.

[24]R. Pollice, M. Bot, I. J. Kobylianskii, I. Shenderovich, P. Chen, *J. Am. Chem. Soc.* **2017**, *139*, 13126–13140.

[25]Y. Segawa, H. Omachi, K. Itami, *Org. Lett.* **2010**, *12*, 2262-2265.

[26]M. Fujitsuka, D. W. Cho, T. Iwamoto, S. Yamago, T. Majima, *Phys. Chem. Chem. Phys.* **2012**, *14*, 14585–14588.

[27]Y. Segawa, A. Fukazawa, S. Matsuura, H. Omachi, S. Yamaguchi, S. Irle, K. Itami, *Org. Biomol. Chem.* **2012**, *10*, 5979-5984.

[28]D. Chen, Y. Wada, Y. Kusakabe, L. Sun, E. Kayahara, K. Suzuki, H. Tanaka, S. Yamago, H. Kaji, E. Zysman-Colman, *Org. Lett.* **2023**, *25*, 998–1002.

[29]E. Kayahara, L. Sun, H. Onishi, K. Suzuki, T. Fukushima, A. Sawada, H. Kaji, S. Yamago, *J. Am. Chem. Soc.* **2017**, *139*, 18480–18483.

[30]B. M. Wong, *J. Phys. Chem. C* **2009**, *113*, 21921–21927.

[31]R. Jasti, J. Bhattacharjee, J. B. Neaton, C. R. Bertozzi, *J. Am. Chem. Soc.* **2008**, *130*, 17646–17647.

[32]T. J. Sisto, M. R. Golder, E. S. Hirst, R. Jasti, *J. Am. Chem. Soc.* **2011**, *133*, 15800–15802.

[33]E. R. Darzi, T. J. Sisto, R. Jasti, *J. Org. Chem.* **2012**, *77*, 6624–6628.

[34]J. Xia, J. W. Bacon, R. Jasti, *Chem. Sci.* **2012**, *3*, 3018–3021.

[35]J. Xia, R. Jasti, *Angew. Chem. Int. Ed.* **2012**, *51*, 2474–2476.

[36]P. J. Evans, E. R. Darzi, R. Jasti, *Nat. Chem.* **2014**, *6*, 404–408.

[37]H. Takaba, H. Omachi, Y. Yamamoto, J. Bouffard, K. Itami, *Angew. Chem. Int. Ed.* **2009**, *48*, 6112-6116.

[38]R. Friederich, M. Nieger, F. Vögtle, *Chem. Ber.* **1993**, *126*, 1723–1732.

[39]H. Omachi, S. Matsuura, Y. Segawa, K. Itami, *Angew. Chem. Int. Ed.* **2010**, *49*, 10202–10205.

[40]Y. Segawa, S. Miyamoto, H. Omachi, S. Matsuura, P. Šenel, T. Sasamori, N. Tokitoh, K. Itami, *Angew. Chem. Int. Ed.* **2011**, *50*, 3244–3248.

[41]Y. Segawa, P. Šenel, S. Matsuura, H. Omachi, K. Itami, *Chem. Lett.* **2011**, *40*, 423–425.

[42]S. Yamago, Y. Watanabe, T. Iwamoto, *Angew. Chem. Int. Ed.* **2010**, *122*, 769–771.

[43]G. Fuhrmann, T. Debaerdemaeker, P. Bäuerle, *Chem. Commun.* **2003**, *8*, 948–949.

[44]E. Kayahara, T. Iwamoto, T. Suzuki, S. Yamago, *Chem. Lett.* **2013**, *42*, 621–623.

[45]E. Kayahara, V. Patel, J. Xia, R. Jasti, S. Yamago, *Synlett* **2015**, *26*, 1615–1619.

[46]Y. Yoshigoe, Y. Tanji, Y. Hata, K. Osakada, S. Saito, E. Kayahara, S. Yamago, Y. Tsuchido, H. Kawai, *JACS Au* **2022**, *2*, 1857–1868.

[47]a) E. Kayahara, R. Qu, S. Yamago, *Angew. Chem. Int. Ed.* **2017**, *56*, 10428-10432; b) E. Kayahara, R. Qu, S. Yamago, *Angew. Chem.* **2017**, *129*, 10564–10568.

[48]N. Kubota, Y. Segawa, K. Itami, *J. Am. Chem. Soc.* **2015**, *137*, 1356–1361.

[49]a) P. Della Sala, A. Capobianco, T. Caruso, C. Talotta, M. de Rosa, P. Neri, A. Peluso, C. Gaeta, *J. Org. Chem.* **2018**, *83*, 220-227; b) F. E. Golling, S. Osella, M. Quernheim, M. Wagner, D. Beljonne, K. Müllen, *Chem. Sci.* **2015**, *6*, 7072–7078; c) D. Lu, H. Wu, Y. Dai, H. Shi, X. Shao, S. Yang, J. Yang, P. Du, *Chem. Commun.* **2016**, *52*, 7164–7167; d) T. Nishiuchi, X. Feng, V. Enkelmann, M. Wagner, K. Müllen, *Chem. Eur. J.* **2012**, *18*, 16621–16625; e) M. Quernheim, F. E. Golling, W. Zhang, M. Wagner, H.-J. Räder, T. Nishiuchi, K. Müllen, *Angew. Chem. Int. Ed.* **2015**, *54*, 10341–10346; f) T. J. Sisto, X. Tian, R. Jasti, *J. Org. Chem.* **2012**, *77*, 5857–5860; g) A. Yagi, Y. Segawa, K. Itami, *J. Am. Chem. Soc.* **2012**, *134*, 2962–2965.

[50]Q. Huang, G. Zhuang, M. Zhang, J. Wang, S. Wang, Y. Wu, S. Yang, P. Du, *J. Am. Chem. Soc.* **2019**, *141*, 18938–18943.

[51]J. M. van Raden, E. J. Leonhardt, L. N. Zakharov, A. Pérez-Guardiola, A. J. Pérez-Jiménez, C. R. Marshall, C. K. Brozek, J. C. Sancho-García, R. Jasti, *J. Org. Chem.* **2020**, *85*, 129–141.

[52]S. Hashimoto, E. Kayahara, Y. Mizuhata, N. Tokitoh, K. Takeuchi, F. Ozawa, S. Yamago, *Org. Lett.* **2018**, *20*, 5973-5976.

[53]J. Xia, M. R. Golder, M. E. Foster, B. M. Wong, R. Jasti, *J. Am. Chem. Soc.* **2012**, *134*, 19709–19715.

[54]C. Huang, Y. Huang, N. G. Akhmedov, B. V. Popp, J. L. Petersen, K. K. Wang, *Org. Lett.* **2014**, *16*, 2672–2675.

[55]S. Li, C. Huang, H. Thakellapalli, B. Farajidizaji, B. V. Popp, J. L. Petersen, K. K. Wang, *Org. Lett.* **2016**, *18*, 2268–2271.

[56]S. Li, M. Aljhdli, H. Thakellapalli, B. Farajidizaji, Y. Zhang, N. G. Akhmedov, C. Milsmann, B. V. Popp, K. K. Wang, *Org. Lett.* **2017**, *19*, 4078–4081.

[57]A.-F. Tran-Van, E. Huxol, J. M. Basler, M. Neuburger, J.-J. Adjizian, C. P. Ewels, H. A. Wegner, *Org. Lett.* **2014**, *16*, 1594–1597.

[58]Y. Miyauchi, K. Johmoto, N. Yasuda, H. Uekusa, S. Fujii, M. Kiguchi, H. Ito, K. Itami, K. Tanaka, *Chem. Eur. J.* **2015**, *21*, 18900–18904.

[59]N. Hayase, Y. Miyauchi, Y. Aida, H. Sugiyama, H. Uekusa, Y. Shibata, K. Tanaka, *Org. Lett.* **2017**, *19*, 2993–2996.

[60]N. Hayase, H. Sugiyama, H. Uekusa, Y. Shibata, K. Tanaka, *Org. Lett.* **2019**, *21*, 3895–3899.

[61]S. Nishigaki, M. Fukui, H. Sugiyama, H. Uekusa, S. Kawauchi, Y. Shibata, K. Tanaka, *Chem. Eur. J.* **2017**, *23*, 7227–7231.

[62]a) H. Omachi, T. Nakayama, E. Takahashi, Y. Segawa, K. Itami, *Nat. Chem.* **2013**, *5*, 572–576; b) R. Jasti, C. R. Bertozzi, *Chem. Phys. Lett.* **2010**, *494*, 1–7.

[63]H. Kwon, C. J. Bruns, *Nano Res.* **2022**, *15*, 5545–5555.

[64]P. Della Sala, C. Talotta, T. Caruso, M. de Rosa, A. Soriente, P. Neri, C. Gaeta, *J. Org. Chem.* **2017**, *82*, 9885–9889.

[65]S. Hashimoto, T. Iwamoto, D. Kurachi, E. Kayahara, S. Yamago, *ChemPlusChem* **2017**, *82*, 1015–1020.

[66]W. Zhang, A. Abdulkarim, F. E. Golling, H. J. Räder, K. Müllen, *Angew. Chem. Int. Ed.* **2017**, *56*, 2645–2648.

[67]Y. Segawa, M. Kuwayama, K. Itami, *Org. Lett.* **2020**, *22*, 1067–1070.

[68]T. Iwamoto, Y. Watanabe, T. Sadahiro, T. Haino, S. Yamago, *Angew. Chem. Int. Ed.* **2011**, *50*, 8342–8344.

[69]B. W. Smith, M. Monthioux, D. E. Luzzi, *Nature* **1998**, *396*, 323–324.

[70]P. Thordarson, *Chem. Soc. Rev.* **2011**, *40*, 1305–1323.

[71]E. Riedel, *Anorganische Chemie*, De Gruyter, Berlin, **2011**.

[72]a) T. Iwamoto, Y. Watanabe, Y. Sakamoto, T. Suzuki, S. Yamago, *J. Am. Chem. Soc.* **2011**, *133*, 8354–8361; b) E. Kayahara, Y. Sakamoto, T. Suzuki, S. Yamago, *Org. Lett.* **2012**, *14*, 3284–3287.

[73]T. Iwamoto, Y. Watanabe, H. Takaya, T. Haino, N. Yasuda, S. Yamago, *Chem. Eur. J.* **2013**, *19*, 14061–14068.

[74]E. Kleinpeter, S. Klod, A. Koch, *J. Org. Chem.* **2008**, *73*, 1498–1507.

[75]a) D. Lu, G. Zhuang, H. Wu, S. Wang, S. Yang, P. Du, *Angew. Chem. Int. Ed.* **2017**, *56*, 158–162; b) D. Lu, G. Zhuang, H. Wu, S. Wang, S. Yang, P. Du, *Angew. Chem.* **2017**, *129*, 164–168.

[76]Y. Tang, J. Li, P. Du, H. Zhang, C. Zheng, H. Lin, X. Du, S. Tao, *Org. Electron.* **2020**, *83*, 105747.

[77]H. Ueno, T. Nishihara, Y. Segawa, K. Itami, *Angew. Chem. Int. Ed.* **2015**, *54*, 3707–3711.

[78]M. Freiberger, I. Solymosi, E. M. Freiberger, A. Hirsch, M. E. Pérez-Ojeda, T. Drewello, *Nanoscale* **2023**, *15*, 5665–5670.

[79]T. Iwamoto, Z. Slanina, N. Mizorogi, J. Guo, T. Akasaka, S. Nagase, H. Takaya, N. Yasuda, T. Kato, S. Yamago, *Chem. Eur. J.* **2014**, *20*, 14403–14409.

[80]Y. Nakanishi, H. Omachi, S. Matsuura, Y. Miyata, R. Kitaura, Y. Segawa, K. Itami, H. Shinohara, *Angew. Chem. Int. Ed.* **2014**, *53*, 3102–3106.

[81]J. Rio, S. Beeck, G. Rotas, S. Ahles, D. Jacquemin, N. Tagmatarchis, C. Ewels, H. A. Wegner, *Angew. Chem. Int. Ed.* **2018**, *57*, 6930–6934.

[82]a) A. Stergiou, J. Rio, J. H. Griwatz, D. Arčon, H. A. Wegner, C. P. Ewels, N. Tagmatarchis, *Angew. Chem. Int. Ed.* **2019**, *58*, 17745–17750; b) A. Stergiou, J. Rio, J. H. Griwatz, D. Arčon, H. A. Wegner, C. P. Ewels, N. Tagmatarchis, *Angew. Chem.* **2019**, *131*, 17909–17914.

[83]Y. Tanuma, A. Stergiou, A. Bužan Bobnar, M. Gaboardi, J. Rio, J. Volkmann, H. A. Wegner, N. Tagmatarchis, C. P. Ewels, D. Arčon, *Nanoscale* **2021**, *13*, 19946–19955.

[84]Y. Xu, B. Wang, R. Kaur, M. B. Minameyer, M. Bothe, T. Drewello, D. M. Guldi, M. von Delius, *Angew. Chem. Int. Ed.* **2018**, *57*, 11549–11553.

[85]J. Jakšić, I. Solymosi, A. Hirsch, M. E. Pérez-Ojeda, A. Mitrović, V. Maslak, *Chem. Eur. J.* **2023**, e202301061.

[86]Y. Xu, R. Kaur, B. Wang, M. B. Minameyer, S. Gsänger, B. Meyer, T. Drewello, D. M. Guldi, M. von Delius, *J. Am. Chem. Soc.* **2018**, *140*, 13413–13420.

[87]C. Bingel, *Chem. Ber.* **1993**, *126*, 1957–1959.

[88]A. Hirsch, I. Lamparth, H. R. Karfunkel, *Angew. Chem. Int. Ed.* **1994**, *33*, 437–438.

[89]E. Ubasart, O. Borodin, C. Fuertes-Espinosa, Y. Xu, C. García-Simón, L. Gómez, J. Juanhuix, F. Gándara, I. Imaz, D. Maspoch, M. von Delius, X. Ribas, *Nat. Chem.* **2021**, *13*, 420–427.

3 Abbreviations

Short form	Long form
CA	Cycloaddition
cod	Cyclooctadiene
CPP	Cycloparaphenylene
DCM	Dichloromethane
DMF	*N*,*N*-dimethylformamide
DMSO	Dimethylsulfoxide
dppf	1,1'-Bis(diphenylphosphino)ferrocene
Et	Ethyl
H_8-BINAP	Bis-(diphenylphospino)-5,5’,6,6’,7,7’,8,8’-octahydro-1,1’-binaphthyl,
	[5,5’,6,6’,7,7’,8,8’-octahydro-[1,1’-binaphthalin]-2,2’-diyl]-bis-[diphenylphosphin]
HOMO	Highest occupied molecular orbital
i-Pr	*Iso*-propyl
LUMO	Lowest unoccupied molecular orbital
Me	Methyl
MOM	Methoxymethyl
n-BuLi	*n*-butyllithium
NICS	Nucleus independent chemical shift
$Pd(OAc)_2$	Palladium(II)acetate
$Pd_2(dba)_3$	Tris(dibenzylideneacetone)dipalladium(0)
PIDA	Phenyliodine(III) diacetate
pin	2,3-Dimethylbutane-2,3-diolate
rt	Room temperature
S-PHOS	Dicyclohexyl(2’,6’-dimethoxy[1,1’-biphenyl]-2-yl)phosphane
SWCNT	Single-walled carbon nanotube
t-Bu	*Tert*-butyl
THF	Tetrahydrofuran
TMS	Trimethylsilyl
UV	Ultraviolet
Vis	Visible
X-Phos	Dicyclohexyl[2’,4’,6’-tris(propan-2-yl)[1,1’-biphenyl]-2-yl]phosphane

4 Contributions to literature

4.1 A Modular Synthesis of Substituted Cycloparaphenylenes

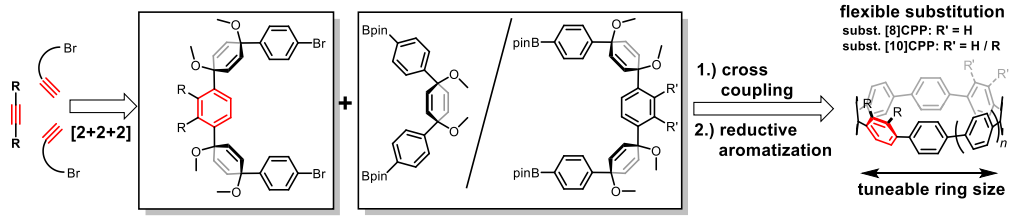

Herein, we report a modular synthesis providing access to substituted cycloparaphenylenes (CPPs) of different sizes. A key synthon introducing two geminal ester units was efficiently prepared by [2+2+2] cycloaddition. This building block can be conveniently converted to macrocyclic precursors controlling the ring size of the final CPP. Efficient reductive aromatization through single-electron transfer provided the substituted nanohoops in a straightforward manner. The *t*-Bu ester substitution pattern enables a tube-like arrangement in the solid-state governed by van der Waals interactions that exhibits one of the tightest packings of CPPs in tube direction, thus opening new avenues in the crystal design of CPPs.

Reprinted with permission from

D. Kohrs, J. Becker, H. A. Wegner, *Chem. Eur. J.* **2022**, *28*, e202104239.

DOI: 10.1002/chem.202104239

Check for updates

Chemistry–A European Journal

Research Article
doi.org/10.1002/chem.202104239

Chemistry Europe
European Chemical Societies Publishing

www.chemeurj.org

A Modular Synthesis of Substituted Cycloparaphenylenes

Daniel Kohrs,[a, c] Jonathan Becker,[b] and Hermann A. Wegner*[a, c]

Abstract: Herein, we report a modular synthesis providing access to substituted cycloparaphenylenes (CPPs) of different sizes. A key synthon introducing two geminal ester units was efficiently prepared by [2+2+2] cycloaddition. This building block can be conveniently converted to macrocyclic precursors controlling the ring size of the final CPP. Efficient reductive aromatization through single-electron transfer provided the substituted nanohoops in a straightforward manner. The *t*Bu ester substitution pattern enables a tube-like arrangement in the solid-state governed by van der Waals interactions that exhibits one of the tightest packings of CPPs in tube direction, thus opening new avenues in the crystal design of CPPs.

Introduction

With their cyclic arrangement of *para*-connected phenyl subunits, CPPs represent the smallest repeatable section of armchair carbon nanotubes. The first synthesis reported by Jasti and Bertozzi opened a new research area around this carbon allotrope.[1] Analogous to ground-breaking studies by Vögtle,[2] the synthesis of an angulated macrocyclic precursor is key to success in tackling the strained nature of the cyclic arrangement of planar phenyl subunits. A variety of ring sizes was realized based on this strategy to build a library of CPPs.[3,4] Thereby, the CPPs can be accessed in a combinatorial fashion from a small number of crucial key compounds by cross-coupling followed by aromatization, thus enabling the preparation of different CPPs. For example, [5]-,[5] [6]-,[6] [8]- and [10]CPP[7] were synthesised from the same five-membered building block. Besides these efforts on the parent CPPs, substituted derivatives were targeted early on, permitting a greater structural diversity, which is of special interest in view of materials applications. Examples include substituted CPPs mimicking larger CNTs cutouts,[8] indeno-fluorene substituted CPPs prepared by intramolecular Friedel-Crafts reactions,[9] or polyfluorinated CPPs reported by the groups of Yamago ([6]- and [9]CPP) and Jasti ([10]CPP).[10] Chiral nanohoops were reported either by an asymmetric synthesis of an helical CPP,[11] or chiral resolution of an racemic precursor,[12] giving an enantiopure CPP derivative. Tetraalkoxy-substituted [10]CPP analogues were synthesized by the group of Yamago by employing the corresponding substituted benzoquinone as a building block.[13] A porphyrin substituted CPP was presented by an analogues approach, introducing a TMS group at an early stage and converting it after CPP formation into an iodo-substituted CPP to which the porphyrin unit was connected by Sonogashira coupling.[14] Our group relied on the [2+2+2] cycloaddition as an efficient method for the introduction of substituents.[15] Strain-reduced macrocycles were accessed by Sonogashira coupling, which incorporated alkynes for a subsequent [2+2+2] cycloaddition, conceding structural alteration on a rather late state. The strategy of [2+2+2] cycloaddition was also adapted by the group of Tanaka for the introduction of *t*Bu esters.[16] Here, in the [2+2+2] cycloaddition not only the substituents are introduced, but also the square-shaped macrocyclic ring is formed. Interestingly, this substituted CPP arranged in a tube-like fashion in the solid-state in contrast to the basket-weaver structure usually found for unsubstituted CPPs. This feature was also observed for [6]- and [8]CPP derivatives decorated with *t*Bu esters.[17] Besides *t*Bu ester substituted CPPs, a carbon nanocage[18] as well as a Möbius-belt shaped [10]CPP[19] derivative were prepared using this method. Employing the [2+2+2] cycloaddition as the macrocyclization step reduces the overall reaction steps but also has a drawback: To access a different sized substituted CPP derivative, a complete new synthetic route needs to be designed.

In this study, we combined the [2+2+2] cycloaddition for an efficient introduction of *t*Bu esters with the modularity of cross-coupling chemistry to provide a modular access to different sized substituted CPPs (Scheme 1).

Results and Discussion

Our synthetic strategy is centred around the building block **10** containing five ring units, half of a [10]CPP (Scheme 2). Suzuki

[a] *D. Kohrs, Prof. Dr. H. A. Wegner*
Institute of Organic Chemistry, Justus Liebig University
Heinrich-Buff-Ring 17, 35392 Giessen (Germany)
E-mail: Hermann.A.Wegner@org.chemie.uni-giessen.de

[b] *Dr. J. Becker*
Institute of Inorganic Chemistry, Justus Liebig University
Heinrich-Buff-Ring 17, 35392 Giessen (Germany)

[c] *D. Kohrs, Prof. Dr. H. A. Wegner*
Center for Materials Research (ZfM/LaMa)
Justus Liebig University Giessen
Heinrich-Buff-Ring 16, 35392 Giessen (Germany)

Supporting information for this article is available on the WWW under https://doi.org/10.1002/chem.202104239

Chemistry–A European Journal
Research Article
doi.org/10.1002/chem.202104239
Chemistry Europe
European Chemical Societies Publishing

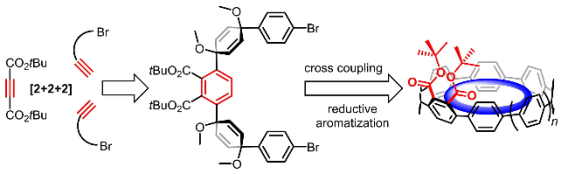

Scheme 1. Synthetic strategy for CPPs decorated with *t*Bu ester.

cross-coupling reaction of such an intermediate as **10** with itself after conversion to the boronic ester or with an unsubstituted intermediate **12** will provide access to two different macrocyclic [10]CPP derivative precursors.[7] The possibility to combine **10** with other building blocks offers a highly modular approach to various substituted CPPs. To showcase the flexibility of our approach an [8]CPP derivative was also targeted.

The synthesis commences with the addition of lithium (trimethylsilyl)acetylide (**3**) and (4-bromophenyl)lithium (**6**) to benzoquinone (**1**) in two sequential steps providing **7** in 59% (Scheme 2). This intermediate was recently reported by the group of Tanaka in their synthesis of a nanocage by a strategy relying on a [2+2+2] cycloaddition.[18] Deviating from their strategy we performed the synthesis by two sequential nucleophilic additions, which improved the overall yield by more than 10% and facilitated the separation. The following cleavage of the silyl protection group and the formation of the methoxy-ethers provided the [2+2+2] cycloaddition precursor **8** in 77%. Building block **8** features the cyclohexadiene unit as angulated phenyl surrogate as well as the alkyne functionality for the subsequent [2+2+2] cycloaddition. For this key step, a catalytic system consisting of a Rh^{I}/(*S*)-H_8-BINAP complex, developed by the group of Tanaka for such [2+2+2] cycloadditions, was applied.[20] The catalyst loading could be reduced to 3% with respect to alkyne **8** providing the product in 72% on a gram scale. The boronic esters **12** and **13**, necessary for the cross-coupling reaction, were prepared according to a literature protocol.[7] The combination of the two entities **10** and **12** in the cross-coupling macrocyclization was realized in 17% yield with Pd^{II}/SPHOS as the catalytic system.[7] In this reaction the formation of a five-membered macrocycle could be detected as a side product originating from an intramolecular homo-coupling of the bis-boronic ester.[5] Finally, the desired di-substituted [10]CPP **18**, which forms a tubular packing in the solid state (Figure 1), could be obtained in 42% isolated yield by aromatization with sodium naphthalide. This flexible approach also provides access to the tetra-substituted CPP **17**, where the two bis-(*t*Bu)-functionalized phenyl rings are positioned vis-à-vis within the nanohoop (Scheme 3). For this purpose, substituted boronic ester **11** was synthesized from key compound **10** by lithium-halogen exchange and quenching with *i*PrOBpin. The same cross-coupling/aromatization sequence gave the desired CPP **17**. As in the previous case, a five-membered macrocycle was observed as side product in the Suzuki cross-coupling macrocyclization. Finally, the reductive aromatization, with sodium naphthalide led to the tetra-substituted CPP **17** in 35% isolated yield.

As a third derivative, [8]CPP derivative **19** was targeted to also showcase the flexibility in ring-size of this approach (Scheme 3). The cross-coupling reaction of **10** and **13** provided the macrocyclic precursor **16** in higher yields compared to the ten-membered derivatives **14** and **15**. This can be rationalized by the absence of a possible intramolecular homo-coupling of the boronic ester. The aromatization delivered the final product in 58% isolated yield. The decreased number of cyclohexadiene moieties, which have to be converted to phenyl rings, combined with the larger scale on which the reaction was performed might be the main reasons for the increased yield.

For the cross-coupling reactions of **10** with **11**–**13**, a C-shape arrangement, as shown in Scheme 3, is necessary. This conformation, however, could be disfavoured by repulsive interactions between the *t*Bu groups from the ester functionalities and methoxy ethers on the sp^3-hybridized positions in the neighboured cyclohexadiene moieties. Single crystals suitable for X-ray analysis of key compound **10** were obtained, which support the desired conformation of this key building block (Figure 2).

Also, the solid-state structure of CPP **18** was obtained by X-ray analysis. Interestingly, it exhibits stacking of the molecules in the [100] direction, forming infinite tubes with slightly shifted entities relative to each other. The rings are tilted towards the

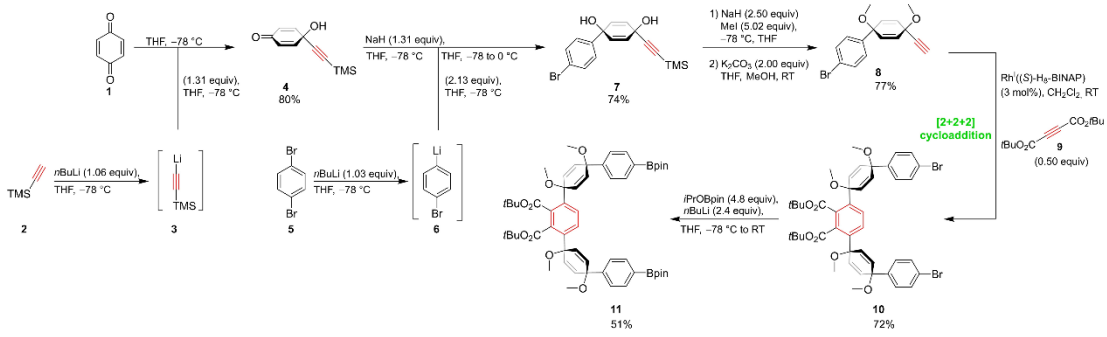

Scheme 2. Synthesis of key building block **10** and its corresponding boronic ester.

Chemistry–A European Journal
Research Article
doi.org/10.1002/chem.202104239
Chemistry Europe
European Chemical Societies Publishing

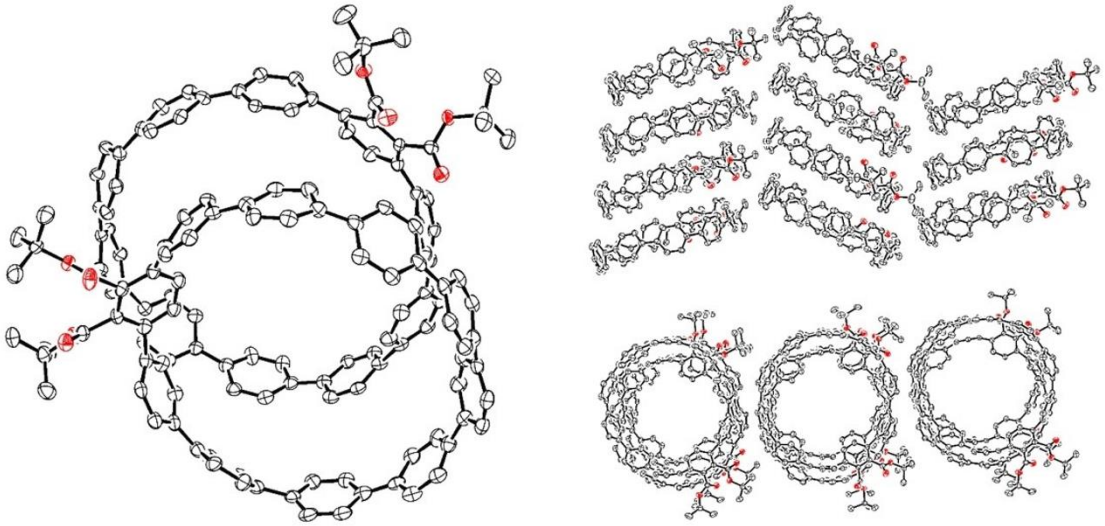

Figure 1. Left: ORTEP plot of the asymmetric unit of the crystal structure of substituted CPP **18**. Solvent molecules and hydrogen atoms are omitted for clarity, thermal ellipsoid are shown at 50% probability. Top right: Columnar packing of bis-substituted CPP **18**; view along the *c*-axis. Bottom: columnar packing of di-substituted CPP **18**; view along the *a*-axis.

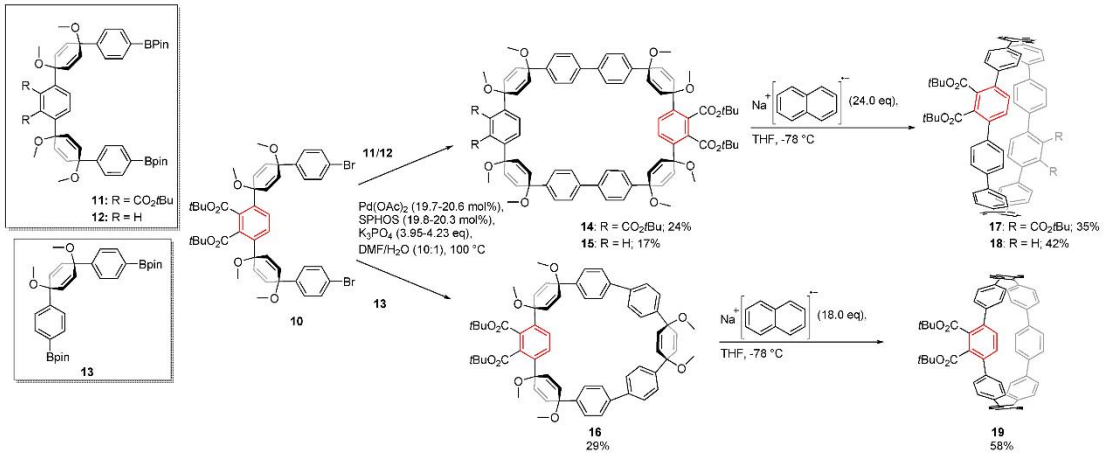

Scheme 3. Synthesis of substituted [8]- and [10]CPPs. The key intermediate **10** was prepared by a [2+2+2] cycloaddition.

2_1 screw axis causing alternating tube directions (Figure 1). In contrast, for unsubstituted CPPs basket-weaver-type packing is typically observed.[4,7,21] The preferred basket-weaver packing of the unsubstituted CPPs can be rationalized by maximizing CH-π interactions. The tubular arrangement is stabilized by van der Waals interactions between *t*Bu groups and phenyl rings, though. With the introduction of the substitution, the formation of CH-π interactions of the CPP core is reduced and the tubular-type packing is more favorable. Additionally, a contribution of weak CH–O hydrogen bonds could play a role. With an average ring to parallel ring distance of about 4.9 Å, the substituted [10]CPP **18** represents one of the tightest packed (in the direction of the tube) CPP structures reported so far. As a side effect, the torsion angles of the substituted aromatic ring with its neighbors are significantly increased, allowing for a flat arrangement of the bulky *t*Bu groups within the plane of the macrocycle.

Optoelectronic properties of the prepared CPPs were investigated by measuring UV/vis absorption spectra and fluorescence spectra (Figure 3). Only small deviations from the absorption maxima of the parent CPPs (340 nm independent of the ring size)[22] were found. Substituted [10]CPP **17** revealed a

Chemistry–A European Journal
Research Article
doi.org/10.1002/chem.202104239
Chemistry Europe
European Chemical Societies Publishing

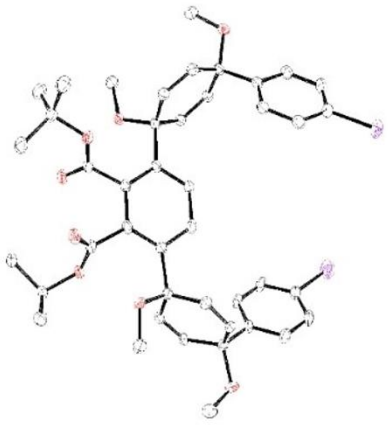

Figure 2. ORTEP plot of *t*Bu ester-substituted dibromide **10**. Hydrogen atoms are omitted for clarity, thermal ellipsoids are shown at 50% probability.

single maximum in its fluorescence spectrum, which is in accordance with our previous reported results on substituted [8]CPPs.[15] In contrast to this, both CPP derivatives substituted at only one phenyl unit show two maxima within their emission spectra. This can be attributed to the change in dihedral angle due to the large substituents influencing the dynamic behavior in the excited state, which has been calculated to be the crucial factor.[23] Additionally, the substituted [8]CPP derivative has a larger Stoke's shift compared to the [10]CPP derivatives and the emission is broader, which is in accordance with results reported for the corresponding unsubstituted CPPs.[22]

Conclusion

In conclusion, a modular synthetic strategy has been developed allowing the flexible introduction of substituents and control of the CPP ring size. The approach features access to CPPs with *t*Bu ester as substituents in different positions and various ring sizes. As examples, two different [10]CPP derivatives and one [8]CPP derivative were prepared by choosing a different cross-coupling partner followed by a reductive aromatization as the final step. The solid-state structure of [10]CPP **18** was studied by X-ray single crystal analysis. A tube-like arrangement was found that exhibits the tightest packing in the tube direction of any CPP known. The higher substituted derivatives reported in the literature have a tubular arrangement governed by substituent–substituent interactions that results in a larger ring-to-ring distance. In contrast, interactions between *t*Bu groups and the unsubstituted phenyl rings of the neighboring CPP are the main reason for the tubular arrangement in our case. Hence, this strategy can serve as general concept for crystal engineering of molecular carbon allotropes.

Experimental Section

Experimental procedures, analytical data of new compounds and details for X-ray crystallographic data are described in the Supporting Information.

Deposition Numbers 2122351 (for **10**), 1996824 (for **18**) contain the supplementary crystallographic data for this paper. These data are provided free of charge by the joint Cambridge Crystallographic Data Centre and Fachinformationszentrum Karlsruhe Access Structures service.

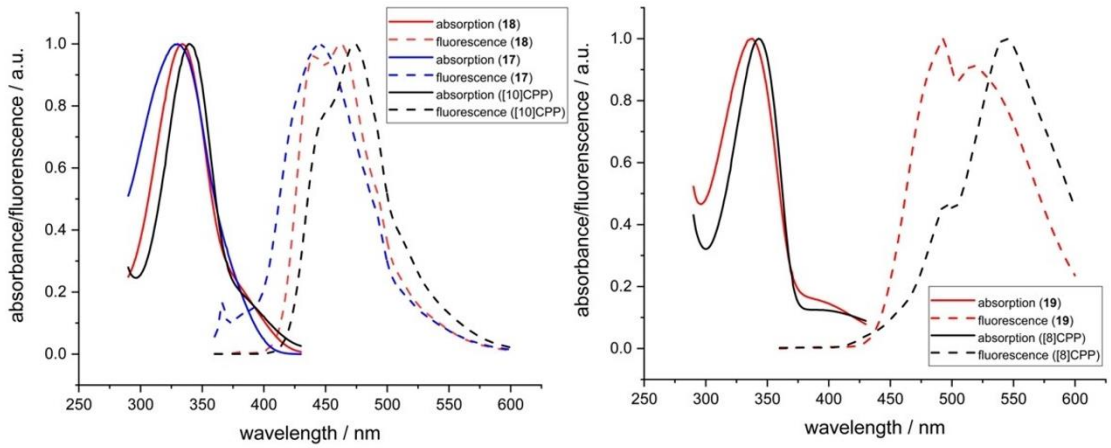

Figure 3. Normalized UV/vis absorption (solid lines) and fluorescence spectra (dashed lines) of left: substituted [10]CPPs **17** (blue, 1.12×10^{-5} M for absorption, 1.12×10^{-6} M for fluorescence), **18** (red, 1.00×10^{-5} M for absorption, 1.00×10^{-6} M for fluorescence) and [10]CPP (black, 1.29×10^{-5} M for absorption and fluorescence; for reference)). Right: substituted [8]CPP **19** (red, 2.05×10^{-5} M for absorption and fluorescence) and [8]CPP (black, 1.12×10^{-5} M for absorption and fluorescence; for reference)). All solutions in toluene.

Chemistry–A European Journal | Research Article doi.org/10.1002/chem.202104239 | Chemistry Europe European Chemical Societies Publishing

Acknowledgements

The authors are grateful to Jan H. Griwatz and Felix Bernt (Justus Liebig University) for a sample of [8]CPP. The authors thank the Justus Liebig University for funding. Open Access funding enabled and organized by Projekt DEAL.

Conflict of Interest

The authors declare no conflict of interest.

Data Availability Statement

The data that support the findings of this study are available in the supplementary material of this article.

Keywords: [2+2+2] cycloaddition · carbon allotropes · cross-coupling · macrocycles · solid-state structures

[1] R. Jasti, J. Bhattacharjee, J. B. Neaton, C. R. Bertozzi, *J. Am. Chem. Soc.* **2008**, *130*, 17646–17647.
[2] R. Friederich, M. Nieger, F. Vögtle, *Chem. Ber.* **1993**, *126*, 1723–1732.
[3] a) E. Kayahara, V. Patel, J. Xia, R. Jasti, S. Yamago, *Synlett* **2015**, *26*, 1615–1619; b) T. J. Sisto, M. R. Golder, E. S. Hirst, R. Jasti, *J. Am. Chem. Soc.* **2011**, *133*, 15800–15802; c) S. Yamago, Y. Watanabe, T. Iwamoto, *Angew. Chem. Int. Ed.* **2010**, *122*, 769–771; *Angew. Chem.* **2010**, *122*, 769–771; d) Y. Segawa, P. Šenel, S. Matsuura, H. Omachi, K. Itami, *Chem. Lett.* **2011**, *40*, 423–425; e) H. Takaba, H. Omachi, Y. Yamamoto, J. Bouffard, K. Itami, *Angew. Chem. Int. Ed.* **2009**, *48*, 6112–6116; *Angew. Chem.* **2009**, *121*, 6228–6232; f) Y. Ishii, Y. Nakanishi, H. Omachi, S. Matsuura, K. Matsui, H. Shinohara, Y. Segawa, K. Itami, *Chem. Sci.* **2012**, *3*, 2340–2345.
[4] E. Kayahara, Y. Sakamoto, T. Suzuki, S. Yamago, *Org. Lett.* **2012**, *14*, 3284–3287.
[5] P. J. Evans, E. R. Darzi, R. Jasti, *Nat. Chem.* **2014**, *6*, 404.
[6] J. Xia, R. Jasti, *Angew. Chem. Int. Ed.* **2012**, *51*, 2474–2476; *Angew. Chem.* **2012**, *124*, 2524–2526.
[7] J. Xia, J. W. Bacon, R. Jasti, *Chem. Sci.* **2012**, *3*, 3018–3021.
[8] a) T. Nishiuchi, X. Feng, V. Enkelmann, M. Wagner, K. Müllen, *Chem. Eur. J.* **2012**, *18*, 16621–16625; b) T. J. Sisto, X. Tian, R. Jasti, *J. Org. Chem.* **2012**, *77*, 5857–5860; c) P. Della Sala, A. Capobianco, T. Caruso, C. Talotta, M. de Rosa, P. Neri, A. Peluso, C. Gaeta, *J. Org. Chem.* **2018**, *83*, 220–227; d) A. Yagi, Y. Segawa, K. Itami, *J. Am. Chem. Soc.* **2012**, *134*, 2962–2965; e) B. Farajidizaji, C. Huang, H. Thakellapalli, S. Li, N. G. Akhmedov, B. V. Popp, J. L. Petersen, K. K. Wang, *J. Org. Chem.* **2017**, *82*, 4458–4464; f) C. Huang, Y. Huang, N. G. Akhmedov, B. V. Popp, J. L. Petersen, K. K. Wang, *Org. Lett.* **2014**, *16*, 2672–2675; g) F. E. Golling, S. Osella, M. Quernheim, M. Wagner, D. Beljonne, K. Müllen, *Chem. Sci.* **2015**, *6*, 7072–7078; h) Q. Huang, G. Zhuang, M. Zhang, J. Wang, S. Wang, Y. Wu, S. Yang, P. Du, *J. Am. Chem. Soc.* **2019**, *141*, 18938–18943; i) D. Lu, H. Wu, Y. Dai, H. Shi, X. Shao, S. Yang, J. Yang, P. Du, *Chem. Commun.* **2016**, *52*, 7164–7167; j) D. Lu, G. Zhuang, H. Wu, S. Wang, S. Yang, P. Du, *Angew. Chem. Int. Ed.* **2017**, *56*, 158–162; *Angew. Chem.* **2017**, *129*, 164–168; k) M. Quernheim, F. E. Golling, W. Zhang, M. Wagner, H.-J. Räder, T. Nishiuchi, K. Müllen, *Angew. Chem. Int. Ed.* **2015**, *54*, 10341–10346; l) J. Xia, M. R. Golder, M. E. Foster, B. M. Wong, R. Jasti, *J. Am. Chem. Soc.* **2012**, *134*, 19709–19715.
[9] S. Li, M. Aljhdli, H. Thakellapalli, B. Farajidizaji, Y. Zhang, N. G. Akhmedov, C. Milsmann, B. V. Popp, K. K. Wang, *Org. Lett.* **2017**, *19*, 4078–4081.
[10] a) S. Hashimoto, E. Kayahara, Y. Mizuhata, N. Tokitoh, K. Takeuchi, F. Ozawa, S. Yamago, *Org. Lett.* **2018**, *20*, 5973–5976; b) J. M. van Raden, E. J. Leonhardt, L. N. Zakharov, A. Pérez-Guardiola, A. J. Pérez-Jiménez, C. R. Marshall, C. K. Brozek, J. C. Sancho-García, R. Jasti, *J. Org. Chem.* **2020**, *85*, 129–141.
[11] J. Nogami, Y. Nagashima, K. Miyamoto, A. Muranaka, M. Uchiyama, K. Tanaka, *Chem. Sci.* **2021**, *12*, 7858.
[12] D. Wassy, M. Hermann, J. S. Wössner, L. Frédéric, G. Pieters, B. Esser, *Chem. Sci.* **2021**, *12*, 10150–10158.
[13] E. Kayahara, L. Sun, H. Onishi, K. Suzuki, T. Fukushima, A. Sawada, H. Kaji, S. Yamago, *J. Am. Chem. Soc.* **2017**, *139*, 18480–18483.
[14] Y. Xu, B. Wang, R. Kaur, M. B. Minameyer, M. Bothe, T. Drewello, D. M. Guldi, M. von Delius, *Angew. Chem. Int. Ed.* **2018**, *57*, 11549–11553; *Angew. Chem.* **2018**, *130*, 11723–11727.
[15] A.-F. Tran-Van, E. Huxol, J. M. Basler, M. Neuburger, J.-J. Adjizian, C. P. Ewels, H. A. Wegner, *Org. Lett.* **2014**, *16*, 1594–1597.
[16] Y. Miyauchi, K. Johmoto, N. Yasuda, H. Uekusa, S. Fujii, M. Kiguchi, H. Ito, K. Itami, K. Tanaka, *Chem. Eur. J.* **2015**, *21*, 18900–18904.
[17] a) N. Hayase, Y. Miyauchi, Y. Aida, H. Sugiyama, H. Uekusa, Y. Shibata, K. Tanaka, *Org. Lett.* **2017**, *19*, 2993–2996; b) N. Hayase, H. Sugiyama, H. Uekusa, Y. Shibata, K. Tanaka, *Org. Lett.* **2019**, *21*, 3895–3899.
[18] N. Hayase, J. Nogami, Y. Shibata, K. Tanaka, *Angew. Chem. Int. Ed.* **2019**, *58*, 9439–9442; *Angew. Chem.* **2019**, *131*, 9539–9542.
[19] S. Nishigaki, Y. Shibata, A. Nakajima, H. Okajima, Y. Masumoto, T. Osawa, A. Muranaka, H. Sugiyama, A. Horikawa, H. Uekusa, et al., *J. Am. Chem. Soc.* **2019**, *141*, 14955–14960.
[20] K. Tanaka, K. Shirasaka, *Org. Lett.* **2003**, *5*, 4697–4699.
[21] a) E. R. Darzi, E. S. Hirst, C. D. Weber, L. N. Zakharov, M. C. Lonergan, R. Jasti, *ACS Cent. Sci.* **2015**, *1*, 335–342; b) N. Ozaki, H. Sakamoto, T. Nishihara, T. Fujimori, Y. Hijikata, R. Kimura, S. Irle, K. Itami, *Angew. Chem. Int. Ed.* **2017**, *56*, 11196–11202; *Angew. Chem.* **2017**, *129*, 11348–11354.
[22] T. Iwamoto, Y. Watanabe, Y. Sakamoto, T. Suzuki, S. Yamago, *J. Am. Chem. Soc.* **2011**, *133*, 8354–8361.
[23] a) C. Camacho, T. A. Niehaus, K. Itami, S. Irle, *Chem. Sci.* **2013**, *4*, 187–195; b) L. Adamska, I. Nayyar, H. Chen, A. K. Swan, N. Oldani, S. Fernandez-Alberti, M. R. Golder, R. Jasti, S. K. Doorn, S. Tretiak, *Nano Lett.* **2014**, *14*, 6539–6546.

Manuscript received: November 26, 2021
Accepted manuscript online: January 10, 2022
Version of record online: January 27, 2022

4.2 Balancing Attraction and Repulsion: The Influence of London Dispersion in [10]Cycloparaphenylene-Fullerene Complexes

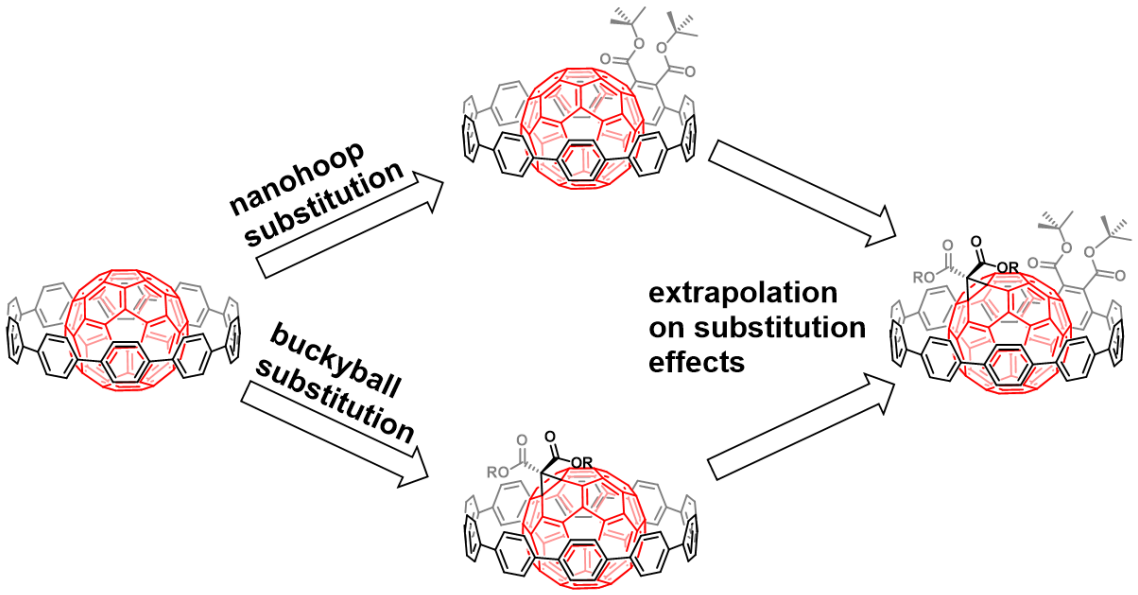

Herein we present a systematic study of the influence of different alkyl chains in malonyl ester fullerene adducts with [10]cycloparaphenylene ([10]CPP]) and a *tert*-butyl (*t*Bu) ester-substituted [10]CPP analogue. The association constants between the nanoring hosts and the fullerene guests were determined by fluorescence quenching experiments. The trends in association were rationalized by an interplay of repulsion arising from an extended volume and London dispersion as an attractive counterpart.

Reprinted with permission from

J. Volkmann, D. Kohrs, H. A. Wegner, *Chem. Eur. J.* **2023**, *29*, e202300268.

DOI: 10.1002/chem.202300268

J. V. and D. K. contributed equally to this work.

Check for updates

Chemistry–A European Journal

Research Article
doi.org/10.1002/chem.202300268

Chemistry Europe
European Chemical Societies Publishing

www.chemeurj.org

Balancing Attraction and Repulsion: The Influence of London Dispersion in [10]Cycloparaphenylene-Fullerene Complexes

Jannis Volkmann[+],[a, b] Daniel Kohrs[+],[a, b] and Hermann A. Wegner*[a, b]

Abstract: Herein we present a systematic study of the influence of different alkyl chains in malonyl ester fullerene adducts with [10]cycloparaphenylene ([10]CPP]) and a *tert*-butyl (*t*Bu) ester-substituted [10]CPP analogue. The association constants between the nanoring hosts and the fullerene guests were determined by fluorescence quenching experiments. The trends in association were rationalized by an interplay of repulsion arising from an extended volume and London dispersion as an attractive counterpart.

Introduction

On a basic level, every noncovalent interaction between two molecular species can be regarded as supramolecular chemistry. One prominent example of molecular structures exploited in supramolecular assemblies, especially in the field of carbon nanomaterials, are fullerenes. Their spheric structure makes them ideal candidates especially for curved host molecules. Cycloparaphenylenes ([*n*]CPP), strained carbon nanohoops,[1] are a prime example of such a molecular motif in this regard. The complex between C_{60} and [10]CPP represents the perfect fit regarding the size of guest and host.[2] Here, mainly π–π interactions between the concave side of the CPP and the convex fullerene surface are the driving force within this process. The high association is rationalized by ideal distance between the aromatic entities, making this peapod a curved analogue of two graphene layers. Generally, the association can be tuned by the complementarity in size, shape and interactions. For instance, changing the size of the CPP from [10] to [8], [9] or [11] decreases the association by more than one order of magnitude (K_{SV}).[2] In methylene bridged macrocycles, such as cyclotriveratrylenes and calixarenes, the increased flexibility increases the complementarity in size, while it decreases in shape.[3,4] Additionally, the extension of such systems, such as the substitution on cyclotriveratrylenes with additional phenyl groups, drastically increases the association.[3] A similar behavior was observed for the π-extension in hexa-*peri*-hexabenzocoronene embedded [12]CPP. While the diameter is too large for an efficient complexation of C_{70}, the extended π-interactions lead to a remarkable high association constant.[5] The conceptual binding motif between fullerene and CPP was used to study a Russian doll-type complex between [15]CPP, [10]CPP and C_{60},[6] as well as the differences to the fullerene derivative C_{70}.[7] The strong interaction between the entities was further used in a π–π templating strategy to build a rotaxane based on fullerenes and one [10]CPP unit.[8] In addition to these all-carbon buckyballs, endohedral fullerenes were studied in this manner as well. Here, the interaction is additionally based on charge transfer.[9] This driving force has also been assigned in the complex between [6,6]-phenyl-C_{61}-butyric acid methyl ester (PCBM), an electron acceptor material in organic solar cells, and a porphyrin unit connect to a [10]CPP unit.[10] Our group exploited this binding motif in order to study the stabilizing effect of the nanoring on a fullerenyl radical,[11] as well as the electronic communication between two CPP units through a dumbbell shaped fullerene dimer.[12] We found that the binding is influenced by London dispersion forces which stabilize the 2:1 complex and thus contribute to a positive cooperativity.

Even though this is an illustrative example of weak forces controlling supramolecular complexes no in-depth study has been done to elucidate the different forces operating. Molecular balances offer an experimental tool to quantify these often neglected weak forces.[13] Crucial for these balances is a high sensitivity for energy changes, as these forces are weak for small molecules, but can reach large values for extended systems, though. Cockroft and co-workers adapted a system originally designed by the group of Wilcox to study alkyl-alkyl interactions.[14] In this system two main conformers, the dispersion promoting folded and the dispersion prohibiting unfolded conformer, could be distinguished and quantified by ^{1}H NMR spectroscopy.[15] An additional example of a balance system relying on the interconversion of two different con-

[a] J. Volkmann,[+] D. Kohrs,[+] Prof. Dr. H. A. Wegner
Institute of Organic Chemistry
Justus Liebig University Giessen
Heinrich-Buff-Ring 17, 35392 Giessen (Germany)
E-mail: Hermann.A.Wegner@org.chemie.uni-giessen.de

[b] J. Volkmann,[+] D. Kohrs,[+] Prof. Dr. H. A. Wegner
Center for Materials research (ZfM/LaMa)
Justus Liebig University Giessen
Heinrich-Buff-Ring 16, 35392 Giessen (Germany)

[+] These authors contributed equally to this work.

Supporting information for this article is available on the WWW under https://doi.org/10.1002/chem.202300268

Chemistry–A European Journal
Research Article
doi.org/10.1002/chem.202300268
Chemistry Europe
European Chemical Societies Publishing

formers is realized in a thiobarbiturate system, in which the *anti* and *syn* relationship between two *tert*-butyl (*t*Bu) groups is analyzed.[16] Furthermore, the bond isomerism in cyclooctatetraene was used for the purpose of investigating London dispersion, as the substituents are only in close proximity in one diastereomer.[17] A balance system consisting of an intermolecular system was presented by Chen and co-workers and is based on N-heterocycles which form a proton-bound dimer.[18] The change of dissociation energy was investigated in solution and in the gas phase as well as computationally.

This approach allows an estimation of dispersive interactions between the substrates by comparing the obtained data in the different states. A further example consisting of two entities is the dimerization of a titanium triscatecholate helicate, in which different ester moieties were investigated on their ability to stabilize the dimers by noncovalent interactions.[19] The symmetry of this system increases its accuracy as the signals obtained are threefold amplified. Our group contributed with the use of azobenzene photoswitches with which we could investigate London dispersion as well as solvent effects.[20,21]

In this study we aim to apply the ability of the [10]CPP-C_{60} host-guest system to enforce close proximity of two molecular entities in order to study the influence of substitution of the buckyball on the binding behavior with [10]CPP and a substituted CPP derivative. For this purpose we employed a bis-*tert*-butyl ester-substituted CPP (s[10]CPP) which we reported earlier.[22] As guest molecules we synthesized and employed malonyl ester-substituted fullerene derivatives. To evaluate the interactions between substituents, the effects of the different substitution on the fullerene or the CPP have to be outlined (Figure 1). The backbone motif consists of [10]CPP and C_{60} whose association is mainly driven by π-π interactions (ΔG_1). The introduction of substituents on the fullerene adds an entropic penalty of reduced rotation in the complex, as well as interactions between the substituents on the fullerene and the unsubstituted [10]CPP (ΔG_2). Attachment of *t*Bu ester on the CPP provides the substituted analogue s[10]CPP, which adds strain energy to the equation which is built by dihedral interactions between the substituted phenyl ring and the neighboring ones as well as interaction energies between the substituents and C_{60} (ΔG_3). The association between substituted fullerenes and s[10]CPP can thus be divided into the measurable energies ΔG_1, ΔG_2, ΔG_3, including the unknown interaction energies as well as the substituent-substituent interaction energy [$\Delta G_{Interactions}(S_F{-}S_C)$], which is then the only unknown variable in this equation.

Results and Discussion

Synthesis of materials

Employing the Bingel-Hirsch reaction to a mixture of C_{60} and symmetric malonyl esters gave access to a library of substituted fullerene derivatives.[23] The employed malonyl esters for this cyclopropanation reaction were formed applying nucleophilic catalysis under Steglich conditions. In this manner, the targeted fullerene derivatives carrying linear as well as branched alkyl chains could be effectively synthesized in two steps from commercially available starting materials (Scheme 1). Besides the linear C_1–C_4 substituents [methyl (Me), ethyl (Et), *n*-propyl (*n*Pr), *n*-butyl (*n*Bu)] different branched substituents [*i*-propyl (*i*Pr), *tert*-butyl (*t*Bu) and 1-adamantyl (Ad)] were incorporated. The unsubstituted nanoring [10]CPP was synthesized following a procedure published by Jasti and co-workers,[24] and *t*Bu ester-substituted [10]CPP was prepared as recently described by us,[22] which follows a "class III" strategy for substituted CPPs,

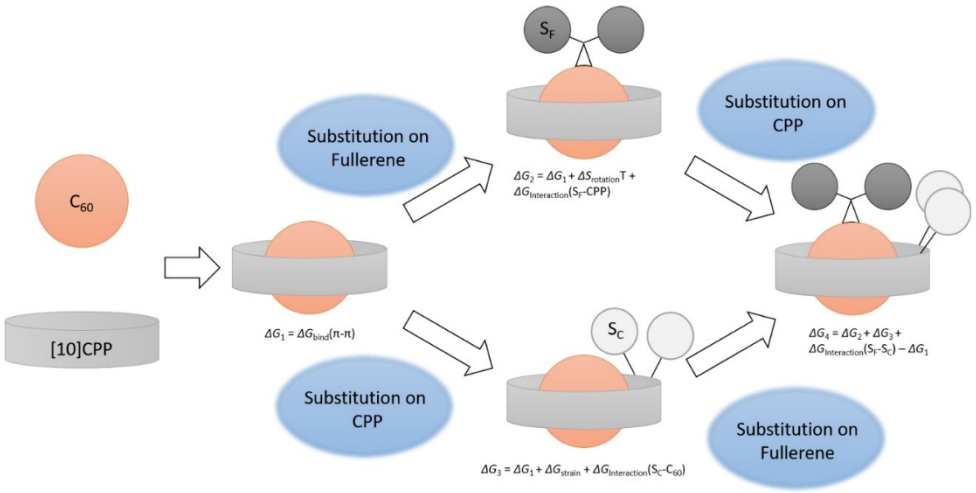

Figure 1. Schematic visualization of the methodological approach for evaluating the noncovalent interactions (S_F = substituents on fullerene, S_C = substituents on s[10]CPP).

Chemistry–A European Journal
Research Article
doi.org/10.1002/chem.202300268
Chemistry Europe
European Chemical Societies Publishing

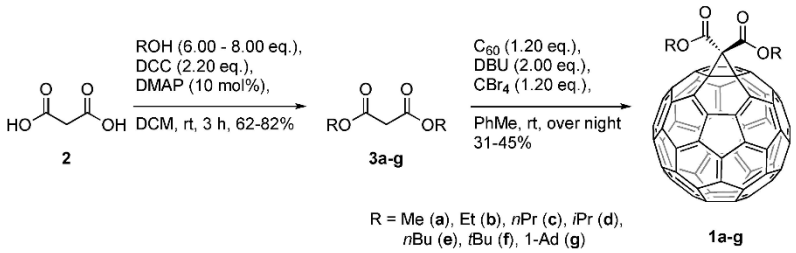

Scheme 1. Synthesis of malonyl ester-substituted fullerenes **1 a–g**.

using a [2+2+2] cycloaddition before macrocyclization through cross coupling allowing an efficient build-up.[25]

In principle the association between the two entities can have two different binding states (*syn* andor *anti*) (Scheme 2) which both contribute to the overall association as they quench the fluorescence of the CPP. The contribution of the substituent-substituent interactions within the assembly can still be estimated as this is the only additional force in the case of both

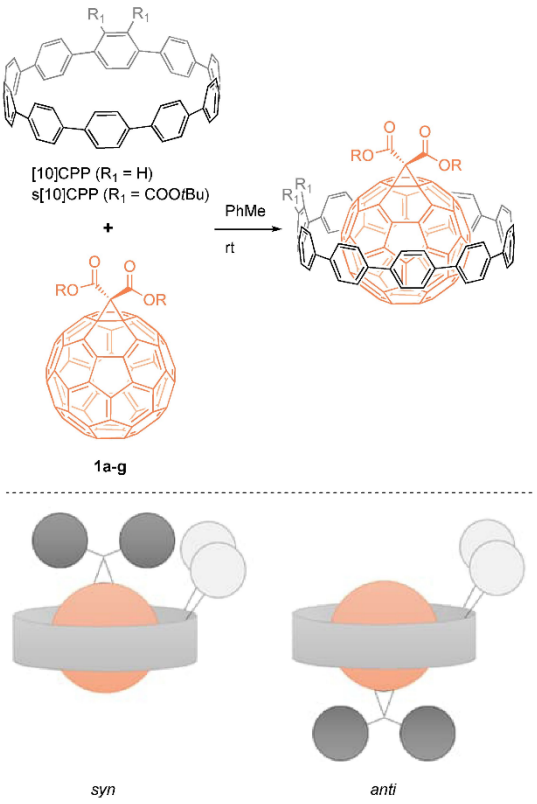

Scheme 2. Top: Representative procedure for the complex formation. Bottom: Schematic visualization of the two binding modes in the case of the s[10]CPP.

substituted entities. To prove the existence of this alignment we conducted a HH NOESY experiment for the complex of s[10]CPP and **1 g** which revealed an noncovalent interaction between the *t*Bu groups and the adamantly groups which can only exist in the *syn* alignment (Figure S3 in the Supporting Information).

The association constants between the substituted fullerenes **1 a–g** and [10]CPP as well as s[10]CPP were determined by fluorescence quenching. Following the decreasing fluorescence intensity of the nanoring upon addition of the fullerene guest allowed operation at low concentrations; this is beneficial for complexes for which large association constants are expected.[26] A triple determination was executed to prove the reliability and test the accuracy of the results. Two emission wavelengths of the s[10]CPP were analyzed which further improved the accuracy of the measurements.

Discussion of association constants

For an easier insight into the interactions between the substituents we considered the associations found in relation to the corresponding complex with bare C_{60}. Thus, we could cancel out additional effects like an increased strain in the nanohoop upon substitution which is built by enforcing a small dihedral angle in the complex or simple substituent-buckyball (S_F-CPP) or substituent-nanohoop (S_C-C_{60}) interactions (Figure 1).

Now we could directly evaluate the impact of a substituent on the binding behavior in the final complex. For a consistent and reliable data set, the association constant of [10]CPP and C_{60} was determined in the first step to gain the necessary ΔG_1, being in good agreement with the values determined by the group of Hirsch,[27] which differ from the original values reported by the group of Yamago.[2] By substitution of the fullerene the association to the nanohoops is decreased which can be rationalized by the locked rotation and, hence, entropic penalty as well as substituent-fullerene interactions (Scheme 1, ΔG_2). Starting with the association of parent [10]CPP with substituted fullerenes we found a maximum for the Me/Et derivatives. The binding constant is in comparison to the value of C_{60} ~80% lower. For longer and more branched alkyl groups it is further decreased (by 80–82%; Figure 2, Table 1). The adamantyl fullerene derivative **1 g** deviates in this context,

Chemistry–A European Journal
Research Article
doi.org/10.1002/chem.202300268
Chemistry Europe
European Chemical Societies Publishing

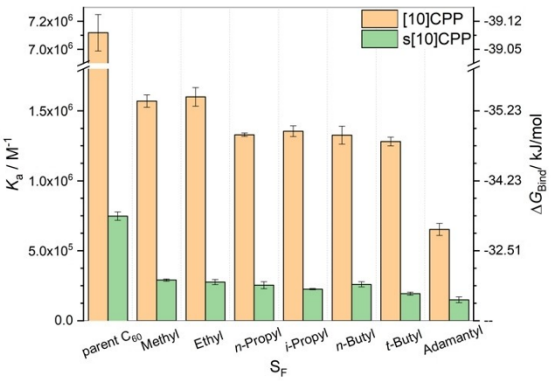

Figure 2. Summary of association constants K_a and binding energies ΔG_{bind} for the fullerene complexes of the parent and *t*Bu ester-substituted [10]CPP.

Table 1. Summary of the determined association energies ΔG_{bind} of the fullerenes C_{60}, and **1a–g** with s[10]CPP and [10]CPP, respectively.

Guest	Energy [kJ mol^{-1}] $\Delta G_{bind,s[10]CPP}$	$\Delta G_{bind,[10]CPP}$
C_{60}	−33.5 ± 0.1	−39.09 ± 0.05
1a	−31.17 ± 0.07	−35.35 ± 0.07
1b	−31.0 ± 0.2	−35.4 ± 0.1
1c	−30.8 ± 0.2	−35.1 ± 0.3
1d	−30.54 ± 0.05	−34.98 ± 0.07
1e	−30.9 ± 0.2	−34.9 ± 0.1
1f	−30.2 ± 0.2	−34.84 ± 0.06
1g	−29.5 ± 0.4	−33.2 ± 0.2

having an association of roughly one order of magnitude lower relative to C_{60}. This finding can be explained by the increased steric demand of this bulky substituent.

Next, we investigated the association behavior between the s[10]CPP and the substituted fullerene derivatives to achieve ΔG_3 and ΔG_4. On a first glance, the association with bare C_{60} is one order of magnitude smaller than for unsubstituted [10]CPP. This corresponds to ~5.5 kJ mol^{-1} and can be attributed to dihedral strain which increases due to planarization in order to achieve efficient complexation. The association constants of s[10]CPP with the linear alkyl substituted fullerene derivatives **1a–c**, **e** are around $^2/_3$ lower relative to the value for C_{60}. The decrease in binding strength is thus lower compared to the case of unsubstituted [10]CPP. In contrast to the complexation of unsubstituted [10]CPP with fullerene derivatives **1a–g**, branching reduced the association in a linear trend with the Ad derivative **1g** bearing the smallest association constant for the complexation with s[10]CPP. Even though the steric interactions between nanoring and fullerene should be more pronounced in the case of the s[10]CPP, the relative change in association for longer alkyl chains is less distinct than in the unsubstituted case with [10]CPP.

To get a better insight into the effect of substitution on the association (energies), the energies were subtracted from the values for C_{60}, thus directly providing the energetic penalties of substitution ($\Delta G_2 - \Delta G_1$ for [10]CPP and $\Delta G_4 - \Delta G_3$ for s[10]CPP).

Figure 3 shows that all substituted derivatives are more endergonic than the complex with C_{60} whereby the complexes with substituted [10]CPP (green bars) pay a smaller penalty than for [10]CPP (orange bars). To envision the differences between the substituted fullerenes, the differences in energy penalties were subtracted and depicted in purple bars. The obtained values are equal to the interaction energies $\Delta G_{Interaction}(S_F - S_C)$. All these values are negative, meaning stabilization occurs for s[10]CPP in contrast to parent [10]CPP (Table 2). Within the fullerene derivatives two strategies were followed: On the one hand increasing the alkyl chain length (Me, Et, *n*Pr, *n*Bu) and on the other increasing branched alkyl substituents (Me, Et, *i*Pr, *t*Bu, Ad) to follow the trend of increasing bulk. Within the set of linear alkyl groups it is surprising that the Me fullerene derivative **1a** is already with 1.4 kJ mol^{-1} stabilized. A further increase in alkyl chain length at the fullerene adduct towards Et fullerene derivative **1b** (1.2 kJ mol^{-1}) and *n*Pr derivative **1c** (1.3 kJ mol^{-1}) does not continue this effect. Only the *n*Bu fullerene derivative **1e** has a higher value in this regard (1.6 kJ mol^{-1}). This is in agreement with an earlier study of our group in which *n*Bu groups had the strongest stabilizing effect on the *Z* isomer of azobenzene.[21] For branched substituents this trend is more obvious: exchanging one H with a methyl group in Et fullerene derivative **1b** does not influence the stabilization (1.2 kJ mol^{-1} for *i*Pr fullerene derivative **1d**) while it is reduced to 0.9 kJ mol^{-1} for the *t*Bu fullerene derivative **1f**. This trend is inverted in the case of the Ad fullerene derivative **1g**. Here the substituents have the strongest stabilizing effect in the set of investigated substituents with 1.9 kJ mol^{-1}. This relation between *t*Bu and the larger Ad group can also be found, for example, in a recent study on the equilibrium in alkyl substituted bifluorenylidenes.[28]

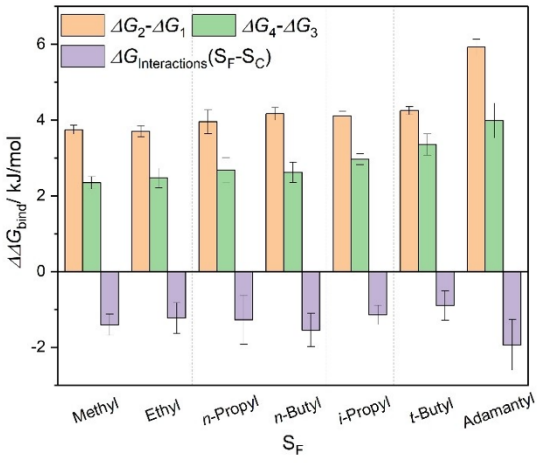

Figure 3. Energy differences relative to the complex with C_{60} for [10]CPP ($\Delta G_2 - \Delta G_1$, orange bars), s[10]CPP ($\Delta G_4 - \Delta G_3$, green bars) and the differences between them ($\Delta G_{Interactions}(S_F - S_C)$, purple bars).

Chemistry–A European Journal
Research Article
doi.org/10.1002/chem.202300268
Chemistry Europe
European Chemical Societies Publishing

Table 2. Energy differences $\Delta G_2-\Delta G_1$, $\Delta G_4-\Delta G_3$ and $\Delta G_{Interaction}(S_F-S_C)$ calculated with equations EQS2 and EQS3 (Supporting Information).

Guest	Energy difference [kJ mol^{-1}] $\Delta G_2-\Delta G_1$	$\Delta G_4-\Delta G_3$	$\Delta G_{Interaction}(S_F-S_C)$
1a	3.75 ± 0.12	2.34 ± 0.16	−1.40 ± 0.28
1b	3.70 ± 0.15	2.47 ± 0.26	−1.23 ± 0.40
1c	3.95 ± 0.32	2.68 ± 0.33	−1.28 ± 0.65
1d	4.11 ± 0.11	2.97 ± 0.14	−1.15 ± 0.26
1e	4.16 ± 0.17	2.62 ± 0.27	−1.55 ± 0.44
1f	4.25 ± 0.11	3.35 ± 0.28	−0.90 ± 0.39
1g	5.92 ± 0.21	3.98 ± 0.46	−1.94 ± 0.67

Conclusion

In conclusion, we have presented a systematic supramolecular study of fullerene Bingel adducts bearing alkyl groups with different chain lengths with [10]CPP and the substituted [10]CPP derivative. We investigated the steric-repulsion versus London dispersion effects between *t*Bu ester and branched, and elongated alkyl chains. Interestingly, we found different trends for the investigated CPP derivatives. In absolute numbers, all cases led to an increased repulsion while adding the substituents to the buckyball. In order to evaluate the influence of substituents, the total interactions were dissected in individual contributions with reference systems that should cancel out additional, undesired interactions, allowing the substituent–substituent interactions to be quantified. These interactions were expected to be small in energy. Hence, the fluorescence quenching method was applied for these supramolecular complexes, as small energy changes can be reliably determined.

Increasing the chain length of the linear alkyl substituents did not have a large effect on the overall binding, whereby the *n*Bu fullerene derivative **1e** showed the strongest stabilization (1.6 kJ mol^{-1}) of the complex with s[10]CPP. Overall, branched alkyl groups (*i*Pr **1d**, *t*Bu **1f**, 1-Ad **1g**) showed a stronger effect, and both s[10]CPP and unsubstituted [10]CPP were more endothermic for larger substituents. However, the effect was more pronounced for [10]CPP, leading to a net stabilization for the Ad-substituted fullerene derivative **1g**.

The presented system allowed low-energy interactions to be quantified efficiently and with high accuracy. Due to the complexity of interactions, only a qualitative rational of the operating effects can be formulated, though. Nevertheless, this proof-of-principle study shows potential for addressing multiple interactions in complex systems. Additionally, it provides guidelines for the design of carbon-based supramolecular functional systems in the future.

Experimental Section

Experimental details are described in the Supporting Information.

Acknowledgements

The authors are grateful for the financial support provided by the Justus Liebig university and the DFG (SPP 1807). The authors are grateful to Dr. Heike Hausmann for NMR measurements. Open Access funding enabled and organized by Projekt DEAL.

Conflict of Interest

The authors declare no conflict of interest.

Data Availability Statement

The data that support the findings of this study are available in the supplementary material of this article.

Keywords: cyclophanes · fullerenes · host-guest systems · pi interactions · supramolecular chemistry

[1] Y. Xu, M. von Delius, *Angew. Chem. Int. Ed.* **2020**, *59*, 559–573; *Angew. Chem.* **2019**, *132*, 567–582.
[2] T. Iwamoto, Y. Watanabe, T. Sadahiro, T. Haino, S. Yamago, *Angew. Chem. Int. Ed.* **2011**, *50*, 8342–8344.
[3] H. Matsubara, A. Hasegawa, K. Shiwaku, K. Asano, M. Uno, S. Takahashi, K. Yamamoto, *Chem. Lett.* **1998**, *27*, 923.
[4] T. Haino, M. Yanase, Y. Fukazawa, *Angew. Chem. Int. Ed.* **1997**, *36*, 259–260; *Angew. Chem.* **1997**, *109*, 288–290.
[5] D. Lu, G. Zhuang, H. Wu, S. Wang, S. Yang, P. Du, *Angew. Chem. Int. Ed.* **2017**, *56*, 158–162; *Angew. Chem.* **2017**, *129*, 164–168.
[6] S. Hashimoto, T. Iwamoto, D. Kurachi, E. Kayahara, S. Yamago, *ChemPlusChem* **2017**, *82*, 1015–1020.
[7] T. Iwamoto, Y. Watanabe, H. Takaya, T. Haino, N. Yasuda, S. Yamago, *Chem. Eur. J.* **2013**, *19*, 14061–14068.
[8] Y. Xu, R. Kaur, B. Wang, M. B. Minameyer, S. Gsänger, B. Meyer, T. Drewello, D. M. Guldi, M. von Delius, *J. Am. Chem. Soc.* **2018**, *140*, 13413–13420.
[9] a) T. Iwamoto, Z. Slanina, N. Mizorogi, J. Guo, T. Akasaka, S. Nagase, H. Takaya, N. Yasuda, T. Kato, S. Yamago, *Chem. Eur. J.* **2014**, *20*, 14403–14409; b) Y. Nakanishi, H. Omachi, S. Matsuura, Y. Miyata, R. Kitaura, Y. Segawa, K. Itami, H. Shinohara, *Angew. Chem. Int. Ed.* **2014**, *53*, 3102–3106; c) H. Ueno, T. Nishihara, Y. Segawa, K. Itami, *Angew. Chem. Int. Ed.* **2015**, *54*, 3707–3711.
[10] Y. Xu, B. Wang, R. Kaur, M. B. Minameyer, M. Bothe, T. Drewello, D. M. Guldi, M. von Delius, *Angew. Chem. Int. Ed.* **2018**, *57*, 11549–11553; *Angew. Chem.* **2018**, *130*, 11723–11727.
[11] a) A. Stergiou, J. Rio, J. H. Griwatz, D. Arčon, H. A. Wegner, C. P. Ewels, N. Tagmatarchis, *Angew. Chem. Int. Ed.* **2019**, *58*, 17745–17750; *Angew. Chem.* **2019**, *131*, 17909–17914; b) Y. Tanuma, A. Stergiou, A. Bužan Bob-

Chemistry–A European Journal
Research Article
doi.org/10.1002/chem.202300268
Chemistry Europe
European Chemical Societies Publishing

nar, M. Gaboardi, J. Rio, J. Volkmann, H. A. Wegner, N. Tagmatarchis, C. P. Ewels, D. Arčon, *Nanoscale* **2021**, *13*, 19946–19955.
[12] J. Rio, S. Beeck, G. Rotas, S. Ahles, D. Jacquemin, N. Tagmatarchis, C. Ewels, H. A. Wegner, *Angew. Chem. Int. Ed.* **2018**, *57*, 6930–6934; *Angew. Chem.* **2018**, *130*, 7046–7050.
[13] a) A. Elmi, S. L. Cockroft, *Acc. Chem. Res.* **2021**, *54*, 92–103; b) M. Giese, M. Albrecht, *ChemPlusChem* **2020**, *85*, 715–724; c) F. Holtrop, K. W. Visscher, A. R. Jupp, J. C. Slootweg in *Adv. Phys. Org. Chem.*, Elsevier, **2020**, pp. 119–141; d) D. J. Liptrot, P. P. Power, *Nat. Chem. Rev.* **2017**, *1*, 4; e) M. A. Strauss, H. A. Wegner, *Eur. J. Org. Chem.* **2019**, *2019*, 295–302; f) J. P. Wagner, P. R. Schreiner, *Angew. Chem. Int. Ed.* **2015**, *54*, 12274–12296; *Angew. Chem.* **2015**, *127*, 12446–12471.
[14] S. Paliwal, S. Geib, C. S. Wilcox, *J. Am. Chem. Soc.* **1994**, *116*, 4497–4498.
[15] L. Yang, C. Adam, G. S. Nichol, S. L. Cockroft, *Nat. Chem.* **2013**, *5*, 1006.
[16] U. Berg, I. Pettersson, *J. Org. Chem.* **1987**, 5177–5184.
[17] M. H. Lyttle, A. Streitwieser, Jr., R. Q. Kluttz, *J. Am. Chem. Soc.* **1981**, *103*, 3232–3233.
[18] R. Pollice, M. Bot, I. J. Kobylianskii, I. Shenderovich, P. Chen, *J. Am. Chem. Soc.* **2017**, *139*, 13126–13140.
[19] D. van Craen, W. H. Rath, M. Huth, L. Kemp, C. Räuber, J. M. Wollschläger, C. A. Schalley, A. Valkonen, K. Rissanen, M. Albrecht, *J. Am. Chem. Soc.* **2017**, *139*, 16959–16966.
[20] a) L. Schweighauser, M. A. Strauss, S. Bellotto, H. A. Wegner, *Angew. Chem. Int. Ed.* **2015**, *54*, 13436–13439; *Angew. Chem.* **2015**, *127*, 13636–13639; b) M. A. Strauss, H. A. Wegner, *Angew. Chem. Int. Ed.* **2019**, *58*, 18552–18556; *Angew. Chem.* **2019**, *131*, 18724–18729; c) M. A. Strauss, H. A. Wegner, *Angew. Chem. Int. Ed.* **2021**, *60*, 779–786; *Angew. Chem.* **2021**, *133*, 792–799.
[21] M. A. Strauss, H. A. Wegner, *ChemPhotoChem* **2019**, *3*, 392–395.
[22] D. Kohrs, J. Becker, H. A. Wegner, *Chem. Eur. J.* **2022**, *28*, e202104239.
[23] a) C. Bingel, *Chem. Ber.* **1993**, *126*, 1957–1959; b) X. Camps, A. Hirsch, *J. Chem. Soc. Perkin Trans. 1* **1997**, 1595–1596.
[24] E. R. Darzi, T. J. Sisto, R. Jasti, *J. Org. Chem.* **2012**, *77*, 6624–6628.
[25] D. Kohrs, J. Volkmann, H. A. Wegner, *Chem. Commun.* **2022**, *58*, 7483–7494.
[26] P. Thordarson, *Chem. Soc. Rev.* **2011**, *40*, 1305–1323.
[27] I. Solymosi, J. Sabin, H. Maid, L. Friedrich, E. Nuin, M. E. Pérez-Ojeda, A. Hirsch, *Org. Mater.* **2022**, *4*, 73–85.
[28] F. M. Wilming, B. Marazzi, P. P. Debes, J. Becker, P. R. Schreiner, *J. Org. Chem.* **2022**, *88*, 1024–1035.

Manuscript received: January 26, 2023
Accepted manuscript online: February 14, 2023
Version of record online: March 3, 2023

4.3 Influence of Substitution on the Supramolecular Chemistry of Cycloparaphenylene-Fullerene Complexes

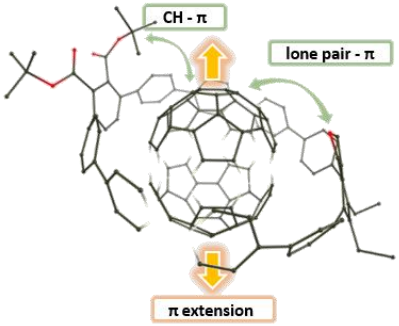

We present a comprehensive host-guest study of four substituted and unsubstituted [10]cycloparaphenylenes with the fullerenes C_{60} and C_{70}. Within this study, the influence on the complexation behavior was investigated experimentally and computationally. Due to the increased steric demand the substitution on the nanohoop results in an energetic penalty, which could be partially compensated by additional substituent-fullerene interactions. These attractive interactions are intensified in the C_{70} complexes and with an increased degree of substitution. For the computational investigation conformer ensembles were taken into account, providing reliable structures with Boltzmann weighted energies. An analysis of the noncovalent interactions elucidates the origin of the enhanced substituent-C_{70} interaction. The ellipsoid fullerene C_{70} can be considered as a π-extended version of C_{60}, which is able to increase the attractive van-der-Waals interactions within these supramolecular complexes.

Reprinted with permission from

D. Kohrs, J. Volkmann, H. A. Wegner, *Eur. J. Org. Chem.* **2023**, *26*, e202300575.

DOI: 10.1002/ejoc.202300575

D. K. and J. V. contributed equally to this work.

Check for updates

EurJOC
European Journal of Organic Chemistry

Research Article
doi.org/10.1002/ejoc.202300575

Chemistry Europe
European Chemical Societies Publishing

www.eurjoc.org

Influence of Substitution on the Supramolecular Chemistry of Cycloparaphenylene-Fullerene Complexes

Daniel Kohrs[+],[a, b] Jannis Volkmann[+],[a, b] and Hermann A. Wegner*[a, b]

We present a comprehensive host-guest study of four substituted and unsubstituted [10]cycloparaphenylenes with the fullerenes C_{60} and C_{70}. Within this study, the influence on the complexation behavior was investigated experimentally and computationally. Due to the increased steric demand the substitution on the nanohoop results in an energetic penalty, which could be partially compensated by additional substituent-fullerene interactions. These attractive interactions are intensified in the C_{70} complexes and with an increased degree of substitution. For the computational investigation conformer ensembles were taken into account, providing reliable structures with Boltzmann weighted energies. An analysis of the noncovalent interactions elucidated the origin of the enhanced substituent-C_{70} interaction. The ellipsoid fullerene C_{70} can be considered as a π-extended version of C_{60}, which is able to increase the attractive van der Waals interactions within these supramolecular complexes.

Introduction

Interactions between not covalently bound molecules are omnipresent, reaching from solvation to protein folding and beyond. In the field of π-conjugated (nano)carbons, π-π interactions play a crucial role between the nanocarbons, as well as in their solvation. The term π-π interaction joins a library of interactions consisting of quadrupole interactions,[1] electrostatic interactions as well as London dispersion among others.[2]

A prime example among these interactions is the π-stacking of two graphene layers within graphite. Here, the lattices stack in a displaced manner with an interlayer distance of 3.40 Å.[3] Wrapped-up graphene sheets, carbon nanotubes (CNT), have an increased and decreased electron density on the concave and convex site, respectively, which makes them suitable candidates to host fullerenes in their electron-rich cavity. The shortest repeatable cut-out of an armchair CNT is a [*n*]cycloparaphenylene ([*n*]CPP) which can thus be seen as the perfect model substrate for single-walled CNTs. After years of throwbacks on the synthetic odyssey towards these strained polyaromatic hydrocarbons,[4] three main strategies were developed to form this class of curved compounds.[5] Having these strategies established, it was possible to investigate a variety of different sized CPPs for which [10]CPP revealed superior supramolecular properties regarding complexation with fullerenes. The [10]CPP@C_{60} complex, for instance, has an exceptional association constant of around 10^7 M^{-1} in toluene.[6] In this complex the distance between the nanohoop and the fullerene coincides with the interlayer distance in graphite. A similar strategy was applied by our group for the stabilization of the azafullerenyl radical $C_{59}N^{\bullet}$,[7] as well as by others for the synthesis of a rotaxane[8] or the complexation of charge-delocalized endofullerenes.[9] In case of bisazafullerene $(C_{59}N)_2$, the fullerene dimer can be encapsulated by two [10]CPPs, whereat the first complexation promotes the second by additional London dispersion forces.[10]

While a substituted *para*-phenylene unit within a CPP influences the association constant due to a decreased diameter and conjugation originating from the larger dihedral angle of the substituted core unit with the adjacent phenylenes, additional interactions – such as London dispersion – can positively contribute to the association (Figure 1). Recently, we investigated these additional interactions in complexes consisting of a di *tert*-butyl ester functionalized [10]CPP as a host unit encapsulating different methanofullerenes, functionalized with branched as well as linear alkyl chains.[11] In all cases, the

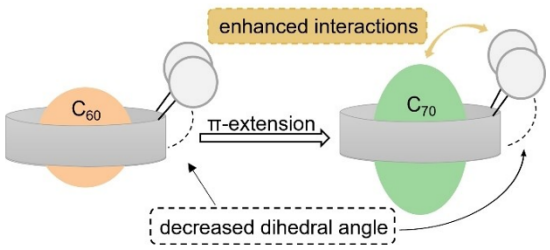

Figure 1. Schematic representation of the proposed enhanced interaction between the π-extended fullerene C_{70} and the substituents on the CPP.

[a] D. Kohrs,[+] J. Volkmann,[+] Prof. Dr. H. A. Wegner
Institute of Organic Chemistry
Justus Liebig University Giessen
Heinrich-Buff-Ring 17, 35392 Giessen (Germany)
E-mail: Hermann.A.Wegner@org.chemie.uni-giessen.de
[b] D. Kohrs,[+] J. Volkmann,[+] Prof. Dr. H. A. Wegner
Center for Materials research (ZfM/LaMa)
Justus Liebig University Giessen
Heinrich-Buff-Ring 16, 35392 Giessen (Germany)
[+] These authors contributed equally to this work.

Supporting information for this article is available on the WWW under https://doi.org/10.1002/ejoc.202300575

EurJOC
European Journal of Organic Chemistry

Research Article
doi.org/10.1002/ejoc.202300575

Chemistry Europe
European Chemical Societies Publishing

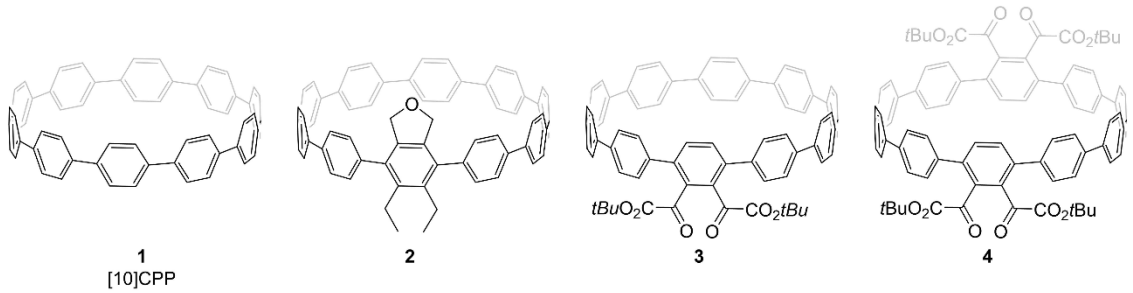

Figure 2. CPPs applied within this study.

attractive interactions dominated, with the dispersion donors *n*-butyl and 1-adamantyl showing the strongest effect. To get an in-depth understanding of the substitution effects in CPP-fullerene complexes, we have herein conducted fluorescence quenching experiments with the previously reported di- and tetra-*tert*-butyl ester functionalized [10]CPPs **3** and **4**, as well as the diethyl phthalane incorporated [10]CPP **2**, in comparison to the parent [10]CPP **1** (Figure 2). The fullerenes C_{60} and C_{70} were employed as guest molecules and the impact of the different shapes of the fullerenes on the association behavior with the substituted nanohoops were investigated experimentally as well as by theoretical calculations.

Results and Discussion

Experimental details

The substituted CPPs – di- and tetra-*tert*-butyl ester functionalized [10]CPPs **3** and **4**, as well as diethyl phthalane incorporated [10]CPP **2** – were synthesized according to previously published syntheses,[12,13] following a similar strategy relying on a combination of a [2+2+2] cycloaddition for the introduction of substituents and a cross-coupling reaction for the selective formation of the 10-membered ring.[14] The unsubstituted [10]CPP **1** was synthesized following a synthesis reported by Jasti and coworkers.[15]

For the determination of the association constants, trifold fluorescence quenching experiments were conducted in toluene and the thus obtained standard deviation was employed for the errors. While the concentration of the emitting host (CPP) was kept constant, the guest concentration was varied, and the quenching of the fluorescence was followed. The data were evaluated by non-linear regression utilizing the online tool "bindfit" by Thordarson.[16] For the determination of the stoichiometry, association mode and association constant the corresponding recommendations by Thordarson were followed. Even though the association constant of parent [10]CPP with C_{70} is literature known, we repeated the experiments to rule out systematic deviations originating from different experimental setups.

Association Constants

The association constants and energies of the different C_{60} and C_{70}/CPP-complexes are summarized in Table 1 and Figure 3. In general, the association drops upon substitution of the nanohoop which is in accordance with our earlier results for methanofullerenes.[11] This trend can be rationalized by the increased dihedral angle between the substituted aromatic ring and the adjacent ones which effectively reduces the inner diameter and thus the cavity available for the fullerene (Figure 1). The dihedral angle has to be reduced upon complex-

Table 1. Summary of the binding energies used for Figure 1 as well as the corresponding association energies for the investigated complexes with the standard deviations after trifold determination. The values 1@C_{60} and 3@C_{60} are taken from ref. [11].

Host	Guest	K_{bind}/M^{-1}	$\Delta G_{bind,measure}$/kJ/mol
1	C_{60}	$7.1 \pm 0.1 \cdot 10^6$	-39.09 ± 0.05
	C_{70}	$4.7 \pm 0.2 \cdot 10^5$	-32.4 ± 0.1
2	C_{60}	$1.15 \pm 0.08 \cdot 10^5$	-28.9 ± 0.2
	C_{70}	$3.75 \pm 0.08 \cdot 10^4$	-26.10 ± 0.06
3	C_{60}	$7.5 \pm 0.3 \cdot 10^5$	-33.5 ± 0.1
	C_{70}	$7.7 \pm 0.3 \cdot 10^4$	-27.88 ± 0.08
4	C_{60}	$1.0 \pm 0.1 \cdot 10^5$	-28.6 ± 0.3
	C_{70}	$4.1 \pm 0.7 \cdot 10^4$	-26.3 ± 0.5

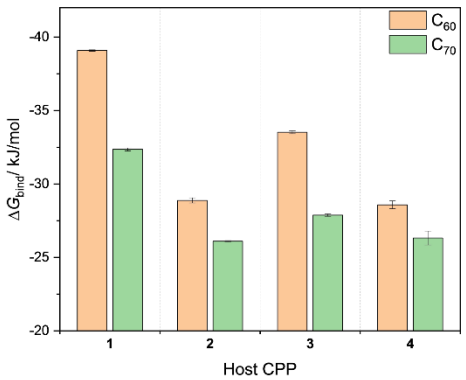

Figure 3. Association energies of the investigated nanohoop molecules with C_{60} as well as C_{70}.

EurJOC
European Journal of Organic Chemistry

Research Article
doi.org/10.1002/ejoc.202300575

Chemistry Europe
European Chemical Societies Publishing

ation – a penalty which has to be paid with association energy. Additionally, this trend amplifies with an increasing degree of substitution and contributes to both, the association with C_{60} and C_{70}. For the two fourfold-substituted derivatives **2** and **4** the values are very similar, indicating a weak influence of the nature of the substituents in the investigated cases.

To analyze the interactions, the binding energies were normalized to the energies of the parent complexes **1**@C_{60} and **1**@C_{70}, respectively (Figure 4, orange and green bars). Thus, the sum of energetic penalty arising from a decreased effective inner diameter and attractive non-covalent interactions can be rationalized. In all cases the association energy is reduced by 10%–30%, correlating to a reduction of the association constant by about one order of magnitude, given the exponential relation between association constant and its energy (Supporting Information, EQ S1). However, it is clearly visible that the relative drop in the association energy is stronger for C_{60} among all substituted CPPs. This fact is supported by the $\Delta\Delta G_{bind,rel}$ values calculated with Equation (1). This value emphasizes the differences between the C_{60} and C_{70} complexes. A value of 100% indicates no influence of the nature of fullerene, while a value $<100\%$ indicates a stabilization of C_{70} over C_{60}, and *vice versa*. In all three cases $\Delta\Delta G_{bind,rel}$ is $<100\%$, showing the stabilizing effect of C_{70} over C_{60} (Figure 4, purple bar).

$$\Delta\Delta G_{bind,rel} = \frac{\Delta G_{bind,rel}(C_{60})}{\Delta G_{bind,rel}(C_{70})} \quad (1)$$

While the lower sphericity of C_{70} leads to a weaker interaction with the nanoring, even in the parent complexes, it bears an additional surface for further interactions in the substituted cases which is the main reason for the smaller penalty paid upon substitution.

C_{70} can be seen as an π-extended C_{60}. The attractive CH-π and lone pair-π interactions of the CPP substituents with the convex surface of the fullerene improve the association and lead to a smaller decrease in association compared to C_{60}. This assumption is supported by the fact that this trend is enhanced upon a higher degree of substitution, possessing thus more interacting entities.

For the twofold substituted CPP **3** the value is very close to 100% and hence, there is only a marginal difference between the fullerenes, which indicates interactions with C_{60} and C_{70} to have a similar quantity. On the other hand, the fourfold substituted CPPs **2** and **4** exhibit a value of around 90%, which could be explained by a similar contact surface between substituents and curved fullerene surface.

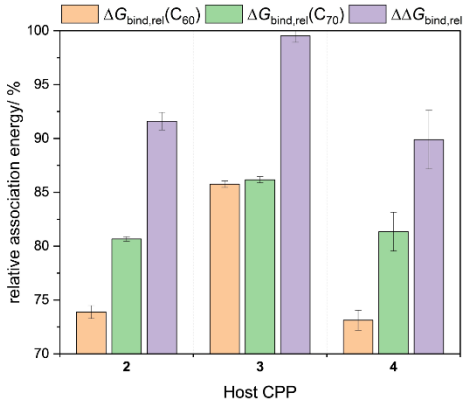

Figure 4. Relative association energies normalized on the association energy of the parent complex with [10]CPP.

Theoretical Investigation

Computational details

The computational details are briefly described in the following while a more exhaustive description can be found in the supplementary information. All density functional theory (DFT) calculations were executed with the software package orca (version 5.0.4).[17] The RIJCOSX approximations,[18–21] utilizing the auxiliary basis set def2-J were used as default. To get reliable geometries and energies, the hosts, as well as the complexes were subjected to the conformer-rotamer ensemble sampling tool (CREST) by Grimme.[22] The obtained ensemble was submitted to the command line energetic sorting of conformer rotamer ensembles (CENSO) workflow,[23] obtaining a narrowed ensemble with geometries and energies on a DFT level. The geometries were obtained by the r2SCAN-3c/mDZ method,[24] accompanied with the solvation model based on molecular electron density (SMD[25]) energy and the modified rigid rotator harmonic oscillator (mRRHO[26]) approach with Grimme's extended tight binding method (xTB-gfn2)[27] based thermodynamic correction. The single point energies were obtained with the hybrid DFT method PBE0 with D4 dispersion correction,[19,20][18,28] combined with the triple-ζ def2-TZVP basis set,[19] in conjuction with the SMD solvent model and the mRRHO(gfn2) approximation for the thermodynamic contribution. The final ensemble represents 99% of the Boltzmann distribution among all observed conformers. Utilizing the Boltzmann weighted energies for the CPPs and complexes, the energy contributions of the present conformers were taken into account. The non-covalent interaction (NCI) in the supramolecular complexes were calculated with the NCIPLOT 4.0 software.[29] Additionally, the data were visualized with vmd,[30] using a color code based on $\mathrm{sign}(\lambda_2)\cdot\rho$ [−1.5 (blue), 0 (green), +1.5 (red)]. The required wavefunctions were obtained with PBE0/def2-TZVP.

Theoretical Evaluation of the Binding Constants

The above-described workflow allows to obtain the structures and energies of a small representative of the most likely ensemble of both, the hosts and the complexes. By that the possible error of taking the less probable (not lowest lying) conformer(s) into account is reduced. Additionally, by utilizing

EurJOC
European Journal of Organic Chemistry

Research Article
doi.org/10.1002/ejoc.202300575

Chemistry Europe
European Chemical Societies Publishing

the Boltzmann weighted energies of the lowest lying conformers, representing 99% of the total energy, mimic the conformational reality of the system even further. In Table 2 and Figure S18 (Supporting Information) the thus obtained calculated association energies are displayed. These energies were determined by the Gibbs free energy of the complex, subtracted with the Gibbs free energies of the host and the guest. In general, the binding is slightly overestimated, which is known for such complexes.[6,31,32]

The non-corrected basis set superposition error (BSSE) can be taken into account as an additional factor. For all investigated CPPs, the overbinding is stronger for the C_{70} complex than the C_{60} ones. This circumstance originates from the calculated binding energy, which is in three of four cases higher for C_{70} than for the corresponding C_{60} complex.

Theoretical Evaluation of the Geometries and Non-covalent Interactions

For the discussion of the non-covalent interactions occurring within the investigated supramolecular complexes, the most abundant conformer (MAC) was utilized for the visualization of intermolecular forces. Within the ensemble of the diethyl phthalane CPP **2**, only conformers with the ether moiety facing inside the cavity were observed. This is in agreement with the crystal structure of the diethyl phthalane incorporated [8]CPP reported earlier by our group.[33] The fact that the ether moiety is facing inside – in both cases, the CPP and its complexes – is further supported by ^{1}H-NMR spectroscopy of the **2**@C_{60} complex (Supporting Information, Figure S13). The optimized geometries of **3** and **4** show that the substituents tend to face out of the nanohoop, minimizing the repulsive interactions which is in agreement with the solid state structure of CPP **3** which we presented earlier.[12]

The NCI plots of the MAC of the four investigated CPPs with the fullerenes are displayed in Figure 5. The parent [10]CPP complexes, show the π-π interactions which are expected to be present in the backbone of the substituted nanohoop as well. In both complexes a large interaction surface can be observed between the nanohoop and the fullerene. As indicated by the green color the interactions are of a weak nature, displaying π-π van der Waals forces. The shape of the NCI plot is similar in both, the C_{60} and the C_{70} complex.

Table 2. Summary of the calculated binding free energies.

Host	Guest	$\Delta G_{bind,calc}$	$\Delta G_{bind,measure}$ kJ/mol	abs. deviation
1	C_{60}	−49.18	−39.09	10.10
	C_{70}	−50.82	−32.35	18.47
2	C_{60}	−35.75	−28.88	6.87
	C_{70}	−33.30	−26.10	7.20
3	C_{60}	−51.32	−33.52	17.80
	C_{70}	−52.22	−27.88	24.34
4	C_{60}	−48.13	−28.58	19.54
	C_{70}	−48.18	−26.28	21.90

For a better understanding of the interactions, NCI scatter-plots of the complexes were depicted. The corresponding graphs for [10]CPP complexes with C_{60} and C_{70} are displayed in Figure 4b. In these 2D plots, the reduced density gradient (RDG) is plotted against the density multiplied by the sign of the second hessian eigenvalue (sign(λ_2)·ρ). Thus, spikes close to sign(λ_2)·ρ = 0 display weak interactions. Both NCI scatter-plots of **1**@C_{60} and **1**@C_{70} have sharp spikes close to sign(λ_2)·ρ = 0, originating from the π-π interactions, which qualitatively appear similar, while being slightly more expressed in the C_{70} complex (green circle) which resembles the more rough interactions in the NCI plot.

Additional interactions can be observed for the complexes of CPP **2**. As the lone pair of the oxygen is facing to the π-surface of the fullerene, strong attractive interactions can be observed, which are indicated by the blue color in the NCI plot. These additional interactions are similar for both complexes (C_{60} and C_{70}). The scatter-plots of both reveal weak interactions close to sign(λ_2)·ρ = 0. Comparing the data of the C_{60} and the C_{70} complex of CPP **2** a stronger interaction can be observed for the C_{70} complex recognizable by the more intense spikes in the scatter plot (green bar). The C_{60} and C_{70} complexes of the CPPs **3** and **4** with their *tert*-butyl esters can form CH-π van der Waals interactions between the *tert*-butyl groups and the guests. In the C_{60} complexes of CPPs **3** and **4**, only the belt-like NCI surface can be observed between the host and the guest which are the result of the concave-convex π-π interaction. Other attractive interactions between the substituents on the nanohoop and the fullerene guest cannot be observed. However, extending the π-surface of the fullerene – by changing from C_{60} to C_{70} – a new NCI surface emerges between the *tert*-butyl substituents of the nanohoop **3** and the egg-shaped fullerene. With a $H_{substituent}$–C_{C70} distance of ~3.8 Å these interactions are in the range of London dispersion forces. The increased number of weak interactions is also represented in the corresponding scatter-plots. Two new spikes appear at very low ρ values (green bar), while the blurry spike at −0.01 is approaching the RDG = 0 line (green circle). This finding supports our interpretation of C_{70} behaving like a π-extended C_{60} in these supramolecular complexes. Interestingly, in none of the observed conformer of **3**@C_{70} both *tert*-butyl groups are facing toward the fullerene core, indicating that sterics and/or dipole moment outnumbers the potential additional London dispersion forces. In case of the more substituted CPP **4** the complexation of C_{70} also induces an additional non-covalent interaction between the *tert*-butyl substituents and the fullerene compared to C_{60}, represented by a light green NCI surface. Surprisingly, only one out of four substituents interacts with the encapsulated fullerene in the MAC.

The insight obtained from the NCI plots and their scatter-plots support our assumptions originating from the experimental data: In all substituted cases the weak interactions are more pronounced for the C_{70} complexes in comparison to the corresponding C_{60} complex visualized by the scatter-plots. This effect appears to be stronger for the substituted nanohoops than for the parent [10]CPP, explaining the stronger beneficial substitution effect for the substituted nanohoops, described by

EurJOC
European Journal of Organic Chemistry

Research Article
doi.org/10.1002/ejoc.202300575

Chemistry Europe
European Chemical Societies Publishing

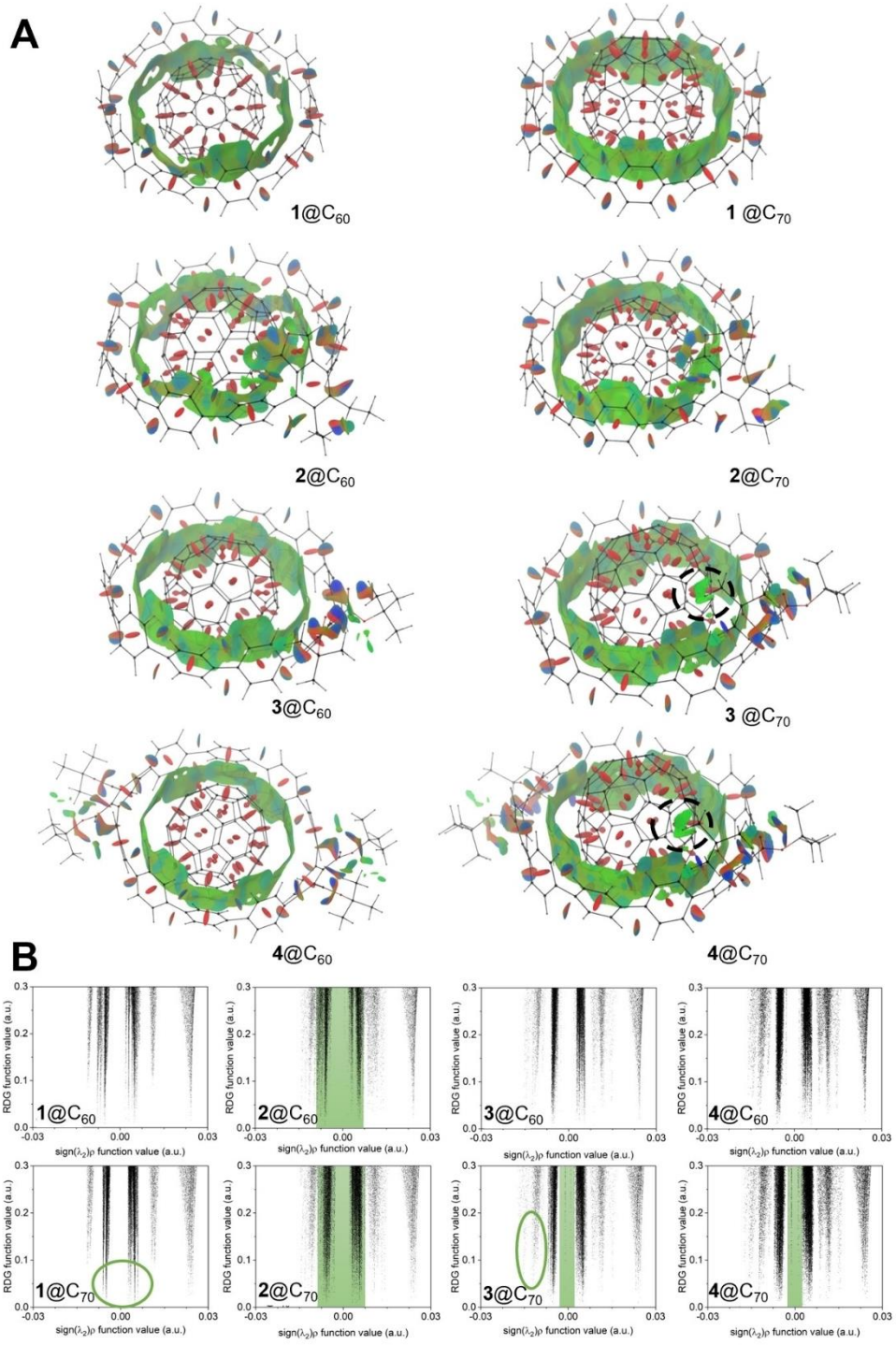

Figure 5. Calculated structures of the MAC of each complex with the isosurface displaying noncovalent interactions (A). Scatter plot (RDG function value vs. sign(λ_2)ρ function value) of the noncovalent interactions of each in A shown complex (B).

the lower relative association energy (Figure 4, purple bar). In the visualized NCI plots the additional interactions with C_{70} are visible for the *tert*-butyl ester functionalized CPPs **3** and **4** while they are not as obvious in case of CPP **2** as in the C_{60} complex

EurJOC
European Journal of Organic Chemistry

Research Article
doi.org/10.1002/ejoc.202300575

Chemistry Europe
European Chemical Societies Publishing

already attractive substituent fullerene interactions can be observed.

Conclusions

In summary, we presented a comprehensive host-guest study of substituted [10]CPPs with the fullerenes C_{60} and C_{70} investigating the association and interactions experimentally, as well as theoretically. With the method of fluorescence quenching the association energies of the complexes could be determined even though the differences are small. The observed trend shows an attractive substituent-fullerene interaction with regard to the ellipsoid fullerene C_{70}, which bears additional π-surface for attractive van der Waals forces. Additionally, the experimental data reveal, that the nature of the substituent has a comparable low impact, in contrast to the degree of substitution. The theoretical investigation was based on the whole ensemble of conformers utilizing the tools CREST and CENSO to obtain reliable structures and energies. Even though, the calculated energies overestimate the binding, these values perform well with respect to the literature cases of [10] and [11]CPP, which report an overbinding of one order of magnitude.[6,31] Visualization and analysis of the noncovalent interactions support the assumptions based on the observed trends by qualitative comparison of the NCI plots. Interactions of the substituents with the encapsulated fullerene – especially in case of C_{70} – reveal the attractive nature of these additional stabilizing effects. The presented results contribute to the understanding of non-covalent interactions within supramolecular complexes and provide quantitative data to design supramolecular carbon structures utilizing non-covalent interactions.

Experimental Section

Materials: Fullerenes C_{60} and C_{70} were purchased from TCI. The four substituted and unsubstituted cycloparaphenylenes were previously synthesized and used without further treatment.[11–13]

C_{60}: ^{13}C NMR (151 MHz, C_6D_6) δ 143.3.

C_{70}: ^{13}C NMR (151 MHz, $CDCl_3$) δ 150.7, 148.2, 147.4, 145.4, 130.9.

[10]CPP **1**: ^{1}H NMR (400 MHz, $CDCl_3$) δ 7.56 (s, 40H), ^{13}C NMR (101 MHz, $CDCl_3$) δ 138.3, 127.5.

Substituted CPP **2**: ^{1}H NMR (400 MHz, CD_2Cl_2): δ 7.64–7.54 (m, 26H), 7.54–7.50 (m, 4H), 7.17–7.13 (m, 4H), 4.01 (s, 4H), 3.04 (q, ^{3}J = 7.4 Hz, 4H), 1.24 (t, ^{3}J = 7.4 Hz, 6H); ^{13}C NMR (101 MHz, CD_2Cl_2): δ 140.1, 139.4, 139.3, 139.2, 138.8, 138.7, 138.6, 138.6, 138.5, 135.9, 130.6, 128.0, 127.9, 127.83, 127.76, 127.72, 127.66, 127.4, 74.6, 23.9, 17.0. Digits were added to show the difference in the chemical shift. HRMS (APCI): calc. for $[C_{66}H_{51}O]^+$: $[M+H]^+$ 859.3935, found 859.3933.

Substituted CPP **3**: ^{1}H NMR (400 MHz, $CDCl_3$): δ 7.60–7.51 (m, 32H), 7.46–7.40 (m, 4H), 6.75 (s, 2H), 1.46 (s, 18H); ^{13}C NMR (101 MHz, $CDCl_3$): δ 167.0, 139.6, 139.4, 138.9, 138.47, 138.45, 138.43, 138.31, 138.28, 134.44, 131.42, 130.12, 127.56, 127.53, 127.51, 126.8, 82.5, 28.02. Digits were added to show the difference in the chemical shift. HRMS (ESI): calc. for $[C_{70}H_{56}O_4+Na]^+$: $[M+Na]^+$ 983.4071, found 983.4072.

Substituted CPP **4**: ^{1}H NMR (600 MHz, CD_2Cl_2): δ 7.61 (s, 16H), 7.59–7.55 (m, 8H), 7.47–7.43 (m, 8H), 6.84 (s, 4H), 1.45 (s, 36H); ^{13}C NMR (151 MHz, CD_2Cl_2): δ 167.5, 140.3, 140.0, 139.7, 139.14, 139.09, 135.1, 132.1, 130.8, 128.23, 128.17, 127.6, 83.1, 28.4. Digits were added to show the difference in the chemical shift. HRMS (ESI): calc. for $[C_{80}H_{72}O_8+2Na]^+$: $[M+2Na]^{2+}$ 603.2505, found 603.2504.

Fluorescence Quenching Experiments: The fluorescence quenching experiments were performed with a FP-8300 fluorescence spectrometer from Jasco. Solvents for spectroscopy were purchased from Merck or Chemsolute (Uvasol® or HPLC quality). The samples were irradiated with a Xe-lamp. Excitation and emission bandwidth were set to 2.5 nm. The fluorescence was measured between 400 nm and 600 nm with a scan speed of 200 nm/min and a data interval of 0.2 nm. The response time was set to 0.5 sec. The titrations with parent [10]CPP were irradiated at 340 nm, with di- and tetra-*tert*-butyl ester substituted [10]CPP at 338 nm and with diethyl phthalane incorporated [10]CPP at 326 nm.

The association constants were determined by threefold titrations. For each titration a 10^{-6} M to 10^{-7} M solution of the CPP was prepared in toluene. These solutions were used as solvent for a 10^{-4} M to 10^{-6} M solution of the different fullerene guests. Starting with 1800 µl of CPP solution the fullerene (in CPP) solution was added in portions of 15–100 µl. After each step of addition, the solution was mixed thoroughly, and a fluorescence spectrum was measured.

For the determination of the association constant the fluorescence (in a.u.) at the maxima (one maximum in case of parent [10]CPP and two maxima in case of the substituted [10]CPPs) were used. The data were plotted with non-linear regression utilizing the online tool "Bindfit" by P. Thordarson.[16] As error of the mean values the standard deviation was used.

Supporting Information

The authors have cited additional references within the Supporting Information.[34]

Acknowledgements

The authors are grateful to Dennis Gerbig for computational support and the Justus Liebig University for financial support. Open Access funding enabled and organized by Projekt DEAL.

Conflict of Interests

The authors declare no conflict of interest.

Data Availability Statement

The data that support the findings of this study are available in the supplementary material of this article.

EurJOC
European Journal of Organic Chemistry

Research Article
doi.org/10.1002/ejoc.202300575

Chemistry Europe
European Chemical Societies Publishing

Keywords: host-guest systems · macrocycles · computational chemistry · substituent effects · noncovalent interactions

[1] C. A. Hunter, J. K. M. Sanders, *J. Am. Chem. Soc.* **1990**, *112*, 5525–5534.
[2] S. E. Wheeler, J. W. G. Bloom, *J. Phys. Chem. A* **2014**, *118*, 6133–6147.
[3] E. Riedel, C. Janiak, *Anorganische Chemie*, De Gruyter, Berlin, **2022**, pp. 554–561.
[4] S. E. Lewis, *Chem. Soc. Rev.* **2015**, *44*, 2221–2304.
[5] a) R. Jasti, J. Bhattacharjee, J. B. Neaton, C. R. Bertozzi, *J. Am. Chem. Soc.* **2008**, *130*, 17646–17647; b) H. Takaba, H. Omachi, Y. Yamamoto, J. Bouffard, K. Itami, *Angew. Chem. Int. Ed.* **2009**, *48*, 6112–6116; c) S. Yamago, Y. Watanabe, T. Iwamoto, *Angew. Chem. Int. Ed.* **2010**, *122*, 769–771.
[6] T. Iwamoto, Y. Watanabe, T. Sadahiro, T. Haino, S. Yamago, *Angew. Chem. Int. Ed.* **2011**, *50*, 8342–8344.
[7] A. Stergiou, J. Rio, J. H. Griwatz, D. Arčon, H. A. Wegner, C. P. Ewels, N. Tagmatarchis, *Angew. Chem. Int. Ed.* **2019**, *58*, 17745–17750.
[8] Y. Xu, R. Kaur, B. Wang, M. B. Minameyer, S. Gsänger, B. Meyer, T. Drewello, D. M. Guldi, M. von Delius, *J. Am. Chem. Soc.* **2018**, *140*, 13413–13420.
[9] H. Ueno, T. Nishihara, Y. Segawa, K. Itami, *Angew. Chem. Int. Ed.* **2015**, *54*, 3707–3711.
[10] J. Rio, S. Beeck, G. Rotas, S. Ahles, D. Jacquemin, N. Tagmatarchis, C. Ewels, H. A. Wegner, *Angew. Chem. Int. Ed.* **2018**, *57*, 6930–6934.
[11] J. Volkmann, D. Kohrs, H. A. Wegner, *Chem. Eur. J.* **2023**, *29*, e202300268.
[12] D. Kohrs, J. Becker, H. A. Wegner, *Chem. Eur. J.* **2022**, *28*, e202104239.
[13] J. Volkmann, D. Kohrs, F. Bernt, H. A. Wegner, *Eur. J. Org. Chem.* **2022**, *2022*, e202101357.
[14] D. Kohrs, J. Volkmann, H. A. Wegner, *Chem. Commun.* **2022**, *58*, 7483–7494.
[15] E. R. Darzi, T. J. Sisto, R. Jasti, *J. Org. Chem.* **2012**, *77*, 6624–6628.
[16] a) http://supramolecular.org; b) D. Brynn Hibbert, P. Thordarson, *Chem. Commun.* **2016**, *52*, 12792–12805; c) P. Thordarson, *Chem. Soc. Rev.* **2011**, *40*, 1305–1323.
[17] a) F. Neese, *WIREs Comput. Mol. Sci.* **2012**, *2*, 73–78; b) F. Neese, *WIREs Comput. Mol. Sci.* **2022**, *12*, e1606.
[18] C. Adamo, V. Barone, *J. Chem. Phys.* **1999**, *110*, 6158–6170.
[19] F. Weigend, R. Ahlrichs, *Phys. Chem. Chem. Phys.* **2005**, *7*, 3297–3305.
[20] B. Helmich-Paris, B. de Souza, F. Neese, R. Izsák, *J. Chem. Phys.* **2021**, *155*, 104109.
[21] F. Weigend, *Phys. Chem. Chem. Phys.* **2006**, *8*, 1057–1065.
[22] P. Pracht, F. Bohle, S. Grimme, *Phys. Chem. Chem. Phys.* **2020**, *22*, 7169–7192.
[23] S. Grimme, F. Bohle, A. Hansen, P. Pracht, S. Spicher, M. Stahn, *J. Phys. Chem. A* **2021**, *125*, 4039–4054.
[24] a) S. Grimme, A. Hansen, S. Ehlert, J.-M. Mewes, *J. Chem. Phys.* **2021**, *154*, 64103; b) J. W. Furness, A. D. Kaplan, J. Ning, J. P. Perdew, J. Sun, *J. Chem. Phys. Lett.* **2020**, *11*, 8208–8215.
[25] A. V. Marenich, C. J. Cramer, D. G. Truhlar, *J. Phys. Chem. B* **2009**, *113*, 6378–6396.
[26] S. Spicher, S. Grimme, *J. Chem. Theory Comput.* **2021**, *17*, 1701–1714.
[27] C. Bannwarth, E. Caldeweyher, S. Ehlert, A. Hansen, P. Pracht, J. Seibert, S. Spicher, S. Grimme, *WIREs Comput. Mol. Sci.* **2021**, *11*, e1493.
[28] E. Caldeweyher, S. Ehlert, A. Hansen, H. Neugebauer, S. Spicher, C. Bannwarth, S. Grimme, *J. Chem. Phys.* **2019**, *150*, 154122.
[29] E. R. Johnson, S. Keinan, P. Mori-Sánchez, J. Contreras-García, A. J. Cohen, W. Yang, *J. Am. Chem. Soc.* **2010**, *132*, 6498–6506.
[30] W. Humphrey, A. Dalke, K. Schulten, *J. Mol. Graphics* **1996**, *14*, 33–38.
[31] T. Iwamoto, Y. Watanabe, H. Takaya, T. Haino, N. Yasuda, S. Yamago, *Chem. Eur. J.* **2013**, *19*, 14061–14068.
[32] J. Antony, R. Sure, S. Grimme, *Chem. Commun.* **2015**, *51*, 1764–1774.
[33] A.-F. Tran-Van, H. A. Wegner, *Beilstein J. Nanotechnol.* **2014**, *5*, 1320–1333.
[34] a) J. G. Brandenburg, C. Bannwarth, A. Hansen, S. Grimme, *J. Chem. Phys.* **2018**, *148*, 64104; b) S. Ehlert, M. Stahn, S. Spicher, S. Grimme, *J. Chem. Theory Comput.* **2021**, *17*, 4250–4261; c) M. Bursch, J.-M. Mewes, A. Hansen, S. Grimme, *Angew. Chem. Int. Ed.* **2022**, *61*, e202205735.

Manuscript received: June 14, 2023
Revised manuscript received: June 20, 2023
Accepted manuscript online: June 21, 2023

5 Additional contributions

5.1 Mechanistic Study of Domino Processes Involving the Bidentate Lewis Acid Catalyzed Inverse Electron-Demand Diels–Alder Reaction

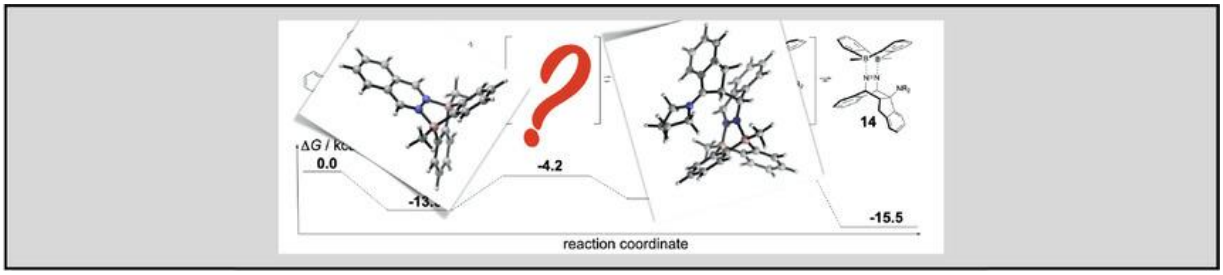

“The detailed understanding of mechanisms is the basis to design new reactions. Herein, we studied the domino bidentate Lewis acid catalyzed inverse electron-demand Diels Alder (IEDDA) reaction developed in our laboratory computationally as well as by synthetic experiments, to characterize different pathways. A quinodimethane intermediate was identified as keystructure, which is the basis for all subsequent transformations: Elimination to an aromatic naphthalene, rearrangement to a dihydroaminonaphthalene and a photo-induced ring opening. These insights allow to optimize the reaction conditions, such as catalytic utilization of amine, as well as to advance new reactions in the future.”

Reprinted with permission from

M. A. Strauss, D. Kohrs, J. Ruhl, H. A. Wegner, *Eur. J. Org. Chem.* **2021**, *2021*, 3866–3873.

DOI: 10.1002/ejoc.202100486

M. A. S. and D. K. contributed equally to this work.

5.2 Synthesis of a Substituted [10]Cycloparaphenylene through[2+2+2] Cycloaddition

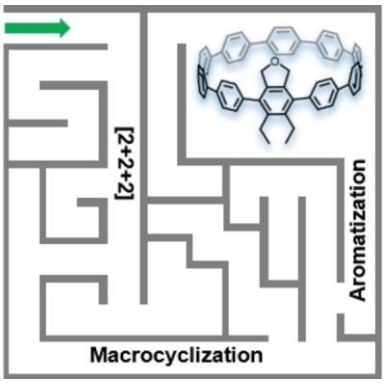

Herein, we report the synthesis and investigation of a substituted [10]cycloparaphenylene (CPP) incorporating a diethylphthalane unit. An efficient strategy relying on a symmetric built-up starting with propargyl ether as [2+2+2] cycloaddition precursor was developed. The straightforward synthesis required overcoming unexpected obstacles within the [2+2+2] cycloaddition, protection and aromatization. These results give valuable insights for accessing CPPs with highly substituted subunits. Finally, a seven-step synthesis with an overall yield of 8% provided the target nanoring, including good to excellent yields for the critical macrocyclization and aromatization. The synthesized nanohoop exhibits a hypsochromic shift in fluorescence and absorption, compared to the unsubstituted [10]CPP. This observation is proposedly caused by an increased torsion angle between the bivalent substituted phenyl moieties and the adjacent units.

Reprinted with permission from

J. Volkmann, D. Kohrs, F. Bernt, H. A. Wegner, *Eur. J. Org. Chem.* **2022**, *2022*, e202101357.

DOI: 10.1002/ejoc.202101357

5.3 Cycloparaphenylenes *via* [2+2+2] cycloaddition

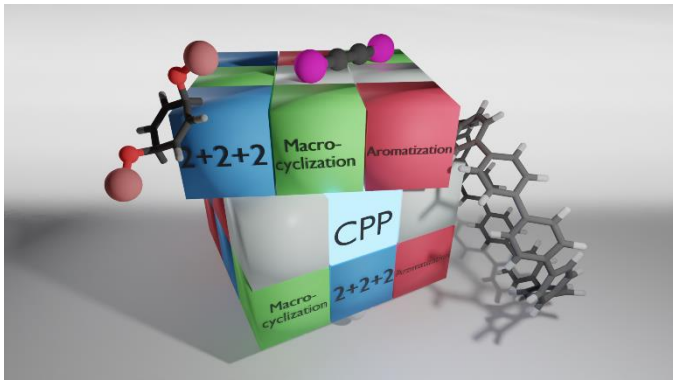

The [2+2+2] cycloaddition (CA) offers great potential as an atom economic method for the formation of substituted aromatic rings. In this article, we highlight the application of this versatile method in synthetic approaches towards substituted cycloparaphenylenes (CPPs). The [2+2+2] CA can take over different tasks within the synthesis depending on the targeted CPP. These approaches were divided into three key steps: aromatization (which finalises the CPP), macrocyclization (the formation of a strain-reduced macrocycle) and the [2+2+2] CA. Based on this analysis the strategies were categorised into four classes based on which task the [2+2+2] CA fulfills. We point out the benefits and drawbacks of each synthetic strategy and summarize our findings to provide the reader with an easy insight into this research field.

Reproduced from

D. Kohrs, J. Volkmann, H. A. Wegner, *Chem. Commun.* **2022**, *58*, 7483–7494.

with permission from the Royal Society of Chemistry.

DOI: 10.1039/D2CC02289C

D. K. and J. V. contributed equally to this work.

6 Acknowledgements

Als erstes möchte ich mich bei Prof. Dr. Hermann A. Wegner bedanken, meine Doktorarbeit in seiner Arbeitsgruppe anfertigen zu dürfen. Vor allem der wissenschaftliche Freiraum und das offene Ohr für neue Projektideen haben meine Entwicklung in den letzten Jahren positiv beeinflusst.

Prof. Dr. Richard Göttlich möchte ich für das Erstellung eines Zweitgutachtens danken.

Ein besonderer Dank gebührt meiner Frau Alena, die mich das ganze Studium hinweg unterstützt und in stressigen Phasen wieder aufgebaut hat.

Meinen Eltern und meiner Schwester möchte ich danken, mich über die Jahre zu der Person gemacht zu haben, die ich heute bin.

Meinen Laborkollegen Julia Ruhl, Christopher Leonhardt, Mari Janse van Rensburg, Jannis Volkmann, Jan Griwatz, Felix Bernt, Marcel Strauss, Anne Kunz, Dominic Schatz, Michel Große, Conrad Averdunk, Giovanni Parolin, Chiara Di Berardino, Finn Schneider, Katinka Grimmeisen, Kai Hanke, Pia Mader, Rouven Fritzius, Silke Müsse, Nathaniel Ukah, Atanu Patra, Longcheng Hong, Jan Geldsetzer, Sebastian Beeck, Sebastian Schmalisch, Sebastian Ahles, Andreas Heindl, Elena Berger und Ronja Kehr mit denen ich über die letzten Jahre zusammengearbeitet habe möchte ich für die nette Arbeitsatmosphäre und den Spaß in und außerhalb des Labors danken.

Keine Doktorarbeit kommt ohne die Hilfe der technischen und administrativen Mitarbeiter aus, die mit ihrer Unterstützung unsere Forschung sehr stark weiterbringen. Daher gebührt auch großer Dank Dr. Heike Hausmann, Anika Bernhardt, Anja Platt, Dr. Raffael Wende, Dr. Dennis Gerbig, Stefan Bernhardt, Steffen Wagner, Edgar Reitz, Anja Beneckenstein, Inna Klein, Brigitte Weinl-Boulakhrouf, Dr. Jörg Neudert, Eike Santowski, Mario Daubner, sowie Doris Verch, Michaela Richter und Maurice Monnard die vor allem halfen anfallende bürokratische Hürden zu überwinden.